INVESTIGATION OF FIELD RELEVANT PARAMETERS FOR MICROBIALLY ENHANCED COALBED METHANE SCALE UP

by

George Addison Platt

A thesis submitted in partial fulfillment
of the requirements for the degree

of

Master of Science

in

Chemical Engineering

MONTANA STATE UNIVERSITY
Bozeman, Montana

July 2019

DEDICATION

This thesis is dedicated to my mother, Janet Huff, who infectiously believes in the importance of generosity, kindness, and curiosity, and to my father, Dudley Platt, who taught me the value of loving your vocation and doing work worth doing.

ACKNOWLEDGEMENTS

Funding for this project was provided by the Department of Energy (DE-FE0024068) and by the United States Geological Survey (USGS) Energy Resources Program. Partial financial support was provided by the National Science Foundation (NSF) under Grant #s CHE-1230632 and 1736255. Environmental samples used in this work were collected at a field site managed by USGS. Any opinions, findings, conclusions, or recommendations expressed herein are those of the author and do not necessarily reflect the views of the DOE, NSF or the USGS. Any use of trade, firm, or product names is for descriptive purposes only and does not imply endorsement by the U.S Government.

I would like to acknowledge my committee members for their guidance and support throughout my graduate work: Dr. Robin Gerlach, Dr. Elliott Barnhart, Dr. Matthew Fields, and Dr. Katherine Davis. I wish to thank the affiliated faculty, staff, and students of the Center for Biofilm Engineering and Department of Chemical and Biological Engineering for their dedication to creating a positive, challenging, and rewarding work and learning environment. I would like to thank the member of the Fields Lab, specifically Dr. Hannah Schweitzer, Dr. Heidi Smith, Dr. Katherine Davis, and Dr. Elliott Barnhart. Getting to conduct field research with this group was a pleasure and privilege due to their incredible wealth of knowledge and expertise, and their unlimited supply of humor and positivity.

Lastly, I would like to thank my friends and family, especially Shawna Pratt, for her continued support and encouragement through earlier morning field trip departures and late nights of writing. Thank you for lightening my load in all aspects of life.

TABLE OF CONTENTS

TABLE OF CONTENTS CONTINUED

LIST OF TABLES

LIST OF TABLES CONTINUED

Table Page

LIST OF TABLES CONTINUED

LIST OF FIGURES

LIST OF FIGURES CONTINUED

Figure Page

LIST OF FIGURES CONTINUED

Figure Page

LIST OF FIGURES CONTINUED

Figure Page

ABSTRACT

Energy production from coal is projected to decline significantly over the next 30 years, due to concerns over anthropogenic carbon emissions, climate change, and cost. As coal-based energy production decreases, the demand for natural gas is expected to increase. Coalbed methane (CBM), a biogenic natural gas resource found in subsurface coal beds, may aid in meeting the projected increase in demand. However, costs associated with traditional CBM extraction currently make utilizing this resource economically prohibitive due to slow coal-to-methane conversion rates and the necessity to treat co-produced water. Algae can be cultivated in co-produced formation water and the addition of very small amounts of this algal biomass can increase coal-to-methane conversion rates. The goal of this work was to determine the optimal algae amendment concentration for the enhancement of microbial coal-to-methane conversion to maximize return on investment.

Concentrations of ^{13}C-labeled algae amendment ranging from 0.01-0.50 g/L (equivalent to 0.0001-0.005 g per g of coal) were tested in coal-containing batch microcosms. Enhanced methane production was observed in all amended microcosms and maximum methane production occurred between 169-203 days earlier than in unamended microcosms. When as little as 0.01 g/L algae amendment was added, $^{13}CH_4$ and $^{12}CH_4$ tracking revealed that the improvement in coal-to-methane conversion kinetics was due to enhanced coal degradation. Increasing amendment concentrations to 0.05-0.50 g/L improved coal-to-methane conversion rates further, but improvements from amendment concentrations above 0.05 g/L were insignificant.

The geologic scope of this CBM enhancement strategy was investigated by studying methane production from five coals ranging in thermal maturity. Biogenic methane was produced from all coals, with subbituminous coals generally producing more methane than thermally mature bituminous coals. The addition of algae amendment to thermally mature coal microcosms resulted in methane production that was comparable to production from unamended, thermally immature coals. This improvement was associated with an increased relative abundance of coal degrading microorganisms. Collectively, this work demonstrates that algae amendment concentrations can be reduced further (to 0.01-0.05 g/L) relative to the previously investigated concentrations (ranging from 0.1-0.5 g/L) and still improve coal-to-methane conversion rates for a range of coal sources.

CHAPTER ONE

INTRODUCTION

Motivation

Transitioning from today's carbon-based economy toward a sustainable energy future presents great challenges in all sectors of society. In the face of climate change, environmental and health concerns arising from the continued use of high-emissions fossil fuels such as coal are leading to a rapid decline in traditional mineral-extraction based economies. The contribution of extraction-based industries to gross domestic product and total employment has been declining for decades [1], resulting in negative socio-economic externalities in communities that have long benefited from fossil fuel based-economies [2]. A fundamental tenant of sustainability is meeting the needs of the present generation without impinging on the ability of future generations to prosper economically, environmentally, and socially, known as the three-pillars of sustainability [3]. The current needs of society are centered around adequate supplies of food, water, materials, and the energy required to provide these necessities [3]. A three-step plan for achieving sustainability has been proposed recently, focusing on the technological contributions from science and engineering [4]. This plan involves (1) short term goals focusing on research and development programs targeting energy efficiency, water resources management, the enhancement of biological processes, and carbon capture and sequestration, (2) a transition regime that focuses on the environmentally-responsible extraction and utilization of natural gas from low-permeability reservoirs such as shale or biogenically derived sources such as coal seams and anaerobic digestion, and (3) long term strategies for the integration of large scale renewable energy (solar, wind, geothermal) into the electricity grid for use at the residential, commercial, and industrial scales [4].

This thesis addresses one of the technical challenges associated with the transition regime proposed above, specifically the extraction and utilization of natural gas from soon-to be under-utilized coal reserves. As renewable energy resources become integrated into the energy portfolio, fossil (coal-fired and gas-fired) power plants will continue to see reduced operational hours and will eventually transition to back-up energy generation during times of peak demand [5]. In the absence of cost-effective large-scale energy storage capabilities, fossil-fired power plants will be forced to deliver variable output to meet intermittent peaks in energy demand, resulting in increased transient phase operation [6]. At full operational load, CO_2 emissions per unit of energy are on average 50-100% higher in coal plants relative to gas plants, and at the minimum compliance load (MCL), the minimum load required for the plant to be compliant with current emissions standards, gas-fired power plants produce less CO_2 and SO_x than coal-fired plants [6]. These emissions reductions, in addition to shorter hot and cold start times in gas-fired power plants, make natural gas a more favorable fuel for flexible electricity generation as renewable energy resources increase. Because natural gas is a more favorable transition fuel, the proportion of total electricity generation from coal is expected to decline from 28% in 2018 to 17% in 2050, while the share from natural gas is expected to increase from 34% to 39%, with most of the demand expected to be met by shale and tight oil resources [7].

Declining production of once-utilized natural gas and coal resources, specifically in the Powder River Basin (PRB) region of southeast Montana and northeast Wyoming, has led to environmental and economic consequences. The Powder River Basin is the largest known coal reserve in the U.S. and a region with a significant history of coalbed methane (CBM) production. The gas-in-place (GIP) in the PRB has been estimated at 1.5 trillion m^3 [8], resulting in a relatively low concentration of gas (1.6 to 2.2 m^3/ton coal). However, when natural gas prices are favorable, CBM production in the PRB is economically viable due to the accessible depth of the coal seams (<300 m), a high concentration of methane (97%), and limited H_2S compared to other

CBM reservoirs. Commercial exploration and production of CBM in the PRB began in the 1980s and reached a peak production of 9.5 billion m^3 in 2005 [9]. The cost to develop a typical CBM well during this time was approximately $165,000 and gas productivity began after a dewatering period of up to 6 months. This dewatering period would produce formation water with high concentrations of total dissolved solids (TDS) and high salinity at a rate of 17,000 gal/day [10]. Technological advances such as hydraulic fracturing made production of natural gas from low permeability oil and shale reservoirs economically viable, resulting in a drastic increase in natural gas supply and a subsequent decrease in gas price, dropping from a peak of $13.42/million BTU in October 2015 to $2.65/million BTU in April 2019 (Henry Hub Natural Gas Spot Price) [11]. As a result, CBM production drastically declined, resulting in 4150 abandoned wells [12] and approximately 4000 lined and unlined holding ponds full of low-quality co-produced water [13]. Based on abandoned well infrastructure alone, approximately $680M of CBM infrastructure is currently inoperable or dormant. Many of these wells are uncapped, resulting in methane leakage to the atmosphere. Furthermore, it has been shown that upstream greenhouse gas emissions from oil and gas extraction is negatively correlated with production [14-16], suggesting that as the economic benefit from CBM production in the PRB declined, the environmental consequences increased.

Beyond the PRB, coalbed and shale gas plays exist across the United States (Figure 1.1). Biogenic methane, produced primarily since the Late Pleistocene, has been found in the Illinois, Michigan, and Gulf of Mexico Basins [17]. Biogenic methane is typically found in shallow, thermally immature coals and shales (vitrinite reflectance, $R_o < 0.6\%$) where formation waters have low salinity (<2 M Cl^-) and low concentrations of SO_4^{2-} (<10 mM). In these systems, methane and carbon dioxide are produced from the syntrophic degradation of the recalcitrant coal organic matter by an anaerobic microbial consortium consisting of fermentative and hydrolytic bacteria, acetogens, and CO_2-reducing and acetate-utilizing methanogenic archaea [18-20].

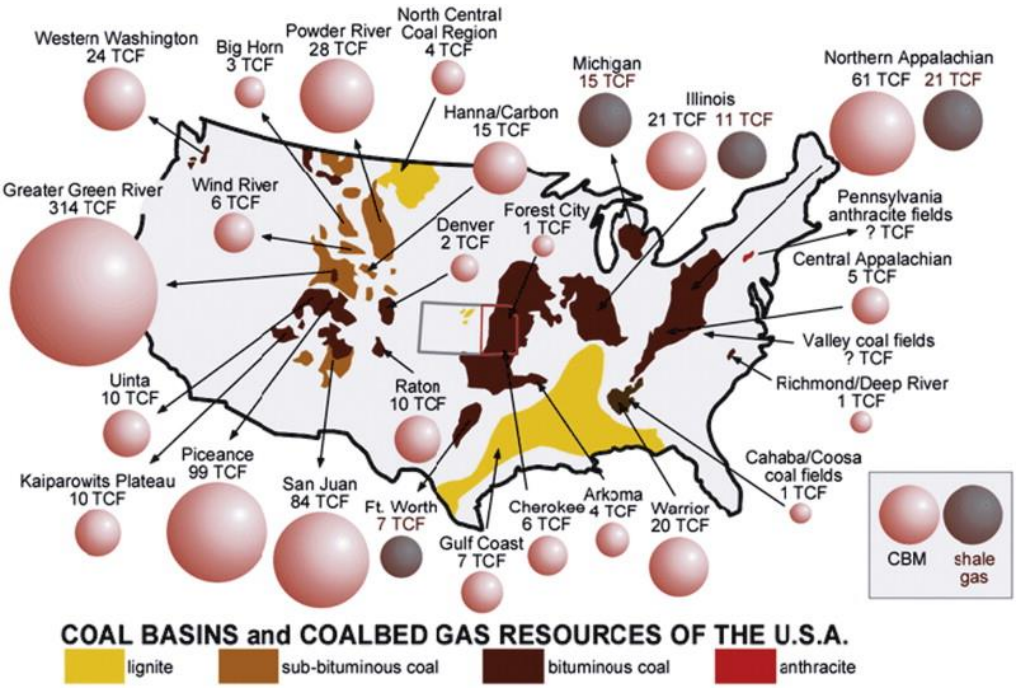

Figure 1.1: Map of U.S sedimentary basins with coalbed methane and fractured shale gas plays including estimates of gas-in-place (Newell et al., 2004).

Additionally, thermogenic hydrocarbon substrates can be utilized by anaerobic microorganisms to produce additional methane, known as secondary gas production [21]. While biogenic gas formation is typically greater in thermally immature sedimentary basins, such as those containing low rank lignite and subbituminous coal, isotopic signatures of biogenic CBM have been found in basins with primarily bituminous coal, such as the northern reaches of the Michigan Basin and the Forest City Basin in eastern Kansas [17, 22]. While biogenic coalbed methane is abundant across the U.S, utilization of these reserves is constrained by the same economic and environmental challenges as the PRB. To take advantage of coalbed methane resources, CBM enhancement technologies that increase in-situ methane production rates, recycle water, and increase profit margins by producing value added byproducts need to be developed.

Thesis Overview

One strategy to enhance *in-situ* coal-to-methane conversion is to introduce an organic amendment into CBM reservoirs to provide coal degrading organisms nutrients that may be limiting in the coal seam environment. The addition of algal biomass has been shown to decrease methane production lag times and increase maximum methane production rates, demonstrating the feasibility of this technique to stimulate microbial coal-to-methane conversion [23, 24]. The growth of algal biomass, which can be used for biofuel production and other value-added products, in co-produced CBM water has been shown [25]. On-site cultivation is advantageous because it eliminates the costs associated with amendment transport and could utilize existing holding pond infrastructure [23]. The addition of algal biomass as a CBM enhancement is promising due to the coupling of improved coal-to-methane kinetics, environmental remediation, and cost reduction (Figure 1.2).

However, only a limited range of amendment concentrations have been investigated [24, 26] and it has been suggested that the microbial metabolism responsible for enhanced methane production may be sensitive to amendment concentration. Optimizing amendment concentration for enhanced coal degradation as opposed to direct amendment conversion is necessary in order to truly utilize microbial communities to harvest the energy stored in coal without long-term effects on overall microbial community composition and structure.

Furthermore, evaluating different amendment concentrations will allow commercial operators to optimize return on investment (ROI). The minimal amendment concentration that provides consistent, demonstrable enhanced coal degradation needs to be determined. By doing so, shifts in microbial communities away from coal degradation can be avoided and surplus algal biomass can be used for the manufacture of value-added byproducts. The first chapter of this thesis seeks to determine the optimum amendment concentration for enhanced coalbed methane

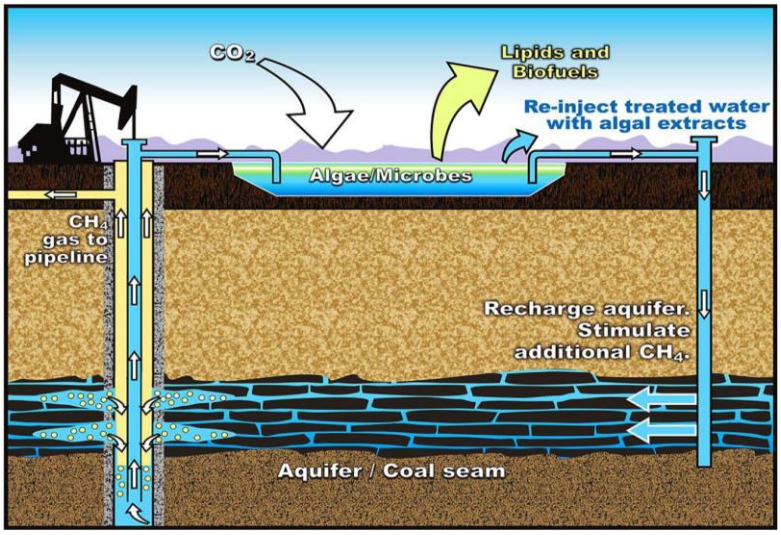

Figure 1.2: Conceptual schematic of microbial CBM enhancement coupled with on-site algae cultivation utilizing pre-existing co-produced holding pond infrastructure from Barnhart et al. (2017).

production. To do so, the mechanism of methane production is evaluated using isotopically labeled ^{13}C-algal amendment, allowing for the ability to track the fate of added amendment into gas products in bench scale, batch microcosms.

In addition to the optimum amendment concentration, the feasibility of algal amendment to stimulate microbial methane production from different coal reserves needs to be evaluated. Due to differences in microbial communities, aqueous geochemistry, ground water infiltration and coal thermal maturity among U.S. CBM reservoirs, the addition of algal amendment needs to be tailored to reservoir conditions. Coal rank, or the degree of coalification due to thermal maturation, is one crucial reservoir variable that needs to be assessed due to associated changes in organic geochemistry that reportedly affect microbial bioavailability [20, 27, 28]. The effect of coal rank on microbial methane production has been shown to be inconclusive in bench scale studies [20, 27-30], while signatures of *in-situ* biogenic methane have been reported in coal basins with different levels of coalification [17]. The second chapter of this thesis attempts to clarify the relationship between coal rank and methane production, focusing on methane yield

potential when using a coal-derived and adapted microbial consortium. Furthermore, the feasibility of using algal amendment to stimulate coal-to-methane conversion in coals of different thermal maturity is assessed to determine the viability of this technique in a range of coal basins.

Lastly, a novel bioelectrochemical technique to enhance microbial coal-to-methane conversion was evaluated in Appendix A of this thesis. Microbial Electrolysis Cells (MECs) have long been a developing technology for enhancing the treatment of complex organic waste streams [31-33]. These systems attempt to address the kinetic and thermodynamic limitations associated with microbial organic matter degradation by adding electrical energy to the system. Due to high energy recovery efficiency when considering the applied electrical input and the energy stored in the organic substrates, MEC technology has garnered interest beyond wastewater treatment applications [34-36]. Specifically, the recently reported high yield bioelectrochemical conversion of coal-to-methane has shed light on the potential to utilize this technology *in-situ* [37]. The highest biogenic coal-to-methane yields reported to date, combined with the potential to reduce geologically sequestered CO_2 and store excess renewable energy (solar, wind) as fuel, makes the idea of catalyzing the microbial coal degradation process using bioelectrochemical techniques worth exploring in detail. Electroactive microorganisms have been identified in anaerobic sludge digestors, subsurface marine environments, and thermophilic oil reservoirs, but the presence of these organisms in mesophilic, biogenic methane producing coal seams has yet to be shown. Consequently, Appendix A of this thesis seeks to determine the effect of an applied electrical voltage on microbial methane production from coal in MEC reactors using PRB coal-derived microorganisms.

CHAPTER TWO

OPTIMIZATION OF ^{13}C-ALGAE AMENDMENT CONCENTRATION FOR ENHANCED COAL DEPENDENT METHANOGENESIS

Contribution of Authors and Co-Authors

Manuscript in Chapter 2

Author: George A. Platt

Contributions: Performed experimental work, analyzed data. Wrote and revised manuscript

Co-Author: Katherine J. Davis

Contributions: Designed and performed experimental work. Contributed to the revision and contents of manuscript with comments and feedback

Co-Author: Elliott P. Barnhart

Contributions: Contributed to experimental design. Contributed to the revision of the manuscript with comments and feedback.

Co-Author: Matthew W. Fields

Contributions: Contributed to experimental design. Contributed to the revision of the manuscript with comments and feedback.

Co-Author: Robin Gerlach

Contributions: Contributed to experimental design. Contributed to data analysis. Contributed to the revision of the manuscript with comments and feedback.

Manuscript Information

Platt, G.P., Davis, K.J., Barnhart, E.P., Fields, M.W., Gerlach, R.

International Journal of Coal Geology

Status of Manuscript:
_X__ Prepared for submission to a peer-reviewed journal
____ Officially submitted to a peer-reviewed journal
____ Accepted by a peer-reviewed journal
____ Published in a peer-reviewed journal

Elsevier

Abstract

The addition of algal biomass to stimulate methane production in coal seams is a promising coalbed methane (CBM) enhancement technique. Previously studies have shown that algal amendment concentrations between 0.1-0.5 g/L can improve methane production rates, but lower amendment concentrations have not yet been evaluated, nor has the effect of increasing the coal-to-amendment ratio. To assess the mechanism of improved coal-to-methane conversion kinetics, isotopically labeled ^{13}C-algal amendment was added to coal microcosms using concentrations ranging from 0.01-0.5 g/L. Methane production rates increased in microcosms with as little as 0.01 g/L algal amendment, and maximum methane production rates were not significantly different between 0.05 g/L and 0.5g/L treatments, ranging from 3.4±0.1 µmol CH_4/g coal/day to 4.0±0.1 µmol CH_4/g coal/day, suggesting that increasing amendment concentration beyond 0.05 g/L does not result in improved coal-to-methane conversion kinetics. Carbon mass balances revealed that microcosms with amendment concentrations between 0.01-0.1 g/L resulted in enhanced methane production that could not be explained by direct amendment conversion alone. $^{12}CH_4$ production rates mirrored total CH_4 production rates in all amended treatments and were significantly higher than the $^{12}CH_4$ production rate in the unamended treatment, suggesting that enhanced methane production is the result of increased coal degradation. Amendment-to-gas conversion ranged from 27.3-46.8% in coal treatments, with no significant differences between amendment concentrations. Overall, these results suggest that a 2 to 10-fold reduction in algal amendment concentration relative to previously investigated concentrations can result in enhanced coal-to-methane conversion.

Introduction

The Powder River Basin (PRB) in southeastern Montana and northeastern Wyoming supplies approximately 40% of U.S. coal. Additionally, biogenic coal bed methane (CBM), an unconventional natural gas resource, is produced in the PRB through the activity of *in situ* bacterial communities that degrade recalcitrant coal into bioavailable intermediates which are in turn consumed by methanogenic archaea to produce methane [18-20, 38-41]. Natural gas is considered a cleaner energy resource than coal, producing approximately half the CO_2 per unit of energy and orders of magnitude less NO_x, CO, and particulate emissions than coal when combusted for electricity production [42, 43]. As a result, the share of electricity generation from coal is expected to decline from 28% in 2018 to 17% in 2050, while the share from natural gas is expected to increase from 34% to 39% [7]. Most of the increase in natural gas production is expected to come from tight oil and shale resources [7], while other sources of onshore production, including CBM, are expected to decline due to unfavorable economic conditions for producing this resource. The decline in CBM production in the PRB has left approximately 4150 abandoned wells [12] and 4000 holding ponds (lined and unlined) full of co-produced formation water [23]. During CBM extraction, water is co-produced, with a typical CBM well in the PRB averaging approximately 17,000 gal/day [10]. Total dissolved solids (TDS) in produced water averages 840 mg/L, which is above the national drinking water standards recommendation of 500 mg/L for potable water [25]. Produced water is also potentially problematic because of high concentrations of Na^+ and low concentrations of Mg^{2+} and Ca^{2+}. As a result, large volumes of produced water require treatment before surface discharge or for use in irrigation [23], which negatively impacts the economic feasibility of CBM production.

One strategy for increasing the economic viability of CBM production is to stimulate biogenic methane production *in-situ* by adding nutrients [38, 44, 45], simple carbon substrates

[29, 46], or a complex organic amendment such as yeast or algae extract [23, 24, 47]. Photosynthetically derived biomass, such as algae, has the potential benefit of on-site cultivation while simultaneously recycling produced water. Hodgskiss et. al isolated and cultivated a native algal species from CBM production water [25] and previous studies have demonstrated the viability of microbially-enhanced coalbed methane (MeCBM) by amending PRB microbial consortia with algal biomass, resulting in increased microbial coal-to-methane conversion [23, 24]. On-site cultivation of algal biomass for use as a stimulant for CBM production has the added benefit of generating lipids for biofuels and other value-added products, as well as sequestering carbon dioxide. While stimulating methane production with an organic amendment is a promising technique for improving the sustainability and economic feasibility of CBM production, it also runs the risk of shifting microbial communities away from coal-degrading organisms[24]. For this reason, an effective organic amendment will promote the microbial growth of coal-degrading organisms, while limiting direct amendment-to-methane conversion.

The goals of this study were as follows: (1) determine the optimum algal amendment concentration for enhanced coal-to-methane conversion to minimize costs and reduce microbial community shifts and (2) determine the fate of algal amendment and the source of enhanced methane production using ^{13}C-labeled biomass.

Methods

Site and Sample Collection

All samples were collected from the previously described Birney Test Site [18], located near Birney, MT in the PRB. Formation water from the Flowers-Goodale (FG) coal bed was pumped and retrieved in June 2017 from the FG-11 well. After two well volumes were pumped and discarded, 6-gal plastic jugs were rinsed twice with formation water before being filled and stored at 4ºC prior to microcosm set up. Coal cores were collected during the July 2013 drilling of

the Flowers-Goodale monitoring wells (FGM-13 and FGP-13). The 2-inch diameter cores were cut into approximately 12-inch long sections and placed in PVC tubes filled with formation water pumped from the FG-11 well. Microbial cultures were collected from the FG-09 well in June 2017 using the diffusive microbial samplers previously described by Barnhart et al. [38]. The slurry from the FG-09 DMS was added to a serum bottle prepared with 5g FG coal and 45 mL of filter sterilized, reduced FG formation water before incubation at 21±1ºC in the dark for 2 months prior to use as inoculum for the microcosms described below.

^{13}C-Labeled Amendment Growth and Preparation

A microalga, *Chlorella* sp. strain SLA-04 (isolated from Soap Lake, WA, USA) was cultured for biomass accumulation [24]. SLA-04 was cultured at 20ºC in Bold's Basal Medium [48] with 2X nitrate in tube photobioreactors as previously described [49] with the following modifications. Five photobioreactors containing 1.2 L of sterile media and inoculated with $5x10^5$ cells/mL were sparged (20%:80% O_2:N_2) to minimize atmospheric CO_2 dissolution. Sodium bicarbonate ($NaH^{13}CO_3$) was initially added at 10mM as the sole inorganic carbon (IC) source. The pH was measured within the first hour of the 14-hour light period and then every 4 hours until the beginning of the dark phase. pH was maintained between 8.5 and 10 by adjusting with 2M HCl or KOH as needed to reduce IC loss through CO_2 off gassing. Dissolved Inorganic Carbon (DIC) was measured twice daily and $NaH^{13}CO_3$ was added as needed to maintain DIC between 5 and 10 mM. Daily cell counts were used to determine stationary phase when the cell counts were the highest, $1.2x10^8$ cell/mL. The biomass was concentrated by centrifugation, dried by lyophilization, and stored at -20ºC until use in coal microcosms. The ^{13}C-labeled algal amendment was sent to the Stable Isotope Facility at the University of California (Davis, CA, USA) for carbon-13 analysis. ^{13}C-algal amendment was 46.8 %C (dry weight), and 94.8% ^{13}C/C. ^{13}C-algae was ground to a fine powder with a ceramic mortar and pestle, and 10X Stock solutions

of ^{13}C-algal amendment concentrate were prepared for final concentrations of 0.5 g/L, 0.1 g/L, 0.05 g/L, and 0.01 g/L using degassed FG formation water in an anaerobic chamber and sealed in serum bottles. Carbon analysis of ^{13}C-algal amendment can be found in Table 2.1

Table 2.1: Carbon analysis of carbon sources in microcosms.

Carbon Source	%C (Dry Weight)	%^{13}C of Total C	δ^{13}C (‰)	Average MW Carbon (g/cmol)
^{13}C-algae	46.8	94.8	1,621,359	12.948
coal	58.1	1.1	-24.1	12.011

Microcosm Setup

All microcosms were set up in triplicate using anoxic techniques in 26 mL Balch tubes sealed with butyl rubber stoppers and aluminum crimp seals. The FG coal core (depth 384-385') was opened in an anaerobic glove bag, where it was dried and crushed. Crushed coal was sieved to an effective size of 0.85-2.00 mm. One mm diameter Borosilicate glass beads were autoclaved and used in lieu of coal to provide carbon-free substrate for controls.

Microcosms were setup in two main categories: different amounts of coal and different amendment concentrations. For the different amounts of coal microcosms, Balch tubes were prepared with 1, 2, or 5 g of prepared coal or glass beads. FG formation water was filtered with a 0.2 µm bottle top filter, sparged overnight with anoxic 5% CO_2 (balance of N_2) and reduced with 1 mM sulfide ($Na_2S^{\bullet}9H_2O$). For each coal amount condition, amended microcosms were set up with a final amendment concentration of 0.1 g/L ^{13}C-algae. Each microcosm was inoculated with 1 mL of previously collected FG enrichment consortium, and prepared formation water was added to obtain a final liquid culture volume of 10 mL. Microcosms with 1g, 2g, and 5g of coal had headspace volumes of 16.0, 15.2, and 12.8 mL, respectively. Using the prepared 10X stock solutions, amended microcosms with final amendment concentrations 0.5 g/L, 0.1 g/L, 0.05 g/L,

and 0.01 g/L and 1g of prepared coal or glass beads were setup as described above, in addition to unamended microcosms. The amount of carbon added to the microcosms as amendment for each concentration can be found in Table 2.2. All microcosms were incubated at 21±1ºC in the dark for 405 days. Headspace gas was sampled and analyzed every 2-6 weeks.

Table 2.2: Amount of carbon added as amendment for each prepared amendment concentration.

Amendment Concentration (g/L)	Cmol added as Amendment (µmol)
0.01	3.6
0.05	18.1
0.1	36.1
0.5	180.7

Headspace Gas Analysis

Headspace gases (CH_4 and CO_2) were analyzed using an SRI Instruments (Torrance, CA, USA) Model 8601 GC equipped with a thermal conductivity detector (TCD) interfaced with PeakSimple Chromatography software. Ultra-high purity helium carrier gas and a Supelco HayeSep-D packed stainless-steel column (6 feet x 1/8" O.D) were used for separation. One mL of headspace gas was sampled from each microcosm and manually injected with a carrier gas pressure of 8 psi and the oven and TCD temperatures of 40ºC and 150ºC, respectively. To measure isotope ratios of $^{13}CH_4$:$^{12}CH_4$ and $^{13}CO_2$:$^{12}CO_2$, 500 µL of headspace gas was manually injected into an Agilent 6890 GC 5973 electron impact ionization mass selective detector (Agilent Technologies, Palo Alto, Ca, USA) equipped with a GS-Carbonplot column (60m x 0.320 mm I.D. x 1.50 µm film thickness) and interfaced with Agilent Enhanced ChemStation software. The following operation parameters were used: 500 uL split ratio 30:1 injection, constant flow at 1 ml/min, injector temperature of 185ºC, interface temperature of 60ºC, and scan range m/z 2-100. Ultra-high purity helium was the carrier gas. Both headspace gas samples were taken simultaneously and 1.5 mL of anoxic 5% CO_2 (balance N_2) was injected to replace the

sample volume. Isotope ratios were analyzed using the GC-MS deconvolution method previous described [50].

Statistical Analysis

Differences in final methane production, methane production rates, carbon dioxide production, carbon dioxide production rates, amendment conversion, $^{12}CH_4$ production, and maximum $^{12}CH_4$ production rate for each amendment concentration for coal and GB samples were compared using a Generalized Linear Model (GLM) with Tukey interaction. GLM models comparing differences in final methane production, methane production rates, carbon dioxide production, carbon dioxide production rates, $^{12}CH_4$ production, and maximum $^{12}CH_4$ production rates with a factor for coal mass and a factor for amendment condition. A p-value less than 0.05 determined significance.

Results

Total Methane Production

All ^{13}C-algae amended coal and GB treatments produced methane during the 405-day study (Figure 2.1). The unamended GB treatment produced 4.2±0.6 µmol CH_4/g coal, suggesting that methane produced from carbon in the inoculum was negligible. At the end of the 405 day period, coal treatments amended with 0.5 g/L, 0.1 g/L, 0.05 g/L, and 0.01 g/L ^{13}C-algae produced 295.5±2.9 µmol CH_4/g coal, 235.6±7.1 µmol CH_4/g coal, 224.4±2.7 µmol CH_4/g coal, and 199.2±24.3 µmol CH_4/g coal, respectively, while the unamended coal treatment produced 163.7±38.6 µmol CH_4/g coal. Coal treatments with amendment concentrations of 0.5 g/L, 0.1 g/L, and 0.05 g/L produced significantly more methane than the unamended treatment ($p<0.05$) The 0.01 g/L treatment grouped statistically with the 0.1 and 0.05 g/L treatment but did not produce

significantly more methane (p=0.35) than the unamended treatment. A complete table of Tukey pairwise comparisons can be found in the Chapter Supplementary Information (Table S2.1). For all amended coal treatments, methane was detected in the microcosm headspace by day 15. For the 0.5 g/L, 0.1 g/L, and 0.05 g/L treatments, methane production sharply increased until day 84. Methane production for the 0.01 g/L and unamended enrichments occurred more slowly and with more variability, reaching a maximum on day 118 and day 287, respectively.

For all amended GB treatments, methane was first detected on day 18. At the end of the 405-day period, GB treatments amended with 0.5 g/L, 0.1 g/L, 0.05 g/L, and 0.01 g/L ^{13}C-algae produced 63.0±2.9 µmol CH_4/g GB, 14.1±1.7 µmol CH_4/g GB, 10.3±1.1 µmol CH_4/g GB, and 4.5±1.1 µmol CH_4/g coal (Figure 2.1). Methane was detected in the unamended GB treatment on day 57 and it ultimately produced 4.2±0.6 µmol CH_4/g GB. The 0.5 g/L GB treatment quickly produced methane until day 84 and produced statistically more methane than all other GB treatments (p<0.05). The remaining amended GB treatments did not exhibit rapid methane production and instead gradually produced low levels of methane for the duration of the experiment.

Methane production rates increased when ^{13}C-algal amendment was added to coal treatments, but not proportionally to the amount of carbon as amendment added. Methane production rates between day 15 and day 84 – a period of time after the lag phase for all amended treatments with consistent methane production - for the 0.5 g/L, 0.1 g/L, 0.05 g/L, and 0.01 g/L amended coal treatments were 4.0±0.1 µmol CH_4/g coal/day, 3.4±0.1 µmol CH_4/g coal/day, 3.4±0.1 µmol CH_4/g coal/day, and 2.1±1.0 µmol CH_4/g coal/day, respectively. The methane

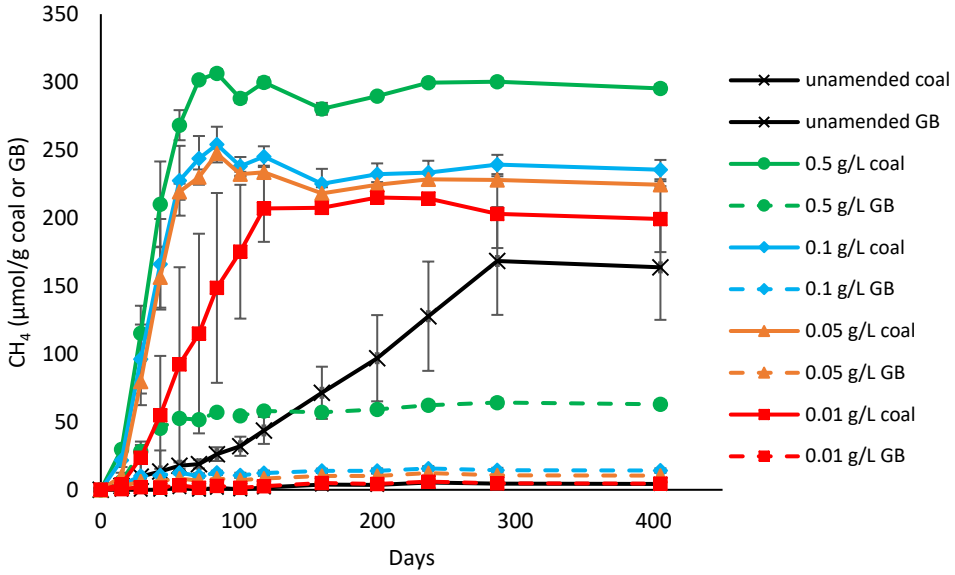

Figure 2.1: Methane produced for ^{13}C-algae amended coal and GB treatments versus time over the course of the 405-day study. All treatments have 1g of solid substrate (coal or GB). Error bars represent one standard deviation of triplicate measurements. Error bars are smaller than the markers if not visible.

production rate for the unamended coal treatment during this time period was 0.3±0.1 µmol CH_4/g coal/day. All amended treatments had statistically higher methane production rates than the unamended treatment during this time interval (p<0.05). Additionally, there was no significant difference between the methane production rate between the 0.5 g/L, 0.1 g/L, and 0.05 g/L treatments (p>0.32), suggesting that increasing amendment concentration above 0.05 g/L does not increase the methane production rate. The 0.01 g/L coal treatment did not group statistically with the higher amendment concentration treatments (Chapter Specific Supplementary Information, Table S2.2) but still had a higher methane production rate than the unamended treatment. However, the time period of days 15-84 was not representative of the highest methane production rate for the unamended coal treatment. Instead, the highest methane production rate for the unamended coal treatment of 0.7±0.2 µmol CH_4/g coal/day occurred between days 71-287. Considering the differences in methane production rate during the most

productive time interval for each treatment, all amended treatments were still greater than the unamended treatment ($p<0.05$). This suggests that the presence of ^{13}C-algal amendment increases the methane production rate and decreases the lag phase for methane production, regardless of amendment concentration, compared to unamended treatments. When methane production rates are normalized to the amount of carbon added as amendment, the efficacy of the added amendment can be evaluated. Normalized methane production rates between the days 15-84 for 0.5 g/L, 0.1 g/L, 0.05 g/L, and 0.01 g/L amended coal treatments were 0.02±0.00 µmol CH_4/µCmol amendment/day, 0.09±0.00 µmol CH_4/µCmol amendment/day, 0.18±0.00 µmol CH_4/µCmol amendment/day, and 0.56±0.27 µmol CH_4 µCmol amendment/day, respectively, suggesting that lower amendment concentrations are utilized more efficaciously than higher concentrations.

Carbon Dioxide Production and Consumption

Carbon dioxide was produced throughout the duration of the study for ^{13}C-algae amended coal treatments (Figure 2.2), while ^{13}C-algae amended GB treatments - except for 0.5 g/L GB - showed a negative production (consumption) of carbon dioxide after accounting for carbon dioxide that was added during sample replacement. For ^{13}C-algae amended coal treatments, carbon dioxide began to increase immediately following inoculation, and continued until day 84-118. The final mass of carbon dioxide produced in the headspace of the microcosms, and the rate at which it changed, generally increased as amendment concentration increased in coal treatments. The final mass of carbon dioxide produced in the 0.5 g/L, 0.1 g/L, 0.05 g/L, 0.01 g/L, and unamended coal treatments was 47.5±0.7 µmol CO_2/g coal, 30.3±4.5 µmol CO_2/g coal, 29.3±2.2 µmol CO_2/g coal, and 22.4±3.3 µmol CO_2/g coal, and 20.1±4.5 µmol CO_2/g coal, respectively. Notably, the 0.01 g/L coal treatment did not have significantly more CO_2 in the headspace than the unamended coal treatment. The final mass of CO_2 produced in the headspace

of GB treatments was 14.2±1.4 µmol CO_2/g coal, -7.7±0.5 µmol CO_2/g coal, -7.9±2.0 µmol CO_2/g coal, -12.8±1.1 µmol CO_2/g coal, and -14.9±0.9 µmol CO_2/g coal for the 0.5 g/L, 0.1 g/L, 0.05 g/L, 0.01 g/L, and unamended GB treatments, respectively.

The CO_2 production rate in coal treatments between days 0-84 generally increased with increasing amendment concentration. For the 0.5 g/L, 0.1 g/L, 0.05 g/L, 0.01 g/L, and unamended coal treatments, CO_2 production rates were 0.5±0.0 µmol CO_2/g coal/day, 0.3±0.0 µmol CO_2/g coal/day, 0.3±0.0 µmol CO_2/g coal/day, 0.2±0.0 µmol CO_2/g coal/day and 0.1±0.0 µmol CO_2/g coal/day. For the 0.5 g/L, 0.1 g/L, 0.05 g/L, 0.01 g/L, and unamended GB between the days 0-84, CO_2 production rates were 0.2±0.0 µmol CO_2/g coal/day, -0.03±0.01 µmol CO_2/g coal/day, -0.03±0.00 µmol CO_2/g coal/day, -0.07±0.00 µmol CO_2/g coal/day, and -0.1±0.0 µmol CO_2/g coal/day. For both coal and GB treatments, the increase in headspace CO_2 and the production rate of CO_2 were not proportional to the amount of carbon added as amendment.

Source of Carbon for Methane Production

To determine whether increased methane production was from enhanced coal conversion or direct amendment conversion, two different analyses were employed. First, it was observed that throughout the duration of the experiment, the amount of methane produced in all ^{13}C-algae amended treatments, regardless of final concentration, was greater than the amount of methane in the unamended coal treatment and corresponding amended glass beads treatments combined (Eqn. 1).

$$CH_{4_{amended\ coal}} > CH_{4_{unamended\ coal}} + CH_{4_{amended\ GB}} \quad \text{Eqn. 1}$$

Methane production from the unamended coal treatment is assumed to be the methane potential from coal conversion alone, while methane production from the amended glass bead treatments is assumed to be the methane potential from amendment conversion alone. Methane produced from

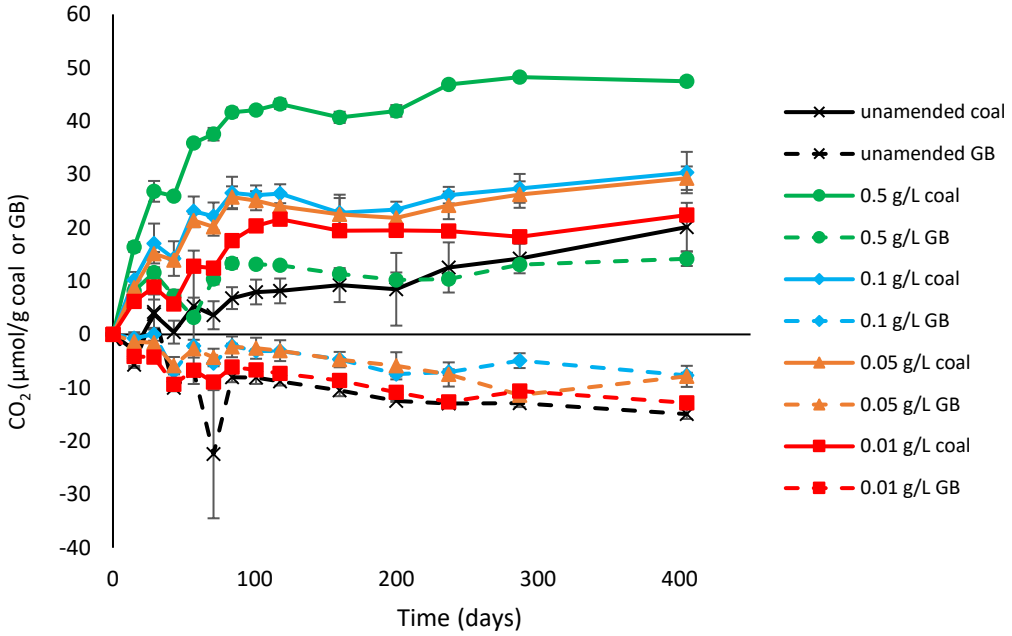

Figure 2.2: Carbon dioxide produced in amended coal and GB treatments versus time over the course of the 405-day study after accounting for CO_2 added during sample replacement. Negative values represent a net consumption of CO_2. All treatments have 1g of solid substrate (coal or GB). Error bars represent one standard deviation of triplicate measurements. Error bars are smaller than the markers if not visible.

amended coal treatments greater than the sum of the individual components is likely from enhanced coal conversion in the presence of amendment rather than direct amendment conversion.

A second analysis based on a carbon balance, as performed previously in Davis et al. (2018), was used to assess the carbon sources for methane production (Figure 2.3). For each amendment concentration, the amount of carbon added as amendment was determined (Table 2.2). Using Eqn. 2, the difference in carbon produced as methane between amended and unamended treatments for each amendment concentration was calculated and normalized by the amount of carbon added as amendment for every sampling point throughout the duration of the experiment.

$$\frac{C_{out}}{C_{in}} = \frac{Cmol\ CH_{4_{amended\ coal}} - Cmol\ CH_{4_{unamended\ coal}}}{Cmol_{amendment}} \quad \text{Eqn. 2}$$

Eqn. 2 assumes that all carbon added as amendment is converted to methane and is not to biomass or inorganic carbon such as CO_2. Thus, any C_{out}/C_{in} ratio greater than one indicates that additional methane produced was due to enhanced coal-to-methane conversion as opposed to direct amendment conversion. By day 43, amended treatments (0.5 g/L coal, 0.1 g/L coal, 0.05 g/L coal, 0.01 g/L coal) had C_{out}/C_{in} ratios greater than one, indicating that the Cmol methane produced exceeded the Cmol added as amendment. All these treatments, except for the 0.5 g/L coal treatment, maintained C_{out}/C_{in} ratios greater than one for the remainder of the study. The C_{out}/C_{in} for the 0.5 g/L coal treatment was above one from days 43-237 before dropping below one, indicating that the additional methane produced is not definitively a result of enhanced coal-to-methane conversion. C_{out}/C_{in} ratios reached a maximum on day 84 for the 0.5 g/L coal, 0.1 g/L coal, and 0.05 g/L coal, while the 0.01 g/L coal treatment reached a maximum on day 118, further reflecting the effect of amendment concentration on methane production rate. After reaching a maximum, C_{out}/C_{in} decreased for all treatments as a result of additional methane production in the unamended treatments while methane production in the amended treatments had mostly ceased and methane concentrations remained mostly constant (cf. Figure 2.2).

Fate of ^{13}C-algal amendment

While it is clear from both analyses above that the addition of ^{13}C-algal amendment to final concentrations between 0.01 g/L and 0.1 g/L increases the rate of coal-to-methane conversion, the mechanism needs to be evaluated. To do this, the conversion of ^{13}C to methane and carbon dioxide was tracked throughout the duration of the experiment for all treatments. In these systems, added carbon can be converted to methane, dissolved or gaseous inorganic carbon (CO_2), soluble organic intermediates, or incorporated into microbial biomass. All treatments

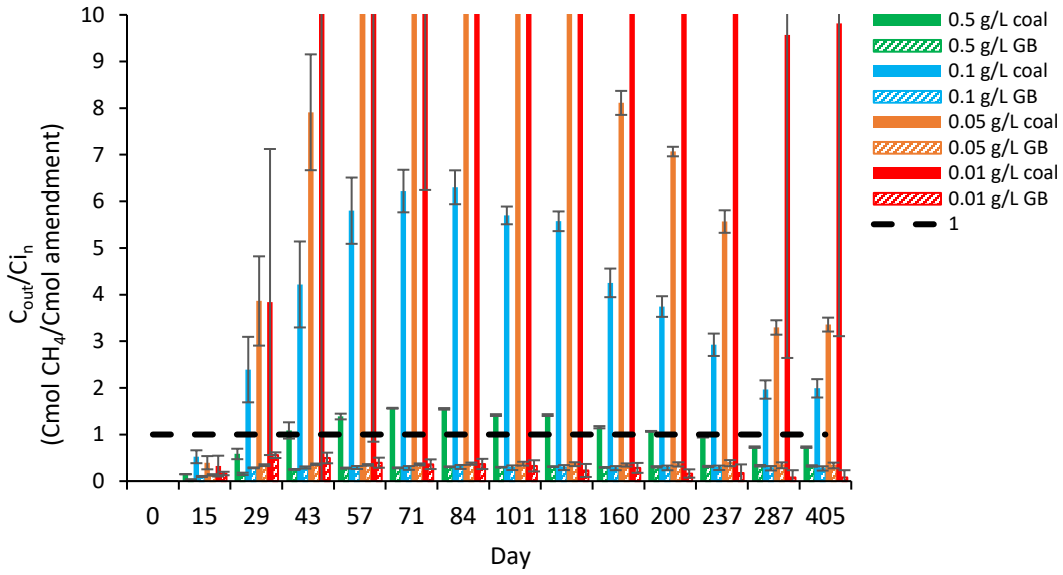

Figure 2.3: Amount of carbon detected as methane relative to the amount of carbon added as amendment for ^{13}C-algae amended coal and GB treatments. C_{out}/C_{in} ratios greater than one represents more surplus carbon detected as methane than carbon added as amendment.

amended with ^{13}C-algal amendment produced methane that contained more than 1.1% $^{13}CH_4$, the approximate natural abundance of ^{13}C in the environment [51], indicating that the microbial consortium used in this study converted at least some amendment to methane, regardless of concentration (Figure 2.4). The percent of CH_4 that was $^{13}CH_4$ increased with increasing amendment concentration ($p<0.01$). By day 405, methane produced in the 0.5 g/L amended coal and 0.5 g/L amended GB treatments was 19.0±0.7% $^{13}CH_4$ and 51.9±3.3% $^{13}CH_4$, respectively. Methane produced in the 0.1 g/L amended coal and 0.1 g/L amended GB treatments was 5.5±0.4% $^{13}CH_4$ and 37.6±9.1% $^{13}CH_4$. For the 0.05 g/L amended treatments, produced methane was 4.1±0.8% $^{13}CH_4$ and 24.7%±13.3% $^{13}CH_4$ for coal and GB, respectively. At the lowest amendment concentration, 0.01 g/L, produced methane was 2.0±0.2% $^{13}CH_4$ and 11.7±2.6% $^{13}CH_4$ for coal and GB, respectively. Methane produced by unamended coal and GB treatments was 1.4±0.0% $^{13}CH_4$ and 0.1±0.1% $^{13}CH_4$, respectively, indicating that methane produced from coal alone or organic matter in the inoculum was comparable to the natural relative abundance of

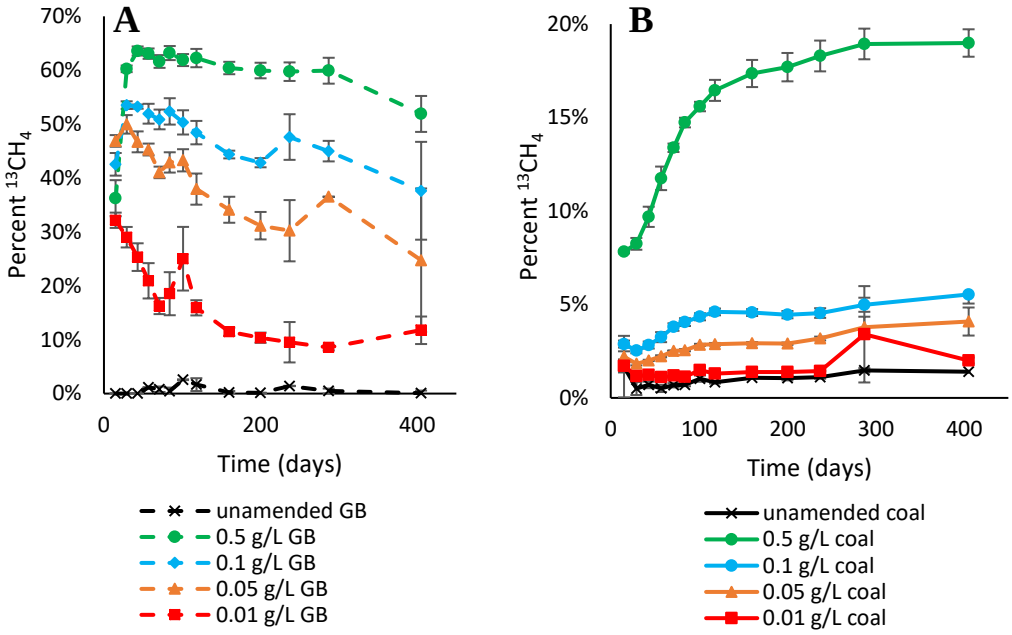

Figure 2.4: Percent of total methane produced that is $^{13}CH_4$ over the course of the 405-day study for (A) ^{13}C-algae amended GB treatments and (B) ^{13}C-algae amended coal treatments. Error bars represent one standard deviation of triplicate measurements. Error bars are smaller than the markers if not visible.

^{13}C considering the sensitivity of the method used. The fraction of total methane that was $^{13}CH_4$ gradually increased as total methane production increased over the course of the 405-day period for all coal treatments, indicating that direct amendment-to-methane conversion is occurring as the fraction of coal that is bioavailable becomes depleted (Figure 2.4B). In GB treatments, the percent of $^{13}CH_4$ increased quickly (Figure 2.4A), reaching a maximum between days 15-43, and then gradually decreased for the remainder of the study. This result suggests that initial methane production in GB treatments was from direct amendment conversion, but methane produced later in the study was derived from another source, such as the reduction of unlabeled CO_2 via hydrogenotrophic methanogenesis, the consumption of unlabeled dissolved organic carbon in the formation water, or the turnover of microbial biomass. Methane production from sources other

than direct amendment conversion in GB treatments provides evidence that these organisms are still metabolically active and viable after amendment has been utilized.

Elevated levels of $^{13}CO_2$ in some amended treatments suggests a fraction of amendment is being converted to CO_2 (Chapter Specific Supplementary Information, Figure S2.1). Treatments with 0.5 g/L amendment exhibited the highest amount of $^{13}CO_2$, reaching as high as 16.5±0.8% and 19.5±0.6% for coal and GB treatments, respectively. Coal treatments with 0.1 g/L coal and 0.05 g/L amendment exhibited variable percentages of $^{13}CO_2$ throughout the duration of the study, reaching as high 4.0±0.2% and 2.5±0.0% on day 200, respectively. Unamended and 0.01 g/L amended coal treatments did not exhibit elevated $^{13}CO_2$ levels relative to natural abundance. A similar trend was observed in amended GB treatments, with 0.1 g/L GB and 0.05 g/L GB reaching a maximum of 4.9±0.2% and 2.9±0.1% $^{13}CO_2$ on day 200, respectively. The 0.01 g/L GB and unamended GB treatments did not exhibit significantly elevated levels of $^{13}CO_2$ during the duration of the experiment. Increased levels of $^{13}CO_2$ at the highest concentration of amendment (0.5 g/L) support the hypothesis that direct amendment conversion is significant at higher concentrations. However, because carbon dioxide is both a substrate and product of methanogenesis depending on the microbial metabolism, and the speciation of aqueous inorganic carbon (CO_3^{2-}, HCO_3^-, H_2CO_3) depends on pH and partial pressure, the mass of $^{13}CO_2$ in the headspace of the microcosms is not a complete measure of amendment to CO_2 conversion.

The fraction of $^{13}CH_4$ detected in microcosm headspace gases is a good approximation for amendment-to-methane conversion. To calculate the extent of amendment conversion in the amended microcosms, the cumulative mass of $^{13}CH_4$ produced was calculated in both amended and unamended treatments. The difference in $^{13}CH_4$ between amended and unamended treatments can be considered the amount of $^{13}CH_4$ produced from the algal amendment alone. Normalizing this difference by the mass of ^{13}C added as algal amendment for each concentration, the amendment-to-methane conversion can be determined (Eq. 3).

$$\%\ conversion = \frac{Cmol\ ^{13}CH_{4_{amended\ coal/GB}} - Cmol\ ^{13}CH_{4_{unamended\ coal/GB}}}{Cmol\ ^{13}C_{added}} \quad \text{Eq. 3}$$

Amendment-to-methane conversion ranged from 25.5-42.7% in coal treatments and 18.2-21.0% in GB treatments (Table 2.3). Differences in amendment-to-methane conversion were not significant based on amendment concentration (p=0.56), but coal treatments generally had higher conversions than GB treatments (p<0.05) (Chapter Specific Supplementary Information, Table S2.3).

Table 2.3: Summary of produced $^{13}CH_4$, $^{13}CO_{2(g)}$, and amendment conversion after 405 days for different concentrations of ^{13}C-algal amendment for coal and GB treatments.

Treatment	Total $^{13}CH_4$ µmol/g coal	Total $^{13}CO_2$ µmol/g coal	% ^{13}C amendment as $^{13}CH_4$	% ^{13}C amendment as $^{13}CO_2$	% ^{13}C amendment as headspace gas
0.5 g/L Coal	48.3±1.3	13.2±0.6	27.0±0.8	7.3±0.3	34.3±1.1
0.5 g/L GB	35.9±2.1	11.6±0.4	21.0±1.3	6.6±0.3	27.5±1.5
0.1 g/L Coal	10.8±0.7	0.5±0.2	25.5±2.1	2.4±0.6	27.3±2.4
0.1 g/L GB	6.2±0.4	0.8±0.5	18.2±1.1	1.5±1.3	19.7±1.5
0.05 g/L Coal	7.3±0.8	1.6±0.0	30.0±4.5	5.4±0.2	35.5±4.6
0.05 g/L GB	3.2±0.5	0.9±0.0	18.9±3.2	3.4±0.3	22.3±2.9
0.01 g/L Coal	3.6±0.9	0.8±0.0	42.7±25.9	4.1±0.9	46.8±26.7
0.01 g/L GB	0.6±0.0	0.5±0.0	17.4±1.2	4.7±0.6	22.1±0.8

Amendment-to-$CO_{2(g)}$ conversion ranged from 2.4-7.3% in coal treatments and 1.5-6.6% in GB treatments. Like methane, observed amendment-to-$CO_{2(g)}$ conversion was generally higher in amended coal treatments than GB treatments (p<0.05). Unlike methane, amendment concentration did have a significant effect on amendment-to-$CO_{2(g)}$ conversion (p<0.05), but no clear relationship could be established (Chapter Specific Supplementary Information, Table

S2.5). Due to the speciation of carbon dioxide in aqueous systems, amendment-to-inorganic carbon conversion is likely underestimated.

Considering both amendment-to-methane and amendment-to-$CO_{2(g)}$ conversion together, the detectable conversion of amendment ranged from 27.3-46.8% in coal treatments and 19.7-27.5% in GB treatments. The differences in total amendment-to-gas conversion between amendment concentrations in coal and GB treatments was not significantly different (p>0.28), suggesting that a similar fraction of amendment is converted to gaseous products, regardless of the initial amendment concentration or substrate type. Because 100% amendment conversion was not observed in all treatments, it is possible that some amendment was not utilized in the microcosms. However, it is more likely that unaccounted ^{13}C was converted to dissolved inorganic carbon, incorporated into microbial biomass, or converted to soluble intermediates such as acetate. In addition, because significant gas adsorption is observed in coal systems, it is likely that some ^{13}C was adsorbed to the solid coal substrate and was undetectable.

Coal-to-Methane Conversion: $^{12}CH_4$

The FG coal used in this study was 58.1% C (dry weight). Assuming a natural abundance of $^{13}CH_4$ in coal (Table 2.1), each microcosm had approximately 532.1 ^{12}C-μmol of coal, which is at least an order of magnitude more than the amount of ^{12}C added as amendment (Table 2.2). As a result, it can be assumed that any $^{12}CH_4$ detected is from coal conversion. All amended and unamended coal microcosms produced significant amounts of $^{12}CH_4$, and $^{12}CH_4$ production was highly correlated with total CH_4 production (Chapter Specific Supplementary Information, Figure S2.2) throughout the 405-day study. Specifically, coal treatments amended with 0.5 g/L, 0.1 g/L, 0.05 g/L, and 0.01 g/L ^{13}C-algal amendment produced 247.1±3.3 μmol $^{12}CH_4$/g coal, 224.8.2±6.5 $^{12}CH_4$/g coal, 217.1±1.9 μmol $^{12}CH_4$/g coal, and 195.6±23.5 μmol $^{12}CH_4$/g coal, while the unamended coal treatment produced 161.6±38.2 μmol $^{12}CH_4$/g coal. The total $^{12}CH_4$ produced in

the 0.5 g/L, 0.1 g/L, and 0.05 g/L amended treatments produced significantly more $^{12}CH_4$ than the unamended coal treatment ($p<0.05$), but they did not produce significantly more $^{12}CH_4$ relative to each other. This provides additional evidence that ^{13}C-algal amendment between the concentrations of 0.05 g/L and 0.5 g/L enhances coal-to-methane conversion, but that increasing amendment concentration above 0.05 g/L does not result in a proportional increase in coal conversion. The coal treatment amended with 0.01 g/L ^{13}C-algae had high variability among replicates and grouped statistically with the 0.05 g/L amended treatments as well as the unamended treatments, suggesting that even at the lowest amendment concentration an increase in coal conversion is possible.

Amending coal treatments with ^{13}C-algal amendment increased the production rate of $^{12}CH_4$ and decreased the lag time for production (Table 2.4, Chapter Specific Supplementary Information, Figure S2.2). $^{12}CH_4$ production increased rapidly in coal treatments amended with 0.5 g/L, 0.1 g/L, and 0.05 g/L ^{13}C-algal amendment until day 84, while the 0.01 g/L coal treatment and the unamended coal treatment consistently produced methane until days 118 and 287, respectively. The $^{12}CH_4$ production rates between day 15 and 84 for coal treatments amended with 0.5 g/L, 0.1 g/L, 0.05 g/L, and 0.01 g/L ^{13}C-algal amendment were 3.4±0.1 μmol $^{12}CH_4$/g coal/day, 3.2±0.1 $^{12}CH_4$/g coal/day, 3.4±0.1 μmol $^{12}CH_4$/g coal/day, and 2.1±1.0 μmol $^{12}CH_4$/g coal/day. Between day 15 and 84, the unamended coal treatment had a $^{12}CH_4$ production rate of 0.3±0.1 μmol $^{12}CH_4$/g coal/day. This methane production rate is not representative of the highest rate of methane production for the unamended coal treatment. Instead, the maximum methane production rate for the unamended coal treatment occurred between day 71 and 287 and was 0.7±0.2 μmol $^{12}CH_4$/g coal/day. Comparing the maximum methane production rates, coal treatments amended with 0.05-0.5 g/L had statistically similar $^{12}CH_4$ production rates that were greater than the 0.01 g/L coal treatment and the unamended coal treatment ($p<0.05$). The coal

Table 2.4: Maximum $^{12}CH_4$ and total CH_4 production rate for amended and unamended coal treatments.

Treatment	$^{12}CH_4$ Rate (μmol $^{12}CH_4$/g coal/day)	Total CH_4 Rate (μmol CH_4/g coal/day)
0.5 g/L coal	3.4±0.1	4.0±0.1
0.1 g/L coal	3.2±0.1	3.4±0.1
0.05 g/L coal	3.4±0.1	3.4±0.1
0.01 g/L coal	2.1±1.0	2.1±1.0
unamended coal	0.7±0.2	0.7±0.2

treatment amended with 0.01 g/L algae also had a higher methane production rate than the unamended coal treatment ($p<0.05$), but it was not as high as the higher amendment concentration treatments (Chapter Specific Supplementary Information, Table S2.6). Increased $^{12}CH_4$ production rates and a decreased production lag time in ^{13}C-algae amended treatments suggests that algal amendment may provide key growth nutrients for coal-degrading organisms that are absent in unamended coal systems.

Discussion

Challenges to conventional CBM extraction include the production of large volumes of low-quality water and limited well lifespans. Techniques to increase methane production in these wells, while simultaneously recycling and treating water, may increase the economic viability of CBM extraction as traditionally coal-dependent communities look for new opportunities to utilize this resource. Enhancement of *in-situ* coalbed methane production using organic amendments has been evaluated previously and preliminary results suggest that organic amendments can increase methane production rate and decrease production lag time [23, 24]. However, the optimum

concentration of amendment has not been evaluated, both in terms of maintaining productive coal degrading microbial populations and cost.

Total methane production increased when ^{13}C-algal amendment was added to coal treatments at concentrations greater than or equal to 0.05 g/L. Methane production rates increased and methane production lag times decreased upon adding algal amendment at concentrations greater than 0.01 g/L compared to unamended coal treatments. Above an amendment concentration of 0.05 g/L, the methane production rate did not significantly increase with increasing amendment concentration, suggesting that above this concentration coal-to-methane conversion is not statistically significantly enhanced. At amendment concentrations between 0.01 g/L to 0.1 g/L, more methane was produced in amended coal treatments than could be explained by direct amendment conversion, suggesting that algal amendment enhances coal to methane conversion, which is consistent with previous studies [24]. Because methane production rates do not increase proportionally to amendment concentration and at the highest amendment concentration (0.5 g/L) there was not explicit evidence of coal-to-methane enhancement (Figure 2.3), the algal amendment is most likely providing key nutrients and carbon for microbial growth, resulting in an increase in microbial biomass, specifically for coal degrading microorganisms. This is supported by lower $^{13}CH_4/^{12}CH_4$ and $^{13}CO_2/^{12}CO_2$ ratios in treatments with amendment concentrations between 0.01-0.1 g/L compared to 0.5 g/L. High $^{13}CH_4/^{12}CH_4$ and $^{13}CO_2/^{12}CO_2$ ratios in the 0.5 g/L treatment suggests that the improvement in methane yield for this treatment relative to the lower amendment concentrations is most likely the result of direct amendment-methane conversion. Total $^{12}CH_4$ production and $^{12}CH_4$ production rate were not different between the 0.05-0.5 g/L coal treatments, providing further evidence that any improvement in methane yield or rate for the 0.5 g/L coal treatment was not from increased coal conversion.

Total CH_4 production mirrored $^{12}CH_4$ production in amended treatments, regardless of amendment concentration, suggesting that the increase in methane production rate and decrease

in production lag time is not due to direct amendment conversion but instead enhanced coal degradation. The degradation and fermentation of the coal geopolymer to methanogenic substrates is the rate-limiting step in the coal-methane pathway [52]. Due to the recalcitrant nature of the coal, the organisms responsible for catalyzing the rate-limiting step are likely energy limited and can maintain cellular viability through the turnover of biomass, as seen in other subsurface environments [53]. Biosynthesis is energetically expensive [54] and for this reason, organisms under energy-limitations that minimize the rate of repair and replacement of biomolecules will significantly decrease their energy expenditure [53]. The introduction of small amounts of algal amendment may provide enough energy for these organisms to increase biosynthesis above their basal minimum, increasing the amount of biomass or activity responsible for coal degradation.

While direct amendment conversion results in additional methane production, it may come at the expense of shifting microbial communities away from coal degrading organisms [24], which may negatively impact long term methane production. Amending *in-situ* coalbed microbial communities with algal biomass can only be considered a viable CBM production stimulation strategy if true enhanced coal-to-methane conversion is demonstrated and if algal biomass is utilized efficiently and economically. Total amendment-to-gas conversion can provide an estimate of how much algal biomass is being converted to gas products. After accounting for $^{13}CH_4$ and $^{13}CO_2$ that may have come from coal, amendment-to-gas conversion ranged from 28.9-46.8%, with no discernable differences in amendment-to-gas conversion between amendment concentrations. This suggests that the same fraction of amendment is converted to gas products regardless of concentration and that >50% of the carbon from the algal biomass amendment ends up in dissolved organic or inorganic carbon, adsorbed to the coal substrate, converted to microbial biomass, or might be not converted at all.

Limited increases in methane production rates and yields at high amendment concentrations, as well as comparable amendment-to-gas conversions, suggest that amendment concentrations should be minimized. In this study, it has been shown that decreasing amendment concentration by 50% (i.e. from 0.1 g/L to 0.05 g/L) did not have a significant effect on total methane yield or rate, or on $^{12}CH_4$ yield or rate, highlighting that the small addition of key growth nutrients enhances coal conversion. This decrease in amendment concentration may result in small reagent cost reductions, which will be beneficial for performing CBM enhancement at scale. By reducing the amount of injected biomass, more may be available for the production of other value-added products, such as biofuels and bioplastics, improving the economics of the system as a whole. Additionally, rapid initial increases in percentages of $^{13}CH_4$ in amended GB treatments suggest that amendment is being utilized by the microbial community. In the absence of oxygen or other external electron acceptors, methane is the final product of the metabolisms necessary to produce microbial biomass. As a result, the detection of $^{13}CH_4$ and $^{13}CO_2$ suggests that the algal amendment is providing key nutrients for microbial growth that in turn enhances coal degradation. The gradual decrease in the fraction of $^{13}CH_4$ after the initial spike suggests that methane is being produced from alternative, unlabeled substrates such as CO_2 via hydrogenotrophic methanogenesis or microbial biomass turnover. Davis et al. (2018) showed that the methanogenic community after 111 days in 0.1 g/L algae amended GB microcosms had high relative abundance of the genus *Methanoregula*, a presumed hydrogenotrophic methanogen, which is consistent with the long-term decrease in $^{13}CH_4$ presented here. Hydrogenotrophic methanogenesis has been reported to be the predominant methanogenesis pathway *in-situ* [18, 23, 24, 38, 55], so the long-term enrichment of hydrogenotrophic organisms due to algal amendment most likely will not impact *in-situ* methane production negatively.

The economic viability of MeCBM by the addition of an algal amendment would be improved by optimizing the amount of algal amendment that is added. The results presented here

suggest that similar improvements in coal degradation occur when reducing the amount of amendment to 10 or even 2% of the originally attempted 0.5 g/L amendment. By adding a small amount of algal amendment, peak methane production occurs approximately 169-203 days earlier than in unamended coal systems. Considering the time-value of money, decreasing production time at this magnitude will increase economic viability of field scale operations. Furthermore, it has been shown that coal-to-methane conversion efficiency decreases after the repeated addition of 0.1 g/L ^{13}C-algal amendment due to an apparent metabolic shift to direct amendment conversion [26]. Economically, repeated stimulation would be advantageous due to the capital and labor costs associated with growing and injecting amendments. Decreasing the amendment concentration from 0.1 g/L to 0.01 g/L may prevent or at least reduce this microbial metabolic shift and make the repeated addition of algal amendment a viable field enhancement strategy, especially when considering groundwater recharge and microbial turnover.

Conclusions

The research presented in this study expands on the current body of knowledge surrounding the effect of algal amendment concentration on enhanced coalbed methane production. It was determined that increasing amendment concentration does not result in proportional increases in methane yield or production rate, which is consistent with previous studies. Furthermore, improvement in methane production from enhanced coal degradation did not increase upon increasing amendment conversion above 0.05 g/L, providing evidence that significant cost reductions can be achieved without a loss in productivity by decreasing amendment concentration. This research provides an improved understanding of MeCBM production using photosynthetically produced biomass and the optimization of associated costs. In light of the significant reduction in biomass required for enhanced methane production, a re-

examination of previously investigated techniques such as repeated algal amendment is warranted at lower amendment concentrations.

Chapter Specific Supplementary Information

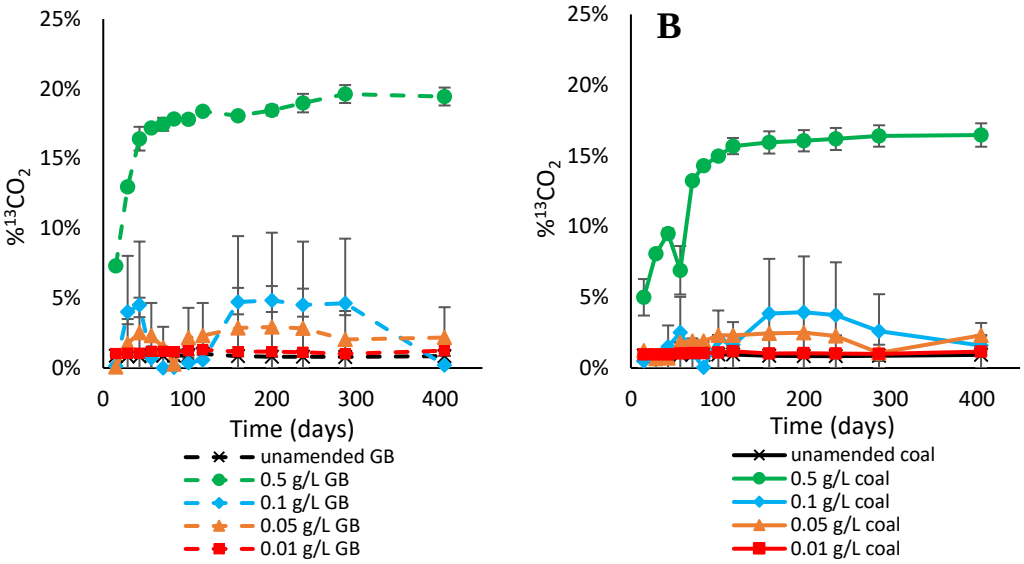

Figure S2.1: Percent of headspace carbon dioxide that is $^{13}CO_2$ over the course of the 405-day study for (A) ^{13}C-algae amended GB treatments and (B) ^{13}C-algae amended coal treatments. Error bars represent one standard deviation of triplicate measurements.

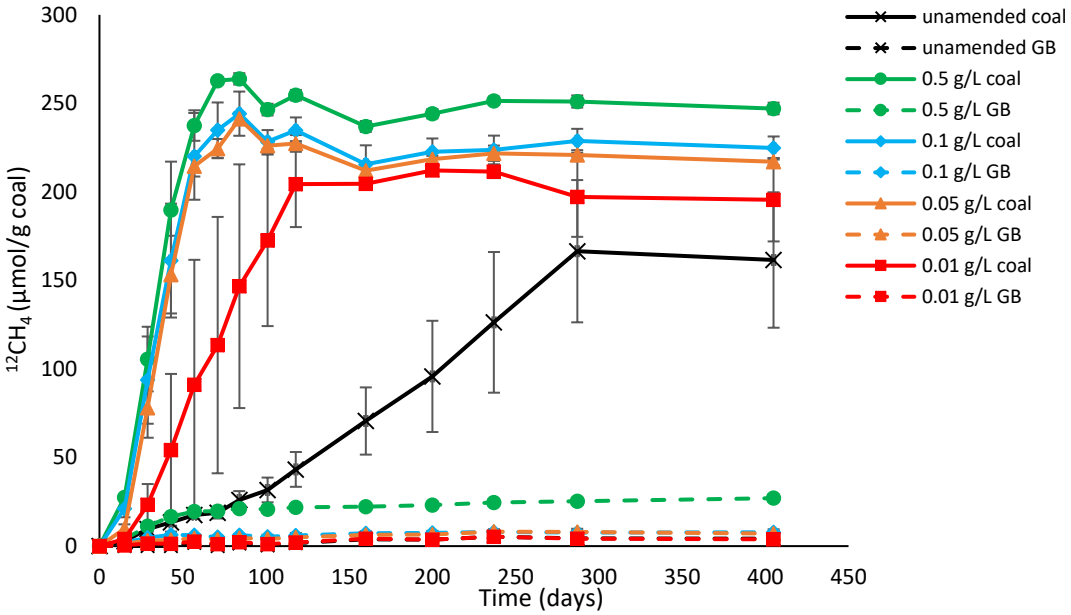

Figure S2.2: $^{12}CH_4$ produced for ^{13}C-algae amended coal and GB treatments versus time over the course of the 405-day study. All treatments have 1g of solid substrate (coal or GB). Error bars represent one standard deviation of triplicate measurements.

Table S2.1:Tukey pairwise comparisons from the Generalized Linear Model comparing cumulative CH_4 production (µmol CH_4/g coal) considering amendment concentration and substrate type. Means that do not share a letter are significantly different.

Treatment	N	Mean	Grouping			
0.50 g/L coal	3	295.451	A			
0.10 g/L coal	6	235.633		B		
0.05 g/L coal	3	224.362		B		
0.01 g/L coal	3	199.172		B	C	
0.00 g/L coal	6	163.683			C	
0.50 g/L GB	3	63.001				D
0.10 g/L GB	3	14.116				D E
0.05 g/L GB	3	10.313				D E
0.01 g/L GB	3	4.536				E
0.00 g/L GB	3	4.240				E

Table S2.2: Tukey pairwise comparisons from the Generalized Linear Model comparing maximum CH_4 production rate (μmol CH_4/g coal/day) considering amendment concentration and substrate type. Means that do not share a letter are significantly different.

Treatment	N	Mean	Grouping		
0.50 g/L coal	3	4.01050	A		
0.05 g/L coal	3	3.44116	A		
0.10 g/L coal	6	3.36627	A		
0.01 g/L coal	3	2.09494		B	
0.50 g/L GB	3	0.74084			C
0.00 g/L coal	6	0.54267			C
0.10 g/L GB	3	0.12868			C
0.05 g/L GB	3	0.08424			C
0.01 g/L GB	3	0.03216			C
0.00 g/L GB	3	0.02144			C

Table S2.3: Tukey pairwise comparisons from the Generalized Linear Model comparing conversion of ^{13}C-algal amendment to CH_4 considering amendment concentration and substrate type. Means that do not share a letter are significantly different.

Treatment	N	Mean	Grouping
0.01 g/L coal	3	0.427317	A
0.05 g/L coal	3	0.300735	A
0.50 g/L coal	3	0.269638	A
0.10 g/L coal	6	0.254507	A
0.50 g/L GB	3	0.209665	A
0.05 g/L GB	3	0.188523	A
0.10 g/L GB	3	0.182312	A
0.01 g/L GB	3	0.173513	A

Table S2.4: Tukey pairwise comparisons from the Generalized Linear Model comparing conversion of ^{13}C-algal amendment to CO_2 considering amendment concentration and substrate type. Means that do not share a letter are significantly different.

Treatment	N	Mean	Grouping				
0.50 g/L coal	3	0.0733255	A				
0.50 g/L GB	3	0.0656512	A	B			
0.05 g/L Coal	3	0.0539922	A	B	C		
0.01 g/L GB	3	0.0470124		B	C		
0.01 g/L Coal	3	0.0406953			C	D	
0.05 g/L GB	3	0.0342551			C	D	E
0.10 g/L Coal	6	0.0243146				D	E
0.10 g/L GB	3	0.0146198					E

Table S2.5: Tukey pairwise comparisons from the Generalized Linear Model comparing conversion of ^{13}C-algal amendment to headspace CH_4 and CO_2 considering amendment concentration and substrate type. Means that do not share a letter are significantly different.

Treatment	N	Mean	Grouping
0.01 g/L coal	3	0.468012	A
0.05 g/L coal	3	0.354727	A
0.50 g/L coal	3	0.342963	A
0.10 g/L coal	6	0.278822	A
0.50 g/L GB	3	0.275316	A
0.05 g/L GB	3	0.222778	A
0.01 g/L GB	3	0.220525	A
0.10 g/L GB	3	0.196932	A

Table S2.6: Tukey pairwise comparisons from the Generalized Linear Model comparing maximum $^{12}CH_4$ production rate (μmol $^{12}CH_4$/g coal/day) considering amendment concentration and substrate type. Means that do not share a letter are significantly different.

Treatment	N	Mean	Grouping		
0.50 g/L coal	3	3.42620	A		
0.05 g/L coal	3	3.35532	A		
0.10 g/L coal	6	3.23292	A		
0.01 g/L coal	3	2.07003		B	
0.00 g/L coal	6	0.53874			C
0.50 g/L GB	3	0.25218			C
0.10 g/L GB	3	0.05882			C
0.05 g/L GB	3	0.04865			C
0.01 g/L GB	3	0.02703			C
0.00 g/L GB	3	0.02133			C

CHAPTER THREE

ALGAL AMENDMENT ENHANCES BIOGENIC METHANE PRODUCTION FROM COALS OF DIFFERENT THERMAL MATURITY

Contribution of Authors and Co-Authors

Manuscript in Chapter 3

Author: George A. Platt

Contributions: Designed and Performed experimental work, analyzed data. Wrote and revised manuscript.

Co-Author: Katherine J. Davis

Contributions: Contributed to experimental design. Contributed to the revision and contents of manuscript with comments and feedback.

Co-Author: Elliott P. Barnhart

Contributions: Contributed to experimental design. Contributed to the revision of the manuscript with comments and feedback.

Co-Author: Hannah D. Schweitzer

Contributions: Performed sequencing for microbial community analysis. Contributed to microbial data analysis.

Co-Author: Heidi J. Smith

Contributions: Performed sequencing for microbial community analysis. Contributed to microbial data analysis.

Co-Author: Matthew W. Fields

Contributions: Contributed to the revision of the manuscript with comments and feedback.

Co-Author: Robin Gerlach

Contributions: Contributed to data analysis. Contributed to the writing and revision of the manuscript with comments and feedback.

Manuscript Information

Platt, G.P., Davis, K.J., Schweitzer, H.D., Smith, H.J., Barnhart, E.P., Fields, M.W., Gerlach, R.

International Journal of Coal Geology

Status of Manuscript:
_X__ Prepared for submission to a peer-reviewed journal
____ Officially submitted to a peer-reviewed journal
____ Accepted by a peer-reviewed journal
____ Published in a peer-reviewed journal

Elsevier

Abstract

Increasing coal rank, the degree of coalification resulting from thermal maturation often quantified by vitrinite reflectance, is thought to negatively affect biogenic coal-to-methane conversion due to a proposed decrease in organic matter bioavailability. The study presented here shows that significant quantities of methane can be produced from coals with a range of thermal maturity using a coal-derived microbial consortium. Methane production from five coals ranging in rank from lignite to low-volatile bituminous coal were evaluated in batch microcosms. Additional microcosms of each coal rank received 0.1 g/L algal biomass to evaluate the effectiveness of organic amendment addition across a range of thermal maturity. Cumulative methane production and methane production rate were generally highest in low rank, subbituminous coals, but no clear association between increasing vitrinite reflectance and decreasing methane production could be determined. The addition of algal amendment resulted in maximum methane production rates that occurred up to 37 days earlier and decreased the time required to reach maximum methane production by 17-19 days. Algae-amended, high rank coal treatments produced comparable amounts of methane to unamended low rank coal treatments, providing evidence that the methane production can be increased in high rank coals to be competitive with low rank coals. Microbial community analysis revealed that archaeal populations were significantly correlated with methane production rate, vitrinite reflectance, percent volatile matter, and fixed carbon, all of which are related to coal rank and composition. Lignite and subbituminous microcosms had high relative abundances of sequences indicative of organisms from the genus *Methanosaeta*, while low-volatile bituminous microcosms had low relative abundance of these sequences, suggesting low rank coals promote acetoclastic methanogenesis. Amended treatments that had significant increases in methane production relative to unamended analogs had high relative abundances of sequences indicative of the

archaeal genus *Methanobacterium*, commonly associated with hydrogenotrophic methanogenesis, and the bacterial family *Pseudomonadaceae*, which contains known hydrocarbon degrading and biosurfactant producing organisms. These results suggest that when algal amendment is most effective at increasing methane production, a shift in microbial community composition towards coal-degrading bacteria and CO_2-reducing methanogens occurs.

Introduction

As the world transitions away from high carbon emitting fossil fuels towards cleaner energy sources, coal reserves may no longer be mined to the current extent, presenting economic challenges for communities that have previously relied on this resource. The utilization of coalbed methane (CBM) can stimulate economic growth in coal-dependent regions of the world and address growing concerns surrounding emissions by providing a lower emissions natural gas fuel instead of coal. Biogenic CBM is produced from the activity of *in-situ* microbial communities that catalyze the conversion of coal to methane in shallow coal beds [18, 19, 23, 38, 40, 46, 55]. However, there are conflicting reports on how coal characteristics promote or inhibit this process.

Rank is one defining characteristic of coal that describes the level of physical and chemical transformation of the organic matter, which is a result of thermal maturation [56-59]. As organic matter is coalified, plant components of similar chemical composition transition into predicable subunits called macerals. Upon burial and geothermal heating, each maceral of the three major maceral groups (inertinite, liptinite, and vitrinite) undergoes unique geochemical changes controlled by vegetation type, Eh, and pH that target specific organic chemistries [57]. The origin of inertinite is somewhat controversial. Scott and Glasspool (2007) argue that inertinite is charcoal formed by wildfire[60], while Hower et al. (2009) hypothesize that is formed from the biological decomposition of plant material and the oxidation of other macerals [61].

Liptinite originates from hydrogen rich plant and algal materials, while vitrinite is the result of the geochemical transformation of humic substances in herbaceous tissues, such as plant roots, leaves, and stems [62]. As coal rank increases, the aromatic structure of vitrinite macerals undergoes ring condensation that results in a shiny appearance [20, 63, 64]. As a result, vitrinite reflectance (R_o), the percent of incident light that is reflected from the surface of these vitrinite macerals, is commonly used as a measure of rank and maturity. Although no physical parameter perfectly explains thermal maturity, vitrinite reflectance does not depend on coal composition or mineral matter, making it a pseudo-independent coal parameter [57].

Coal rank is designated –from lowest to highest– as lignite, subbituminous, bituminous, and anthracite [57]. It is commonly assumed that the bioavailability of the recalcitrant coal organic matter decreases with rank increases due to the loss of heteroatoms such as oxygen, sulfur, and nitrogen, along with the condensation of the aromatic lignin-derived structures to higher order polyaromatic sheets [20, 27, 28, 65]. However, this claim has also been contested by multiple studies [27, 30]. Fallgren et al. (2013) suggests that methane production increases with coal rank when enrichments were set up in microcosms using coal samples from Argonne National Laboratory's Premium Coal Sample Program [27]. In contrast, Wawrik et al (2012) found no correlation between coal rank and methane production when enrichments were prepared using coal samples from the Upper Cretaceous Fruitland Coal Formation in the San Juan Basin [30] However, a meta-analysis of published biogenic methanogenesis rates supported an increase in methanogenesis as rank decreased [20], and an enrichment study using fourteen coals of different rank as the sole carbon source showed a significant increase in methane production as rank decreased due to an increase in low molecular weight acids desorbing from the coal and increased bioavailability[28]. These studies draw conflicting conclusions but were ascertained using different enrichment methods. As a result, there is still uncertainty regarding the correlation between rank and biogenic methane production, if one exists at all.

In addition to understanding how coal rank affects biogenic methane production, the feasibility of microbially enhanced coalbed methane (MeCBM) production needs to be explored across diverse coal geologies before it can be utilized commercially across a wide range of coal basins. One such MeCBM technique is the addition of an organic amendment, such as algal biomass, to *in-situ* microbial communities in order to provide essential nutrients and additional substrates to enhance coal dependent methane production [19, 23, 26]. To the authors' knowledge, the addition of an organic amendment to stimulate methane production in high rank, low methane producing coals has yet to be evaluated. If effective, stimulating methane production from high ranked coals will allow more coal reserves to be utilized while mitigating some of the negative consequences associated with traditional extraction techniques. The study presented here aims to assess the relationship between coal rank and microbial methane production and the feasibility of organic amendment addition to stimulate methane production across different coal ranks.

Methods

Coal Sample Collection and Processing

Coal samples were obtained from the Argonne National Laboratory's Premium Coal Sample Program (Argonne, IL, USA). The location, rank, and collection date for each coal sample are shown in Table 3.1. The collection and processing methods for these coals are detailed in Vorres et al. (1990) [66]. To summarize, the lignite sample was collected from the Beulah-Zap coal seam in the Williston Basin (North Dakota, USA). The seam was approximately 18 feet thick at the collection area and collection was done by accumulating core samples spaced approximately 20' apart[66].

Table 3.1: Coal samples of different ranks used in this study. Sample locations and collection dates from Vorres et al. (1990).

Sample ID	Coal Source	State	ASTM Rank	Collection Year
Lignite	Beulah-Zap	North Dakota	Lignite	1986
SubC	Flowers-Goodale	Montana	Subbituminous C	2013
SubB	Wyodak Anderson	Wyoming	Subbituminous B	1985
HV Bit (Pittsburgh)	Pittsburgh #8	Pennsylvania	High Volatile Bituminous	1986
HV Bit (Stockton)	Lewiston-Stockton	West Virginia	High Volatile Bituminous	1986
LV Bit	Pocahontas #3	Virginia	Low Volatile Bituminous	1986

One high volatile bituminous coal sample was collected from the Lewiston-Stockton seam of the Kanawha formation about 20 miles east of Charleston, West Virginia, while the other was obtained from the Pittsburgh #8 seam approximately 60 miles south of Pittsburgh, Pennsylvania. Both collection sites had a seam thickness of 6’ [66]. The low volatile bituminous coal sample was collected from the Pocahontas #3 seam in Buchanan County, Virginia, and the seam thickness was 6’. The subbituminous B coal sample was collected from the Wyodak-Anderson seam approximately 6 miles northeast of Gillette, WY. The seam was approximately 120’ thick at the collection site and the sample used for processing consisted of a 6” core spanning the thickness of the seam [66]. In addition to the Argon samples, a subbituminous C coal sample was collected from the Flowers-Goodale (FG) seam in the Powder River Basin in Rosebud County near Birney, Montana. Core samples from a well designated FGP-13 were extruded into a wooden trough and cleaned to remove drilling fluids. Samples were transferred to a disposable glove bag filled with N_2 where the exposed outer core was removed [18]. Proximate and ultimate

analyses of the coal samples from the Argonne National Laboratory's Premium Coal Sample Program [66] and the Flowers-Goodale subbituminous C sample can be found in Table 3.2. FG proximate and ultimate analysis was obtained from Barnhart et al. (2016) [18]. All analyses were determined on a dry weight basis, except for percent hydrogen, which is reported on a dry, mineral-matter free basis, and heating value, which is reported on an as-received basis.

Table 3.2: Elemental and Proximate analyses of each coal sample. The subbituminous C data for ash, sulfur, hydrogen, heating value, and volatile matter was obtained from supplementary information in Barnhart et al. 2016.

Sample ID	Ash (%)	Sulfur (%)	Fixed Carbon (%)	Hydrogen (%)	R_o (%)	VM (%)	Heating Value (BTU/lb)
Lignite	10.0	0.80	45.3	4.9	0.25	44.9	7454
SubC	7.4	0.26	53.6	6.6	0.40	39.2	8703
SubB	5.3	0.63	45.9	5.4	0.32	44.7	8426
HV Bit (Pittsburgh)	9.0	2.19	59.4	5.4	0.81	37.8	13404
HV Bit (Stockton)	20.0	0.71	53.5	5.4	0.89	30.2	11524
LV Bit	5.0	0.66	76.6	4.5	1.68	18.6	14926

Site and Sample Collection

All water and microbial samples were collected from the Birney Test Site, previously described by Barnhart et al. (2016), located near Birney, MT in the Powder River Basin (PRB) [18]. Formation water from the FG coal bed was obtained in June 2016. Water from the FG-09 well was collected in 6-gal plastic jugs after pumping two well volumes and rinsing the jugs twice with formation water before filling and storing them at 4°C until microcosm set up. Coal cores were collected during the July 2013 drilling of the FG monitoring (FGM-13) and FG pumping (FGP-13) wells. The 2-inch diameter cores were cut into approximately 12-inch long sections and placed in PVC tubes filled with formation water pumped from the FG-11 well, which accesses the same FG coal source and aquifer. The tubes were sealed with flexible rubber caps to allow room

for gas desorption. Microbial cultures were collected from the SS-13 well, which accesses the interface between the FG coal and the overlying sandstone, in September 2015 using the down-well samplers described by Barnhart et al. (2013) [38]. The slurry from the SS-13 sampler was added to a serum bottle prepared with 5g FG coal and 45 mL of filter sterilized, reduced formation water before being allowed to incubate at 21 ± 1^{o}C in the dark for 361 days prior to being used as inoculum for the microcosms described below.

Establishment of Enrichment Cultures

Coal samples received from the Argonne National Laboratory's Premium Coal Sample Program were stored in glass ampules and opened in the anaerobic chamber. The FG coal core (depth 384-385') was opened in the anaerobic chamber, where it was dried and crushed. Crushed coal was sieved to an effective size of less than 850 μm. 0.2 μm bottle top filtered formation water was sparged overnight with anoxic 5% CO_2 (balance of N_2) and treated with 1 mM sulfide ($Na_2S^{\bullet}9H_2O$) to remove residual oxygen. 1 mM resazurin was added to the reduced formation water as a redox indicator. Enrichment cultures were prepared in an anaerobic chamber by adding one gram of each coal sample to autoclaved Balch tubes. To obtain a final liquid culture volume of 10 mL, each microcosm received 1 mL of previously collected enrichment culture described above and a balance of prepared formation water. The tubes were sealed with autoclaved butyl rubber stoppers and aluminum crimps. Amended and unamended enrichments containing 1 mm borosilicate glass beads (GB) were set up as carbon-free substrate controls. For each coal treatment (each coal and glass beads), triplicate treatments were prepared and either amended with an organic amendment or remain unamended. The amendment, a microalgal (*Chlorella* sp. strain SLA-04) concentrate, was added to a final concentration of 0.1 g/L, as previously described [24]. Both amended and unamended enrichments were removed from the anaerobic chamber and

the headspace was replaced with a 5% CO_2 gas mixture (balance of N_2). Treatments were incubated in the dark at room temperature (21 ± 1°C) for the duration of the 116-day experiment.

Headspace Gas Measurements and Analysis

Headspace gases (CH_4 and CO_2) were analyzed using an SRI Instruments (Torrance, CA, USA) Model 8601 GC equipped with a thermal conductivity detector (TCD) interfaced with PeakSimple Chromatography software. Ultra-high purity helium carrier gas and a Supelco HayeSep-D packed stainless-steel column (6 feet x 1/8" O.D) were used for separation. 1 mL of headspace gas was sampled from each microcosm and manually injected with a carrier gas pressure of 8psi and the oven and TCD temperatures set to 40ºC and 150ºC, respectively. To prevent creating a negative pressure in the tubes, 1 mL of anoxic 5% CO_2 (balance N_2) was injected to replace the sample volume removed. Reactors were sampled approximately every 2 weeks for the duration of the 116-day experiment.

Microbial Community Analysis

On day 116, one replicate of each treatment was destructively sampled for DNA analysis, according to the protocol described in Davis et al. (2018) [24]. Briefly, the coal or GB and liquid fractions were separated by decanting the liquid fraction in a 15 mL Falcon conical centrifuge tube. The coal or GBs were transferred to separate 15 mL Falcon tubes. One mL of 10% sodium dodecyl sulfate (SDS) was added to each gram of coal or GBs and tubes were placed in a 70ºC water bath for 30 min. The liquid fraction was centrifuged and the supernatant decanted and discarded to leave approximately 2 mL with the pellet. Both sample fractions were stored at -80ºC until extraction. Just prior to the DNA extraction, the coal/SDS mixture was heated in a 70ºC water bath for an additional 30 minutes. Sample DNA was extracted using the FastDNA Spin Kit for Soil (MP Biomedical, Solon, OH) according the manufacturer's instructions with minor protocol changes, as reported in Davis et al. (2018). After extraction, the DNA was

prepared for PCR amplification using the OneStep™ PCR Clean Up (Zymo Research, Irvine, CA). Extracted DNA was quantified using a Qubit fluorometer and dsDNA HS Assay Kits (Thermo Fischer Scientific, Carlsbad, CA, USA). The 16S rRNA genes were PCR-amplified for 30 cycles with DreamTaq PCR Master Mix (Thermo Fischer Scientific, Carlsbad, CA, USA) and an annealing temperature of 55ºC for 30 s using the universal prokaryotic primers Pro341F (5'-CCTACGGGNBGCASCAG-3') and Pro805R (5'GACTACNVGGGTATCTAATCC-3'), which amplify the V4 region of the 16s rRNA gene of bacteria [67]. Additionally, the archaea specific primers 751F (– CCGACGGTGAGRGRYGAA) and 1204R (- TTMGGGGCATRCIKACCT) were used to amplify the 16S rRNA gene of archaea [68].

Amplicons were checked by agarose gel electrophoresis with GelRed DNA stains (Biotium, Freemont, CA, USA). Library preparation for Illumina MiSeq was carried out following Illumina's standard protocol "16S Metagenonic Sequencing Library Preparation" prior to being loaded for sequencing on the MiSeq v.3 platform (San Diego, CA, USA). To summarize, following PCR cleanup, purification, and indexing, DNA concentration was determined using PicoGreen stain (Quant-IT, Invitrogen, Carlsbad, CA, US). DNA concentrations were normalized and pooled with a 12.5% PhiX control library. Sequence reads were analyzed using the MiSeq standard operating procedure of the Mothur software package [69]. Forward and reverse reads were joined into contigs using QIIME [70]. The sequences were aligned using SILVA [71]. The aligned reads were quality filtered, chimeras were removed, and OTUs and phylotypes were classified with an 80% confidence using the RDP database [72, 73]. Mothur version 1.38.1 was used to calculate species richness using Inverse Simpson Index (Chapter Specific Supplementary Information, Table S3.1, Table S3.2).

Statistical Analysis

A Generalized Linear Model was fitted to the total amount methane produced, maximum methane production rate, total carbon dioxide production, and carbon dioxide production rate with a factor for coal sample (rank) and a factor for the presence or absence of algal amendment using the statistical software Minitab v.18. A p-value less than 0.05 was deemed to determine statistical significance. Microbial community statistical analyses were performed in R v3.5.3. Heatmaps of bacterial and archaeal relative abundances of combined OTUs based on phylotype at a minimum of 2.5% in at least one sample were generated using the CRAN packages Heatplus, Vegan, RColorBrewer, and ggplots. Principle Coordinate Analyses (PCoA) using Bray-Curtis Dissimilarity distances and non-transformed, combined OTU (based on phylotype) relative abundance (>2.5%) were used to explore differences in bacterial and archaeal community composition between enrichments. The environmental fitting function found in the CRAN package vegan was used to correlate community composition and coal sample metadata.

Results

Methane Production

Methane production was observed in all unamended enrichments, except for the negative control enrichment containing glass beads instead of coal (Figure 3.1A), suggesting that coal-to-methane conversion occurred in all coal samples. Methane production was first detected on day 38 in all unamended treatments. The duration of methane production varied among enrichments, with Lignite producing increasing amounts of methane until day 75, SubC until day 92, SubB until day 56, HV Bit (Pittsburgh) until day 75, HV Bit (Stockton) producing until day 75, and LV Bit until day 116. At the time of destructive sampling, cumulative methane production differed among enrichments. The unamended Lignite, SubC, SubB, HV Bit (Pittsburgh), HV Bit

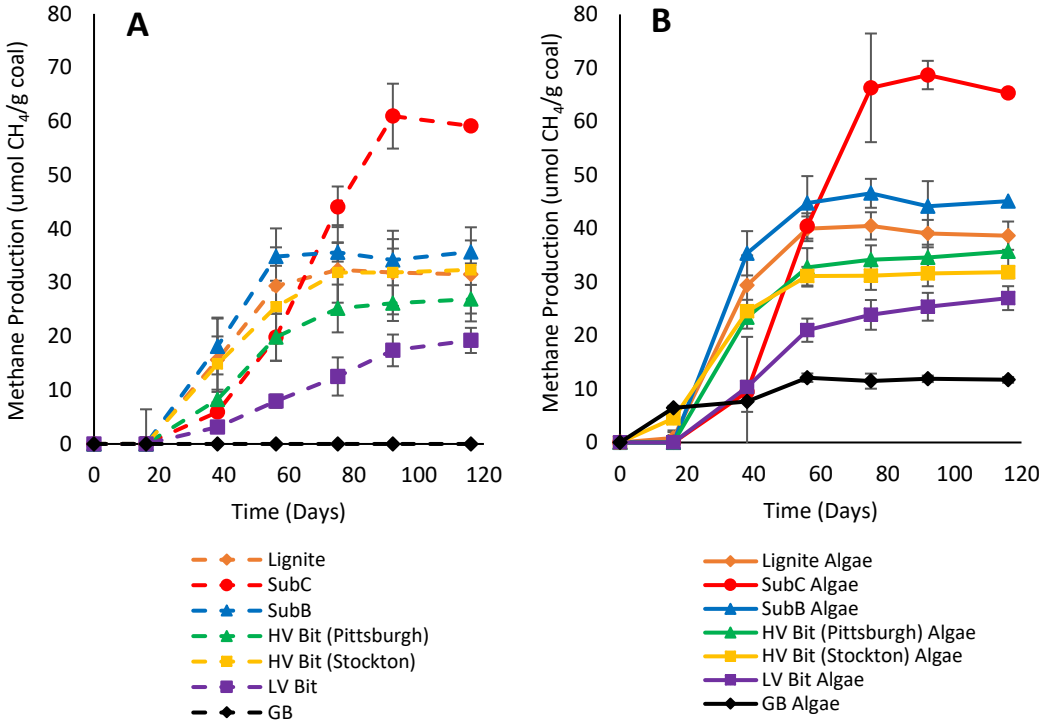

Figure 3.1: Methane production versus time for (A) unamended enrichment and (B) SLA-04 algae extract amended treatments. Algae extract was added to a final concentration of 0.1 g/L. Error bars represent one standard deviation and are smaller than the markers where not visible.

(Stockton), LV Bit, and GB enrichments produced 31.6±8.8 µmol CH_4/g coal, 59.2±6.0 µmol CH_4/g coal, 35.7±2.1 µmol CH_4/g coal, 26.9±2.7 µmol CH_4/g coal, 32.4±6.2 µmol CH_4/g coal, 19.3±2.3 µmol CH_4/g coal, and 0.0±0.0 µmol CH_4/g coal, respectively.

Methane was first detected in Lignite Algae and GB Algae on day 16. The remaining amended enrichments showed detectable methane production by day 38 (Figure 3.1B). The duration of methane production in algae amended treatments varied. For the Lignite Algae, SubC Algae, SubB Algae, HV Bit (Pittsburgh) Algae, HV Bit (Stockton) Algae, LV Bit Algae, and GB Algae, methane production appeared to cease on day 56, 75, 56, 56, 56, 56, and 116, respectively. At the end of the 116-day study, Lignite Algae, SubC Algae, SubB Algae, HV Bit (Pittsburgh), HV Bit (Stockton), LV Bit Algae, and GB Algae had produced 38.7±2.6 µmol CH_4/g coal,

65.3±2.7 µmol CH_4/g coal, 45.1±4.7 µmol CH_4/g coal, 35.7±3.1 µmol CH_4/g coal, 31.8±1.1 µmol CH_4/g coal, CH_4/g coal, 27.0±2.2 µmol CH_4/g coal, and 11.7±0.5 µmol CH_4/g coal, respectively.

All unamended coal enrichments except for the unamended LV Bit enrichment (p=0.56) produced more methane than the amended and unamended GB (p<0.05*)*, indicating that the microbial community was able to convert some fraction of the coal substrate to methane. Methane was not observed in the unamended GB treatment, indicating that methane production from dissolved organics in the inoculum was negligible and that the source of methane in coal- or amendment-containing treatments was from coal or algal amendment. Additionally, coal rank had a statistically significant effect on total methane production in both unamended and amended enrichments (p<0.05), although there was not an obvious statistical trend as vitrinite reflectance increased or decreased. For example, the highest rank coal evaluated in this study (LV Bit, R_O=1.68%) produced the lowest amount of methane considering only coal samples but grouped statistically with the lowest rank coal in this study (Lignite, R_O=0.25%). The amended and unamended subbituminous C samples (SubC Algae, SubC, R_O=0.40%) produced the highest amount of methane, as expected from a low rank coal. The remaining enrichments grouped statistically within these bounds, but without a strong correlation with vitrinite reflectance. A complete table of Tukey pairwise comparisons can be found in the Chapter Specific Supplementary Information, Table S3.4. The presence of algal amendment generally resulted in an increase in total methane production (p<0.05), suggesting that methane production can be stimulated in different ranks of coal. Controlling for coal sample, no pairwise comparison (amended vs. unamended) resulted in a statistically significant difference in total methane production (Figure 3.2). However, comparing amended high rank samples to unamended low rank samples, comparable methane production was achieved. For example, methane production in the amended low volatile bituminous sample (LV Bit Algae) grouped statistically with the unamended subbituminous B (SubB) enrichment and both unamended high volatile bituminous

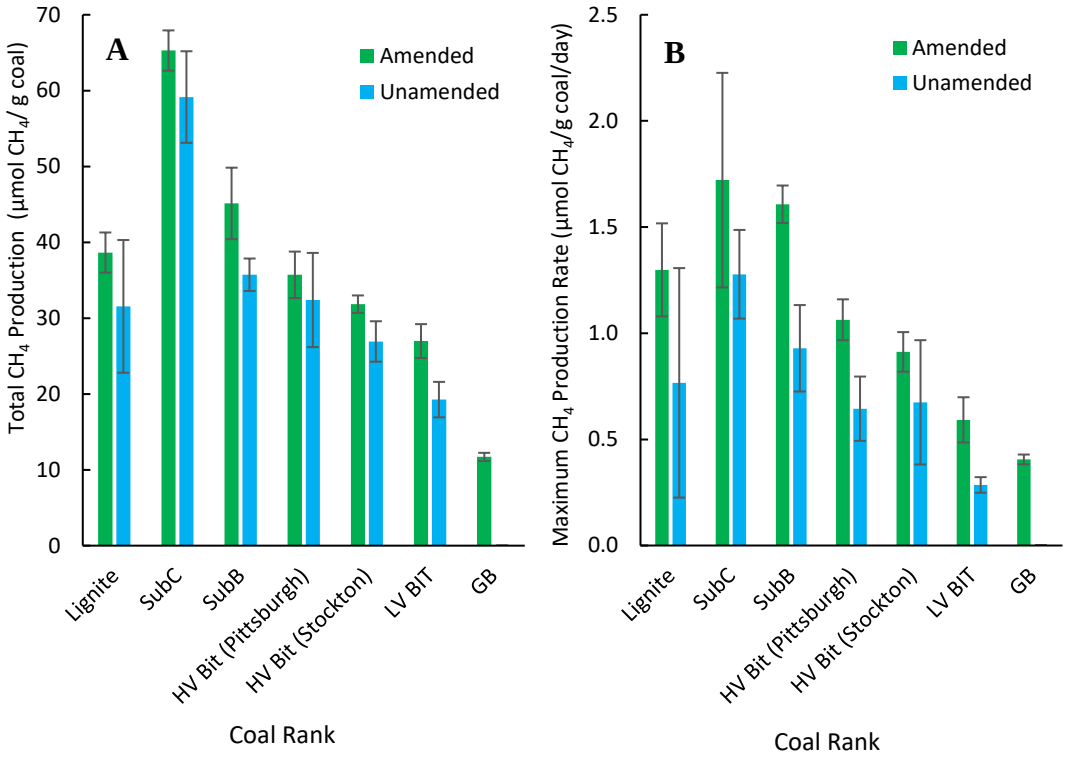

Figure 3.2: (A) Methane production for unamended enrichments and amended enrichments for coal seams of different rank and (B) Maximum methane production rate of coal rank for both amended and unamended enrichments. Maximum methane production rates occurred during different time intervals (see text), depending on the enrichment. Error bars represent one standard deviation.

enrichments (HV Bit (Stockton) and HV Bit (Pittsburgh)). This result suggests that the biogenic methane production potential of high rank coals can be increased to be competitive with lower rank coals by the addition of low amounts of algae or similar amendments.

Maximum methane production rates, and the time interval when they occurred, differed between coal enrichments. The maximum methane production rate for the unamended Lignite enrichment was 0.77±0.54 µmol CH_4/g coal/day between days 38 and 56. The maximum methane production rate for the unamended SubC and SubB enrichments were 1.28±0.21 µmol CH_4/g coal/day between day 56 and 75 and 0.93±0.20 µmol CH_4/g coal/day between day 38 and 56, respectively. The maximum methane production rates for the unamended high volatile

bituminous enrichments HV Bit (Pittsburgh) and HV Bit (Stockton) were 0.64±0.15 µmol CH_4/g coal/day between day 38 and 56 and 0.67±0.29 µmol CH_4/g coal/day, respectively. Lastly, the maximum methane production rate for the unamended low volatile bituminous enrichment, LV Bit, was 0.29±0.04 µmol CH_4/g coal/day between day 75 and 92. Coal rank had a statistically significant effect on maximum methane production rate (p<0.05), with the highest rank coal enrichment (LV Bit, R_O=1.68%) having the slowest methane production rate. However, a clear trend between increasing coal rank and methane production rate could not be determined.

The addition of algal amendment also had a statistically significant effect on methane production rate (p<0.05), with algae-amended treatments generally exhibiting greater methane production rates. Additionally, the effect of algal amendment on methane production rate did not depend on vitrinite reflectance (p=0.78), suggesting that algal amendment can stimulate methane production regardless of coal rank. Complete statistical analysis results and Tukey pairwise grouping can be found in Chapter Specific Supplementary Information, Table S3.5 The maximum methane production rate for the amended Lignite Algae enrichment was 1.30±0.22 µmol CH_4/g coal/day, occurring between day 16 and 38. The maximum methane production rate for the amended SubC Algae and SubB Algae enrichments were 1.72±0.51 µmol CH_4/g coal/day and 1.61±0.09 µmol CH_4/g coal/day, occurring between day 38 and 56 and day 16 and 38, respectively. The amended high volatile bituminous treatments, HV Bit (Pittsburgh) and HV Bit (Stockton), had maximum methane production rates of 1.06±0.10 µmol CH_4/g coal/day between day 16 and 38 and 0.91±0.09 µmol CH_4/g coal/day between day 16 and 38. Lastly, the maximum methane production rates for the amended LV Bit and amended GB Algae treatments were 0.59±0.11 µmol CH_4/g coal/day and 0.41±0.02 µmol CH_4/g coal/day, respectively. Notably, amended treatments had earlier maximum methane production rates compared to corresponding unamended treatments, except for the HV Bit (Stockton) treatments, which had maximum methane production rates between the same sampling days. Maximum methane production rates

in amended treatments were 18-37 days earlier and methane production leveled out 17-19 days earlier in Lignite Algae, SubC Algae, HV Bit (Pittsburgh) Algae and HV Bit (Stockton) Algae, suggesting that the presence of the algal amendment decreased the lag time before methane production in these treatments. The SubB Algae and LV Bit Algae ceased methane production approximately at the same time as the corresponding unamended treatments, but greater maximum methane production rates were observed ($p<0.05$). These results suggest that while final methane production may not increase, the addition of algal amendment can decrease lag times before methane production commences and can increase production rates across different coal ranks.

Carbon Dioxide Production and Consumption

Depending on the methanogenic pathway, inorganic carbon (CO_2) can be either a substrate or a product. Thus, the mass of CO_2 produced in the headspace of the enrichments was monitored for the duration of the experiment. Production of inorganic carbon in unamended enrichments was associated with coal rank ($p<0.05$), with subbituminous coals generally producing more CO_2 than bituminous coals. After accounting for CO_2 added during sampling, unamended Lignite, SubC, SubB, HV Bit (Pittsburgh), HV Bit (Stockton), LV Bit, and GB enrichments produced 1.1±1.7 µmol CO_2/g coal, 72.0±4.7 µmol CO_2/g coal, 15.2±2.6 µmol CO_2/g coal, 6.0±1.5 µmol CO_2/g coal, 3.6±5.6 µmol CO_2/g coal, 3.7±1.2 µmol CO_2/g coal, and -3.1±2.1 µmol CO_2/g coal, respectively by the end of the 116-day study. A "negative" production in the GB treatment headspace suggests that CO_2 was consumed. Because no methane was detected in this treatment, the consumption of CO_2 is likely the result of CO_2 dissolution into the aqueous phase and subsequent speciation into H_2CO_3, HCO_3^-, and CO_3^{2-} as opposed to hydrogenotrophic methanogenesis. While subbituminous coals generally produced more CO_2, the lignite treatment did not follow this trend, grouping more closely with the low volatile bituminous

coal (LV Bit). An increased production of inorganic carbon in the low rank coals suggests increased degradation of organic matter, which is supported by generally higher amount of methane production in these treatments.

Amended Lignite Algae, SubC Algae, SubB Algae, HV Bit (Pittsburgh) Algae, HV Bit (Stockton) Algae, LV Bit Algae, and GB Algae enrichments produced 4.6±0.3 µmol CO_2/g coal, 75.8±0.4 µmol CO_2/g coal, 23.6±3.5 µmol CO_2/g coal, 12.8±1.9 µmol CO_2/g coal, 12.6±2.7 µmol CO_2/g coal, 2.6±6.5 µmol CO_2/g coal, and 7.8±2.5 µmol CO_2/g coal, respectively. Once again, amended subbituminous enrichments produced more CO_2 than amended high volatile and low volatile bituminous samples. Consistent with the unamended lignite treatment, the amended lignite treatment did not group with the low rank coals and instead produced similar amounts of CO_2 as the higher rank bituminous coals. The effect of algal amendment on CO_2 production was significant (p<0.05), while the interaction between algal amendment and rank was not (p=0.29), suggesting that the effect of algal amendment does not depend on the rank of the coal sample. Controlling for coal sample, there were no instances in which algae-amended treatments produced significantly more CO_2 than analogous unamended treatments. Instead, amended bituminous enrichments produced similar amounts of CO_2 as unamended subbituminous and lignite enrichments, suggesting that the addition of algal amendment may increase coal degradation and methanogenesis to comparable levels of unamended low rank coals. A complete table of Tukey pairwise comparisons can be found in the Chapter Specific Supplementary Information, Table S3.6)

Maximum CO_2 production rates occurred between day 0-16 for the amended and unamended coal enrichments, except for the amended and unamended lignite sample, which had a maximum production rate between day 38 and 56, and the amended low volatile bituminous treatment (LV Bit Algae), which had a maximum production rate between day 56 and 75. Unamended Lignite, SubC, SubB, HV Bit (Pittsburgh), HV Bit (Stockton), LV Bit, and GB

enrichments produced 0.6±0.1 µmol CO_2/g coal/day, 3.3±0.2 µmol CO_2/g coal/day, 0.7±0.1 µmol CO_2/g coal/day, 0.3±0.1 µmol CO_2/g coal/day, 0.2±0.3 µmol CO_2/g coal/day, 0.2±0.1 µmol CO_2/g coal/day, and -0.4±0.0 µmol CO_2/g coal/day, respectively by the end of the 116-day study. Similarly, amended enrichments Lignite Algae, SubC Algae, SubB Algae, HV Bit (Pittsburgh) Algae, HV Bit (Stockton) Algae, LV Bit Algae, and GB Algae enrichments produced 0.2±0.2 µmol CO_2/g coal/day, 3.5±0.0 µmol CO_2/g coal/day, 1.1±0.2 µmol CO_2/g coal/day, 0.6±0.1 µmol CO_2/g coal/day, 0.6±0.1 µmol CO_2/g coal/day, 0.1±0.1 µmol CO_2/g coal/day, and 0.4±0.1 µmol CO_2/g coal/day, respectively. As with total CO_2 production, the maximum production rate was generally higher in subbituminous coals than in bituminous coals (Chapter Specific Supplementary Information, Table S3.7). Lignite treatments had maximum CO_2 production rates that occurred 40 days later than subbituminous and high volatile bituminous treatments and were closer in magnitude to the low volatile bituminous treatments. Once again, the effect of algae was statistically significant ($p<0.05$), with amended treatments generally having greater CO_2 production rates than the corresponding unamended treatments. The effect of algae on maximum CO_2 production rate was not dependent on the rank of coal ($p=0.20$), with the grouping of treatments generally mirroring total CO_2 production and methane production. In both amended and unamended coal enrichments, maximum CO_2 production rates occurred earlier than maximum methane production rates, except for the amended and unamended lignite treatments and the amended low volatile bituminous treatment. This result suggests that initial production of CO_2 may be the result of coal degradation as opposed to acetoclastic or methylotrophic methanogenesis.

Microbial Community Analysis

Characterization of Bacterial and Archaeal Community Composition:

Microbial community analysis revealed an average of 102±42 observed bacterial operation taxonomic units

(OTUs) and 144±69 observed archaeal OTUs among all sequenced coal treatments. Archaeal DNA from the SubC Algae treatment and both bacterial and archaeal DNA from the GB treatment was not successfully amplified, therefore these treatments were omitted from the following analyses. Sequences indicative of species found in the bacterial family Geobacteraceae were found in all enrichments at relative abundances (11-67%) with no apparent dependency on rank or presence of algal amendment (Figure 3.3). Sequences indicative of species found in the bacterial family Pseudomonadaceae (5-46%) were also present in all enrichments and were most abundant in both LV Bit and both SubB enrichments (39-46%) as compared to the other enrichments (5-29%). These enrichments, in addition to HV Bit (Pittsburgh) Algae, had less than 0.01% abundance of unclassified species from the candidate phylum Cloacamonas, while other enrichments had relative abundances as high as 15% (SubC) for this phylum. Sequences indicative of species found in the Syntrophaceae family, previously associated with the degradation of crude oil alkanes [74] were present in all enrichments at low relative abundance (1-9%).

Sequences indicative of species in the archaeal genera *Methanobacterium* (16-65%), *Methanosaeta* (14-50%), *Methanoregula* (2-37%), *Methanolobus* (2-10%) and *Methanospirillum* (5-22%) were found in all sequenced enrichments, indicating relatively homogenous archaeal populations in all enrichments (Figure 3.4). OTUs from the genus *Methanosaeta* had high relative abundance (41%-45%) in low rank coal enrichments (Lignite, Lignite Algae, SubB, and SubC) and low relative abundance (16%, 17%) in the highest rank enrichments (LV Bit, LV Bit Algae). The LV Bit Algae, HV Bit (Pittsburgh) Algae, and Sub B Algae enrichments all showed high relative abundance (52%-65%) of *Methanobacterium*, a genus associated with hydrogenotrophic methanogenesis [75] compared to other enrichments (16%-26%). These enrichments also had a lower relative abundance of *Methanosaeta* (17%-28%), a group of methanogenic archaea that have been described to produce methane from acetate [76]. Members of the genus

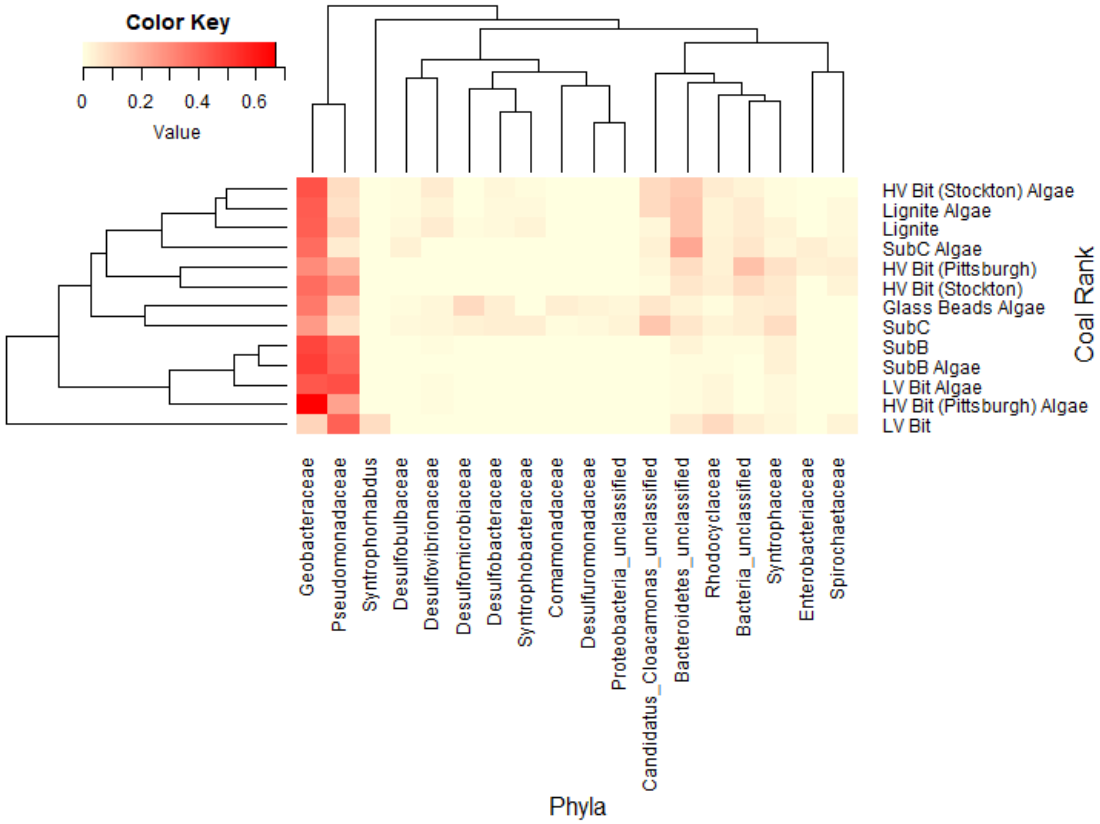

Figure 3.3: Heatmap of bacterial relative abundance of OTUs combined by phylotype. Phylotypes without a relative abundance of 2.5% in at least one sample were omitted.

Methanosarcina, which have been shown to utilize all three known methanogenesis pathways [77], were not found in any enrichments except LV Bit, which had a high relative abundance (28%) of this genus. The highest abundance of the genus *Methanoregula*, often associated with hydrogenotrophic methanogenesis [78], was found in the GB Algae enrichment (37%).

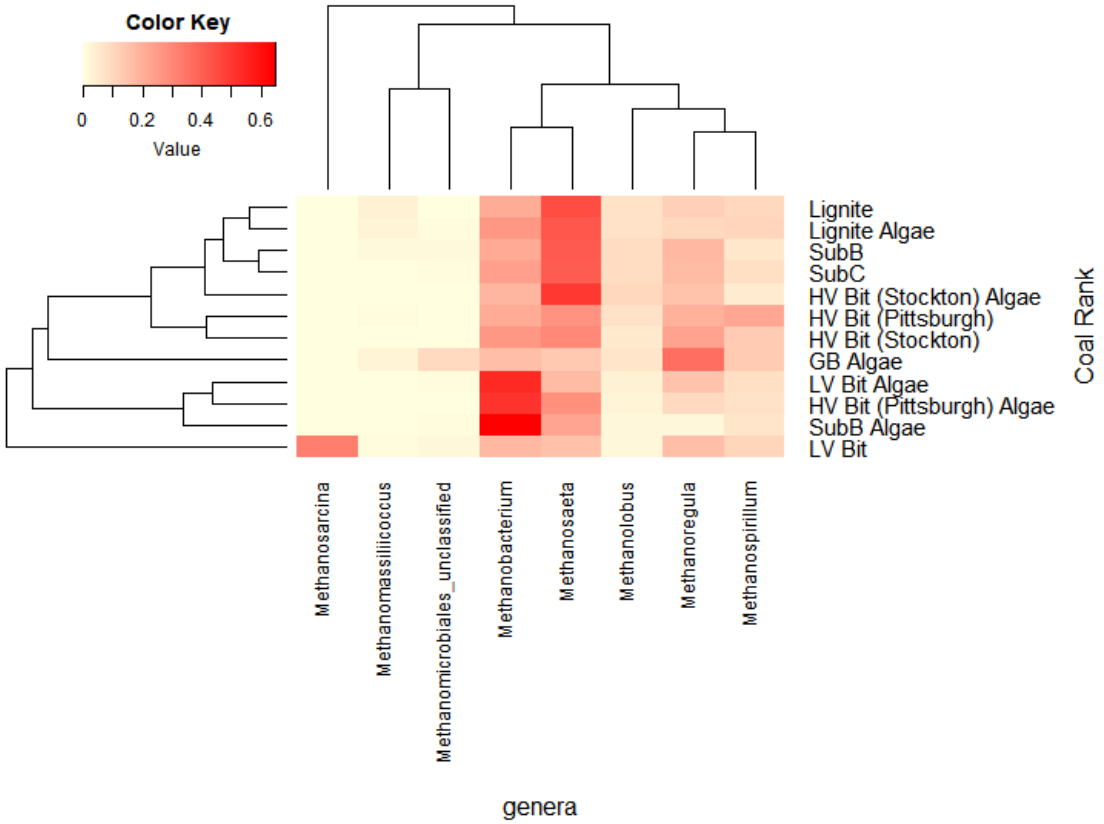

Figure 3.4: Heatmap of archaea relative abundance of OTUs combined by phylotype. Phylotypes without a relative abundance of 2.5% in at least one sample were omitted.

Microbial Community Composition and Coal Properties: Principal Coordinate Analyses (PCoA) were used to elucidate differences in bacterial and archaeal community composition between amended and unamended enrichments grown on coals of different thermal maturity (Figure 3.5, Figure 3.6). For the bacterial communities, no discernable clustering was apparent based on community composition alone. Based on the bacterial PCoA diagram (Figure 3.5), the amended SubC Algae, HV Bit (Stockton) Algae, HV Bit (Pittsburgh), and LV Bit Algae enrichments showed community composition shifts relative to their unamended analogs. A component of all shifts was along PCoA axis 2, which was correlated with OTUs from the family Geobacteraceae. The shift associated with the HV Bit (Stockton) Algae was also associated with a shift along PCoA 1, which was correlated with unclassified OTUs from the phylum

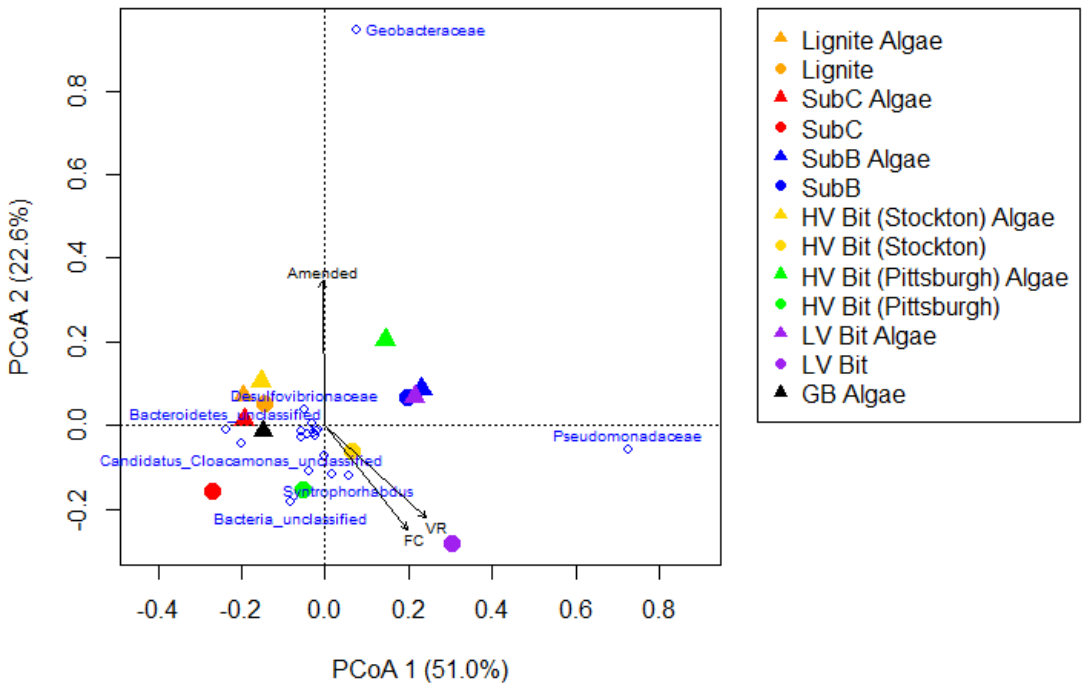

Figure 3.5: Principle Coordinate Analysis (PCoA) of non-transformed bacterial relative abundance based on OTUs combined by common phylotype with vectors representing significantly (or partially significant, $p<0.10$) correlated coal composition and gas production parameters.

Bacteroidetes and OTUs from the candidate phylum Cloacamonas. The shift associated with the HV Bit (Pittsburgh) Algae enrichment also contained a component in the positive PCoA axis 1 direction, associated with OTUs from the bacterial family Pseudomonadaceae. Environmental fitting with coal proximate and ultimate analysis and methane production revealed no significant correlations at the 95% confidence level. Weak correlations between bacterial community composition and the presence of algal amendment (Amended, $r^2=0.47$, $p=0.06$), vitrinite reflectance (R_o, $r^2=0.42$, $p=0.08$), and fixed carbon (FC, $r^2=0.39$, $p=0.10$) were observed. These results suggest that bacterial community composition may be affected by coal properties and the addition of algal amendment, but demonstrably significant correlations could not be verified.

PCoA analysis for archaeal community composition showed tight clustering of unamended enrichments apart from the unamended low volatile bituminous treatment (LV Bit). Similar to shifts in bacterial community composition, algal amendment resulted in significant shifts in archaeal community composition for the SubB, HV Bit (Pittsburgh), and LV Bit enrichments (Figure 3.6). This archaeal community shift appears to be associated with OTUs from the genus *Methanobacterium*, which is associated with hydrogenotrophic methanogenesis. Community composition for unamended enrichments was associated with OTUs from the genera *Methanolobus* and *Methanosaeta*, which have been described to generally be unable to reduce carbon dioxide in the presence of hydrogen and instead utilize methyl compounds [79] and acetate [76], respectively. Significant correlations were revealed between archaeal community composition and percent volatile matter (VM, $r^2 = 0.57$, p=0.05), fixed carbon (FC, $r^2 = 0.68$, p=0.02), vitrinite reflectance (VR, $r^2 = 0.65$, p=0.03), maximum methane production rate ($r^2 = 0.68$, p=0.01), the presence of algal amendment (Amended, $r^2 = 0.51$, p=0.04), and heating value (HV, $r^2 = 0.53$, p=0.05). Like the bacterial community composition, no correlation was found with total methane production, ash, sulfur, or hydrogen. Significant correlations between archaeal community composition and coal properties suggests that coal composition and rank affect the availability of intermediate substrates used for methanogenesis. Due to the syntrophic nature of coal-to-methane conversion, available intermediates for methanogenesis are also dependent on the ability of hydrolytic and fermentative bacteria to produce them.

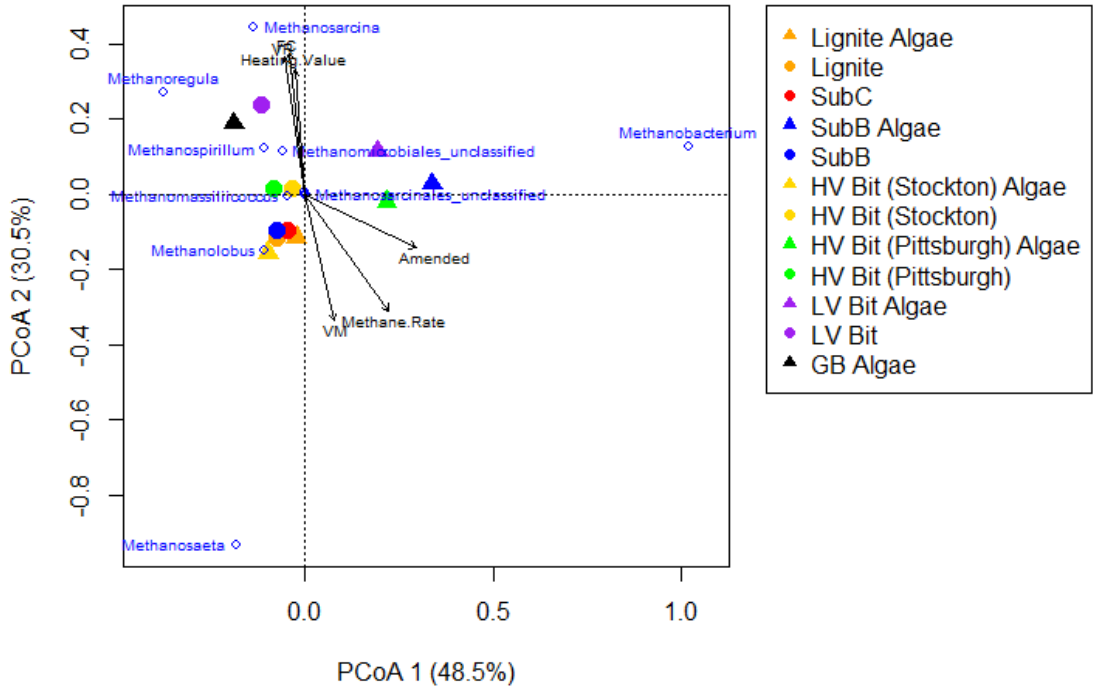

Figure 3.6: Principle Coordinate Analysis (PCoA) of non-transformed archaeal relative abundance based on OTUs combined by common phylotype with vectors representing significantly (or partially significant, $p<0.10$) correlated coal composition and gas production parameters.

Discussion

For MeCBM strategies to be commercially viable, it will be important to determine their effectiveness across a range of coal thermal maturity. While low rank coals are typically targeted for CBM production, enhancing methane production in higher rank coals may be necessary in order to fully utilize the in-ground resource and potentially the waste generated during mining and coal combustion pre-treatment. Enrichments amended with algae generally produced more methane and had higher methane production rates then unamended treatments, and enrichments amended with algae had earlier maximum methane production rates relative to their unamended

analogs. After amending with algae, the high ranked coals, like HV Bit (Stockton) and HV Bit (Pittsburgh), showed comparable amounts of headspace methane to lower rank coals such as the SubB and Lignite that were unamended, suggesting that amended high rank coals seams could be used as a concurrent source of methane in parallel with methane producing low rank coal seams. Previous studies have shown that adding algal amendment to coal enrichments stimulates methane production by enhancing coal degradation, likely by providing hydrolytic and fermentative bacteria with limiting nutrients [19, 23, 24, 26]. In this study, increased methane production could not be explicitly shown to be from enhanced coal degradation based on carbon mass balance analyses alone, suggesting that the microbial consortium may have converted amendment directly to methane. While enrichments amended with algae did not always exhibit an increase in total methane yield, they did show greater methane production rates and decreased lag times, which is important for commercial-scale applications and highlights the feasibility of stimulating methane production using an organic amendment across a range of coal ranks and thus coal basins.

This investigation provides the first results that indicate that coal-derived microbial communities can produce significant quantities of methane from many different ranks of coal, and that organisms capable of utilizing complex organic matter are involved in this process. It was found that coal rank has a significant effect on methane production, with subbituminous coals producing more methane than bituminous coals. These results are consistent with previous published studies [20, 28], but contradict a study conducted by Fallgren et al. (2013) [27], who used the same coal samples from the Argonne Premium Laboratory. Robbins et al. (2016) investigated methane production in enrichments inoculated with biomass from a wide range of organic substrate-degrading organisms (termite guts, digester fluid, koala feces, lake sediment, and CBM production water) using fourteen coals of different rank as the sole carbon source. When methane production leveled out after 50 days, Robbins et al. (2016) reported methane

yields from 0.2-26.4 μmol CH_4/g coal. These methane yields are comparable to the unamended yields observed in this study through 50 days (6.2-28.7 μmol CH_4/g coal), but generally lower than the yields observed in this study through 116 days (19.3-59.2 μmol CH_4/g coal).

Compared to Fallgren et al. (2013), the methane yields in this study through 60 days were 71.7% - 99.2% higher (Chapter Specific Supplementary Information, Table S3.3) and showed a negative correlation between increasing coal rank and methane production, apart from the lignite sample. The increase in methane yield in this study and the opposite trend may highlight the importance of coal-derived organisms associated with the degradation of the coal geopolymer. Fallgren et al. also used Argon coal samples but used a different methanogenic enrichment culture from coal formation water. There is evidence that the planktonic microbial community associated with coal formation water is not indicative of the coal-associated microbial community [55]. For this reason, the discrepancy between methane yields from the same coal samples may have been due to an absence of coal degrading organisms in the formation water culture. Our results suggest that the presence of a native, coal-derived microbial community may play a more influential role in coalbed methane production than coal rank, and that previous studies investigating the relationship between rank and methane production have likely underestimated the methane potential from high rank coals. Moving forward, to accurately predict *in-situ* methane production, coal-associated microbial communities should be used in laboratory studies, with care taken to mimic *in-situ* conditions.

Additionally, adsorption capacity is related to coal micropore structure development, which is dependent on coal rank and maceral composition [80]. In this study, the lignite coal deviated from the proposed methane-rank correlation. This deviation could be attributed to preferential methane sorption over CO_2 at low pressures [81, 82]. Busch et al. (2003) showed that the Beulah-Zap lignite coal used in this study had an extraordinarily high methane adsorption capacity relative to other lignite coals, suggesting that the coal-to-methane conversion of this

sample may have been consistent with expected methane production based on rank but was undetectable due to high adsorption capacity. In the low-pressure range, it is well documented that adsorption capacity increases with a decreasing amount of volatile matter and an increase in vitrinite reflectance, resulting in an increase in coal micro-porosity at higher rank [83, 84]. Because absolute and preferential CH_4/CO_2 adsorption changes with coal rank and maceral composition, the amount of biological methane produced from high rank coals in laboratory studies may need re-evaluation. Additionally, it has also been reported that microbial conversion of coal effects coal pore structure [85] and thus adsorption capacity, further complicating the issue. If the degree of microbial coal degradation is dependent on rank, so might changes in adsorption capacity.

Microbial community composition was found to be correlated with coal composition and the coal proximate analysis results. Bacterial community composition was dominated by sequences indicative of species from the families Geobacteraceae and Pseudomonadaceae. These microbial communities have previously been identified in other *in-situ* CBM investigations although the results presented here are the first to indicate they can remain dominant across the coal ranks investigated here [38, 55, 86-88]. Species from the family Geobacteraceae, well known for containing organisms capable of acetate and monoaromatic hydrocarbon oxidation, have previously been detected in coal mine deposits [87-90] and appear to play a role in the breakdown of complex organic matter. Members of the family Pseudomonadaceae, who are facultative anaerobes often capable of utilizing n-alkanes, polyaromatic hydrocarbons, and heterocyclic compounds, are indeed often associated with the hydrolysis of coal geopolymer hydrocarbons into bioavailable intermediates [91-94]. They are also well-known biosurfactant producers, which has been hypothesized to be an important enzymatic process involved in coal degradation [18, 86, 92, 95-97]. Although the mechanism of increased methane production could not be directly ascertained from observed methane yields and rates, the shift in bacterial populations towards

Pseudomonadaceae organisms in the most productive amended enrichments suggests that additional methane may be the result of enhanced coal hydrolysis rather than direct amendment conversion. This shift was not found in the GB Algae enrichment, further supporting the hypothesis that the presence of algae may have selected for coal degrading organisms in some enrichments. Furthermore, the enrichment of members of Pseudomonadaceae family in both subbituminous and low volatile bituminous treatments suggests that the addition of algal amendment can select for coal-degrading organisms in high and low rank coals, supporting the hypothesis that enhanced degradation of coal from low bioavailable coals is possible.

The archaeal communities in both amended and unamended enrichments were composed mostly of organisms from the genera *Methanobacterium*, *Methanosaeta*, *Methanoregula*, *Methanolobus* and *Methanospirillum*. Amended enrichments that resulted in the largest increase in methane production were enriched for *Methanobacterium*, a mesophilic hydrogenotrophic methanogen [75]. Interestingly, the amended GB enrichment did not cluster with these treatments (Figure 3.6) and instead was associated with high relative abundance of *Methanoregula*, also associated with hydrogenotrophy. This result suggests that organisms involved in enhanced coal-associated methanogenesis are different from those who produce methane via direct amendment conversion. Organisms from the genus *Methanosaeta* were more abundant in the low rank coal enrichments than higher rank enrichments, suggesting that the bioavailability of low rank coal promotes acetoclastic methanogenesis, which is consistent with previous coalbed stimulation results [44]. Furthermore, Robbins et al. (2016) suggested that the increase in methane production from low rank coals is directly related to higher acetate concentrations, which is consistent with the results of this study.

Archaeal communities were found to be correlated with percent volatile matter, vitrinite reflectance, fixed carbon, maximum methane production rate, and the presence of algal amendment (Figure 3.6), indicating a dependence on coal rank, coal composition, and algal

amendment. The significant correlation between archaeal community composition and the presence of algal amendment suggests that methanogens are more dependent on substrate availability than bacterial populations in these systems. Considering the enrichment of organisms from the bacterial family Pseudomonadaceae, the source of hydrogenotrophic methanogenesis substrates in amended treatments is likely from enhanced coal degradation. The enrichment of organisms previously shown to be capable of hydrogenotrophic methanogenesis is evidence that methane production in higher ranked coals can be stimulated, even with low *in-situ* acetate concentrations. Additionally, the limited abundance of acetoclastic methanogens in high rank coal enrichments may be explained by the high abundance of Geobacteraceae, who are known acetate scavengers when appropriate electron acceptors are available. It is possible that members of the family Geobacteraceae outcompete acetoclastic methanogens when acetate concentrations are low, providing another explanation for lower methane production in high rank coals.

Conclusions

The research presented in this study aims to clarify the relationship between biogenic methane production and coal rank. It was found that methane production is generally higher in subbituminous coals than in thermally mature bituminous coal. Importantly, this study shows that significant biogenic methane yields are possible from coals that were previously thought to have limited bioavailability, and that previously reported methane yields from high rank coals were likely an under-estimate due to the lack of an active coal-degrading microbial community. Furthermore, this study affirms the assertation that archaeal community and methanogenesis pathways are sensitive to coal rank, with low rank coals promoting acetoclastic methanogenesis, as previously reported. This study re-examined the biogenic methane yield from previously investigated coals and found significantly higher methane yields, highlighting the importance of using coal-associated, *in-situ* microbial consortia in laboratory studies in order to potentially more

accurately predict biogenic methane potential, which is crucial for CBM exploration and field scale-up. Additionally, it was determined that the addition of algal amendment can enhance methane production rates and decrease lag times until the onset of methane production across a variety of coal ranks by shifting microbial communities towards known hydrocarbon degrading organisms that have previously been identified in coal environments. This result expands the viability of this stimulation technique to previously overlooked CBM resources. Further investigation is needed to describe the mechanisms of MeCBM production in high rank coals to ensure field-scale feasibility.

Chapter Specific Supplementary Information

Table S3.1: Archaeal species richness using Inverse Simpson Index of sequenced coal samples.

Coal Sample	Number of Sequences	Coverage	Observed OTUs	Chao	Inverse Simpson
Lignite Algae	32785	0.999603	165	167	9.5
Lignite	47278	0.99981	211	212	10.3
SubC	18778	0.999148	111	115	9.1
SubB Algae	404	0.987624	23	26	3.7
SubB	39756	0.999698	260	261	10.6
HV Bit (Stockton) Algae	59073	0.999865	196	197	8.7
HV Bit (Stockton)	14431	0.998961	105	109	9.9
HV Bit (Pittsburgh) Algae	7764	0.99781	68	78	6.0
HV Bit (Pittsburgh)	42878	0.999813	176	177	11.9
LV Bit Algae	10408	0.998751	69	75	5.5
LV Bit	26580	0.999586	161	162	8.3
GB Algae	28622	0.999441	190	192	12.4
Sequencing Control	4	0.75	2	2	2.0

Table S3.2: Bacterial species richness using Inverse Simpson Index of sequenced coal samples.

Coal Sample	Number of Sequences	Coverage	Observed OTUs	Chao	Inverse Simpson
SubC Algae	26970	0.999852	151	151	4.7
SubC	30070	0.999834	182	182	7.4
SubB Algae	20928	0.999857	45	46	3.0
SubB	20652	0.999806	83	83	2.3
HV Bit (Stockton) Algae	16921	0.999645	104	105	3.5
HV Bit (Stockton)	7973	0.999749	81	81	3.5
HV Bit (Pittsburgh) Algae	36917	0.999946	89	89	1.8
HV Bit (Pittsburgh)	7883	0.999239	83	84	5.5
LV Bit Algae	44695	0.999911	102	102	2.4
LV Bit	4520	0.999115	96	96	8.4
GB Algae	19763	0.999848	110	110	5.7
Sequencing Control	36851	1.000000	18	18	1.5

Table S3.3: Methane yield in headspace through 60 days of incubation. Percent difference is calculated as the difference between the observed methane yield and the observed methane yield in Fallgren et al., 2013 for the same coal samples.

Coal Rank	Platt (this study) (μmol CH_4/g coal)	Fallgren et al. (2013) (μmol CH_4/g coal)	Percent Difference
Lignite	29.39	0.24	99.2
SubC	24.40	-	-
SubB	34.27	0.38	98.9
HV Bit (Stockton)	26.28	-	-
HV Bit (Pittsburgh)	20.53	1.41	93.1
LV Bit	8.72	2.47	71.7

Table S3.4: Tukey Pairwise Comparisons from Generalized Linear Model comparing cumulative CH_4 production (μmol CH_4/g coal) considering amendment condition and coal rank. Means that do not share a letter are significantly different.

Treatment	N	Mean	Grouping				
SubC Algae	3	65.2883	A				
SubC	3	59.1528	A				
SubB Algae	3	45.1272		B			
Lignite Algae	3	38.6500		B	C		
SubB	3	35.7184		B	C		
HV Bit (Pittsburgh) Algae	3	35.7121		B	C		
HV Bit (Stockton)	3	32.3924			C		
HV Bit (Stockton) Algae	3	31.8380			C		
Lignite	3	31.5495			C		
LV Bit Algae	3	26.9764			C	D	
HV Bit (Pittsburgh)	3	26.9232			C	D	
LV Bit	3	19.2581				D	E
GB Algae	3	11.7026					E F
GB	3	0.0000					F

Table S3.5: Tukey pairwise comparisons from Generalized Linear Model comparing coal rank. Means that do not share a letter are significantly different.

Treatment	N	Mean	Grouping					
SubC Algae	3	1.72108	A					
SubB Algae	3	1.60735	A	B				
Lignite Algae	3	1.29841	A	B	C			
SubC	3	1.27764	A	B	C			
HV Bit (Pittsburgh) Algae	3	1.06343	A	B	C	D		
SubB	3	0.92906		B	C	D	E	
HV Bit (Stockton) Algae	3	0.91194		B	C	D	E	
Lignite	3	0.76619			C	D	E	
HV Bit (Stockton)	3	0.67441			C	D	E	F
HV Bit (Pittsburgh)	3	0.64437			C	D	E	F
LV Bit Algae	3	0.59193			C	D	E	F
GB Algae	3	0.40550				D	E	F
LV Bit	3	0.28540					E	F
GB	3	0.00000						F

Table S3.6: Tukey pairwise comparisons from Generalized Linear Model comparing cumulative CO_2 production (μmol CO_2/g coal) considering amendment condition and coal rank. Means that do not share a letter are significantly different.

Treatment	N	Mean	Grouping			
SubC Algae	3	75.8366	A			
SubC	3	71.9528	A			
SubB Algae	3	23.6338		B		
SubB	3	15.1586		B	C	
HV Bit (Pittsburgh) Algae	3	12.7888		B	C	D
HV Bit (Stockton) Algae	3	12.5944		B	C	D
GB Algae	3	7.8076			C	D	E
HV Bit (Pittsburgh) Algae	3	6.0129			C	D	E
Lignite Algae	3	4.6446			C	D	E
LV Bit	3	3.6965			C	D	E
HV Bit (Stockton)	3	3.5477			C	D	E
LV Bit Algae	3	2.5888				D	E
Lignite	3	1.1087				D	E
GB	3	-3.1177					E

Table S3.7: Tukey Pairwise Comparisons from Generalized Linear Model comparing maximum CO_2 production rate (μmol CO_2/g coal/day) considering amendment condition and coal rank. Means that do not share a letter are significantly different.

Treatment	N	Mean	Grouping			
SubC Algae	3	3.44847	A			
SubC	3	3.27046	A			
SubB Algae	3	1.11503		B		
SubB	3	0.70846		B	C	
HV Bit (Pittsburgh) Algae	3	0.61349		B	C	D
HV Bit (Stockton) Algae	3	0.60235		B	C	D
GB Algae	3	0.35883			C	D	E
HV Bit (Pittsburgh)	3	0.27709			C	D	E
Lignite Algae	3	0.19060			C	D	E
LV Bit	3	0.15502			C	D	E
HV Bit (Stockton)	3	0.15483			C	D	E
LV Bit Algae	3	0.09988				D	E
Lignite	3	0.03722				D	E
GB	3	-0.15739					E

CHAPTER FOUR

CONCLUSIONS, FUTURE WORK, AND IMPLICATIONS

Conclusions

This thesis builds on the body of work evaluating the feasibility and effectiveness of stimulating *in-situ* microbial coal-to-methane conversion by amending CBM systems with algal biomass. In summary, it was demonstrated that the addition of algal amendment at concentrations as low as 0.01 g/L improved microbial coal-to-methane kinetics relative to unamended systems. Additionally, biogenic methane potential from coals of different thermal maturity using a coal-derived microbial consortium were shown to be significantly higher than previously reported studies, suggesting that coals previously deemed bio-unavailable are capable of bioconversion when a coal adapted microbial community is used. Furthermore, it was demonstrated that the addition of algal amendment to high rank, thermally mature coals increases methane yields to levels comparable to those achieved from unamended lower rank coals. Lastly, the feasibility of catalyzing coal-to-methane conversion using bioelectrochemical means was evaluated in MEC reactors, and it was demonstrated that coal-derived microorganisms have the potential to utilize solid electrodes as terminal electron acceptors.

In Chapter Two, it was determined that amendment concentration can be reduced significantly and still achieve demonstrable enhanced coal degradation, resulting in improved methane production rates and decreased lag times. The addition of 0.05 g/L algal amendment, a 50% reduction relative to previously investigated concentrations, results in equivalent maximum methane production rates and equivalent time required to reach maximum cumulative methane production. The addition of 0.01 g/L algal amendment, still resulted in improved methane

production kinetics relative to unamended systems, with maximum methane production occurring 169 days earlier. Considering the time-value of money, improving methane production rates with the small addition of algal amendment may improve the economic feasibility of field scale application. Furthermore, $^{12}CH_4$ data and carbon mass balances showed that at the lowest amendment concentrations tested to date (0.01-0.05 g/L), improvements in methane production kinetics were due to enhanced coal degradation as opposed to direct amendment conversion, suggesting that algal amendment is likely targeting hydrolytic and fermentative bacteria responsible for the initial degradation of the coal geopolymer. This result provides additional evidence that adding small amounts of algal amendment will not result in microbial community shifts away from coal-degrading organisms. Lastly, the knowledge that a 10-fold reduction in algal amendment still results in improved methane production kinetics suggests that recently investigated strategies such as repeated amendment addition may be more viable than previously thought.

In Chapter Three, it was demonstrated that significant biogenic methane yields from thermally mature (high rank) coals are possible when using a coal-derived and -adapted microbial consortium. Subbituminous coals generally produced more methane than higher ranked bituminous coals, suggesting that coal rank affects biogenic methane production and the methanogenesis pathway. Lignite and subbituminous coals tended to promote the enrichment of microbial community members previously described to be associated with acetoclastic methanogenesis, while bituminous coals had higher relative abundance of methanogens associated with hydrogenotrophic methanogenesis. Bacterial community composition did not have a clear dependency on coal rank and known hydrocarbon degrading bacteria were detected in all coal microcosms. Algae amended high rank coal microcosms produced similar amounts of methane and had similar methane production rates compared to unamended low rank coals, suggesting that algal amendment can increase coal-to-methane conversion potential in thermally

mature coals, increasing the potential scope of this technology. Additionally, algal amendment decreased methane production lag times across the range of thermal maturity, providing evidence that the addition of algal amendment for enhanced CBM production has promise in coal basins throughout the U.S.

Finally, in Appendix A, PRB coal-derived microrganisms were shown to be electroactive in Microbial Electrolysis Cells (MECs) fed with coal substrate. Produced current and Confocal Laser-Scanning Microscopy (CLSM) SYBR Green images in these systems demonstrated that putative exoelectrogens present in the microbial community were able to utilize coal hydrolysis and fermentation products to transfer electrons directly to solid electrodes. Additionally, cathodic hydrogen evolution followed by methane production in some coal-fed MEC treatments suggests that protons produced during coal-degradation were reduced at the MEC cathode and utilized by hydrogenotrophic methanogens. An overall insignificant effect of applied voltage on methane recovery, low current density, and low cathodic reduction efficiency indicates exoelectrogens and/or electrotrophs were substrate- or diffusion-limited and that more research focusing on electrode design is warranted before this technique can be shown to be a viable option for CBM enhancement.

Future Work

To continue progress towards field-scale application of microbially enhanced CBM techniques, additional research should focus on addressing the injection and transport of algal amendment in coal seams, and how algal amendment addition effects coal microstructure. Post-cultivation processing of algal amendment may influence injection strategies due to additional transport considerations. The optimization of algae injection, groundwater infiltration, and coal seam transmissivity will need to be coordinated in order to maximize effectiveness. Additionally, algal amendment was demonstrated to enhance coal degradation, suggesting that coal

microstructure may change. Because most of the *in-situ* produced gases are adsorbed to the coal geopolymer and held in place by hydrostatic pressure, gas adsorption likely will be affected, having downstream implications on gas-in-place (GIP), dewatering techniques, and repeated stimulation attempts. Furthermore, if changes in coal microstructure due to increased microbial degradation results in increased gas adsorption, the potential for re-using these coal seams for CO_2 sequestration may increase after extractable methane is depleted.

Additional field-relevant research should focus on the addition of algal amendment to different coal systems using microbial consortia derived from those specific coal environments. Microbial community composition is crucial for coal degradation, and algal amendment may affect *in-situ* coal communities differently. Nutrient introduction from groundwater infiltration varies across CBM reservoirs, suggesting that the type of limiting substrate may vary basin to basin. Additionally, if signatures of secondary gas production from thermogenic coal intermediates are detected, the effect of algal amendment may change due to the *in-situ* microbial communities' adaptation to different coal-derived substrates. Fundamental research assessing key, active microbial community members in the presence of algal amendment across a range of coal basins will allow for better targeted CBM enhancement.

Implications

Anthropogenic atmospheric carbon emissions are causing rapid climate change that will pose challenges to our society economically, socially, and environmentally. The most recent climate reports suggest that a drastic reduction in greenhouse gas emissions in addition to carbon capture and sequestration (CCS) technology will be necessary in order to avoid irreversible societal harm from a changing climate. As a result, the utilization of high emissions fossil fuels such as coal will continue to decline, threatening economies dependent on this resource. The transition from coal to zero-carbon energy solutions will involve a period of increased natural gas

utilization. During this time, technical solutions should attempt to salvage the economic benefit and utilize the stored energy from soon-to-be underutilized coal reserves, paying specific attention to how these resources and existing infrastructure can contribute to the path towards sustainable energy and climate change solutions. One path forward includes the enhancement and utilization of CBM during the natural gas transition period and the simultaneous development of coal seam carbon sequestration technology. While energy production will -and should- transition to renewable, zero-emissions technologies, it is likely that greenhouse gas emissions from manufacturing, agriculture, and chemical industries will still need to be mitigated. Consequently, microbially enhanced CBM production and subsequent coal seam CCS, along with an improved fundamental understanding of carbon cycling by terrestrial subsurface microbial communities, can play a pivotal role in short and long-term climate change solutions.

APPENDICES

APPENDIX A

EFFECT OF APPLIED VOLTAGE ON COAL TO METHANE CONVERSION AND COAL SEAM MICROBIAL COMMUNITIES

Motivation

Microbial electrolysis cells (MECs) are bioelectrochemical systems that utilize an applied voltage to polarize electrodes to provide favorable thermodynamic conditions for the oxidation of organic matter and the production of value-added products. MECs are emerging as a promising wastewater treatment technology because of their potential to turn traditionally energy-consuming unit operations into energy producers [31, 33, 98, 99]. In MECs, complex organic matter is degraded by anaerobic microorganisms and electrons are transferred directly to a conducting, positively charged anode by electro-active microorganisms known as exoelectrogens [100-105]. During the degradation and oxidation of available organic matter, protons are produced and diffuse to the negatively charge cathode, where they are reduced by the electrons transferred to the anode in the presence of an applied voltage, thus completing the circuit [31]. Hydrogen is typically the desired product in MECs because of the growth of the fuel cell market and other industries (such as petrochemical and fertilizer industries) that utilize H_2 as a feedstock [99]. Furthermore, at this time, hydrogen can be stored and transported more efficiently than electricity generated from decentralized, small-scale renewable sources such as solar and wind [106]. However, the microbial consortium in MECs that degrade complex waste streams often contain hydrogen and acetate utilizing methanogens [107-110]. At high hydrogen concentrations, the growth of hydrogenotrophic methanogens is favored [31, 111], resulting in hydrogen gas that is contaminated with methane. For this reason, it has been suggested that methane should be the target product in MECs [112-114]. As energy production shifts away from coal towards renewable resources, natural gas will be a crucial transition fuel due to lower carbon emissions per unit of energy produced and its ability to easily provide supplemental energy during periods of high electricity demand [11].

Coalbed methane is an unconventional source of biogenic natural gas that is produced by a consortium of anaerobic microorganisms that catalyze the conversion of coal to methane [18, 19, 40, 46, 52]. Due to the recalcitrant nature of coal, the rate of biogenic methane production *in-situ* is often too slow for commercial extraction using traditional dewatering techniques to be economically feasible based on the current natural gas market [19, 23, 24, 46, 115]. Attempts to enhance coal-to-methane conversion have focused on the addition of organic amendments targeting coal degrading organisms with limiting nutrients [23, 24, 26, 29, 44, 47, 115] and the addition of biosurfactants [86] and chemical oxidants [116, 117] to enhance bioavailability. Recently, MEC techniques have been proposed to increase coal-to-methane conversion by providing favorable thermodynamic conditions for the degradation of the coal geopolymer and to enhance the reduction of carbon dioxide to methane [34, 37, 118]. To date, the highest biogenic coal-to-methane yields have been produced by polarizing electrodes in MECs, subsequently enriching exoelectrogenic fermentative bacteria and electrotrophic methanogenic archaea that are able to transfer electrons to and from the polarized electrodes directly [37]. In this system, methane yields were orders of magnitude higher than organic amendment enhancement strategies [24, 44, 47]. The recent discovery that direct interspecies electron transfer (DIET) between electroactive microorganisms enhances methane production in anaerobic sludge digestion and other organic waste streams [112-114, 119-127] suggests that this technique may be a viable option to overcome the kinetic and thermodynamic limitations associated with coal degradation.

Background

Thermodynamics and Energy Efficiency

MECs provide favorable thermodynamic conditions for the degradation of organic matter and value-added product formation by supplementing the gap in required energy between microbial electrolysis (autotrophic production of hydrogen from water by photosynthetic bacteria

and algae) and pure electrochemical electrolysis by utilizing the stored chemical energy in organic material. Considering an MEC fed with acetate, a common organic fermentation product detected in coalbed methane systems, the desired reaction is the oxidation of acetate to hydrogen.

$$CH_3COO^- + 4H_2O \rightarrow 2HCO_3^- + H^+ + 4H_2 \qquad \text{Eq. A.1}$$

Under standard biological conditions (pH=7, T=25ºC, P=1 bar) the Gibbs Free Energy of reaction ($\Delta G_r^{\circ\prime}$) is +104.6 kJ/mol, implying that the oxidation of acetate is not thermodynamically spontaneous. To overcome this thermodynamic limitation, additional energy must be added to the system. In MECs, the additional energy required is supplied via the applied voltage. The additional energy required to drive the reaction forward must be greater than the standard reduction potential, E^o, of the reaction. The standard reduction potential is calculated using Equation 2:

$$E^o = \frac{-\Delta G_r^{\circ\prime}}{mF} \qquad \text{Eq. A.2}$$

where m is the amount of electrons (mol e^-) transferred in the reaction and F is Faraday's constant, F=96,485 C/mol e^-. For the oxidation of acetate under biologically relevant conditions, the standard reduction potential is -0.14 V. In theory, the input of 0.14 V will provide enough energy to drive the oxidation of acetate to hydrogen forward. In practice, the actual energy requirement is >0.4V due to internal losses in the system. Irreversible losses include anodic overpotentials (φ_A), cathodic overpotentials (φ_C), and Ohmic Loss (IR_Ω). Anodic and cathodic overpotential losses include those associated with bacterial metabolism, and all losses are a function of current (I). As a result, the actual applied energy required (E_{AP}) and the standard reduction potential are related by [31],

$$E_{AP} = E^o - (\sum \varphi_A + |\sum \varphi_C| + IR_\Omega) \qquad \text{Eq. A.3}$$

Including an external resistor in the MEC circuit to measure current adds an additional voltage loss to the system, $IR_{ext.}$ Therefore, the actual voltage applied over the anode and cathode is less

than the voltage sourced from the power source (E_{PS}). Because the additional resistance is in series with the rest of the MEC circuit, the applied voltage can easily be corrected by

$$E_{AP} = E_{PS} - IR_{ext} \quad \text{Eq. A.4}$$

Now that the voltage sourced from the power supply is defined, the work added to the system (W_E) can be shown to be

$$W_E = \sum_{i=1}^{n} (I_i E_{PS} \Delta t - I_i^2 R_{ext} \Delta t) \quad \text{Eq. A.5}$$

where I_i is the current (A) calculated from the voltage drop (V) across the external resistor (Ω). The work added to the system is measured over each time interval Δt (s) for *n* data points in the operating cycle. For small intervals in time, it is assumed the current, I_i, is constant within the interval.

The expected product yield based on the measured current and system efficiency relative to the electrical input and chemical energy stored in the substrate can now be determined. Assuming all electrons are converted into desired cathodic products (H_2), the theoretical yield of direct cathodic reduction, n_{CE}, can be determined by Eq. A.6 [31]

$$n_{CE} = \frac{\int_{t=0}^{t} Idt}{F m_{H_2}} \quad \text{Eq. A.6}$$

where m_{H_2} = 2 mol e^-/mol H_2, the number of electrons transferred from the cathode to produce one mole of hydrogen. It follows that the cathodic reduction efficiency can be determined by

$$r_{cat} = \frac{n_{H_2}}{n_{CE}} \quad \text{Eq. A.7}$$

where n_{H_2} is the actual number of moles of hydrogen recovered. Ideally, MEC design and operation will maximize r_{cat} while minimizing irreversible losses and electrical input (W_E).

Microbial Interactions and Electron Fate in Microbial Electrolysis Cells

MECs add an additional layer of complexity to the microbial interactions associated with the anaerobic degradation of complex organic matter. For example, the process of coal-to-methane conversion begins with the hydrolysis and fermentation of the recalcitrant geopolymer. The hydrolytic processes produce organic substrates such as polyaromatic hydrocarbons, monoaromatic carboxylic acids and long-chain fatty acids. Fermentative bacteria convert these substrates to short-chain volatile fatty acids, CO_2, H_2, and HS^-, which in turn are metabolized by acetogens to produce additional H_2 and acetate. Finally, hydrogenotrophic, acetoclastic, and methylotrophic methanogenic archaea utilize CO_2 and H_2, acetate, and C1-substrates, respectively, to produce CH_4. In MEC systems, fermentative and acetate-oxidizing exoelectrogens compete with non-electroactive organisms for substrates to produce electrical current. The complexity arises from the production and consumption of acetate and hydrogen in these systems. Homo-acetogens can reduce CO_2 in the presence of molecular hydrogen (generated from bioelectrochemical cathodic reduction or fermentation) to produce additional acetate, which can subsequently be consumed by exoelectrogens to produce additional current. This process, known as a current loop, suppresses MEC performance by generating current without value-added product recovery. Additionally, the reduction of protons and CO_2 can be catalyzed directly or indirectly by electrotrophic archaea at the cathode, producing hydrogen and methane in processes known as electrohydrogenesis and electromethanogenesis [121, 123, 124, 128, 129]. Because of the syntrophic nature of complex organic matter degradation and substrate competition, large bodies of work have been dedicated to studying the thermodynamics and kinetics of microbial metabolism in MECs to optimize performance [100, 101, 103, 130].

Objective

While recent bioelectrochemical coal-to-methane conversion research is promising, to the author's knowledge, the presence and viability of native, coal-associated electroactive microorganisms have yet to be demonstrated. Due to the economic and environmental costs associated with traditional surface coal mining, enhanced coalbed methane production via electromethanogenesis should be demonstrated to be viable under *in-situ* conditions. Previous MEC research has identified the presence of mesophilic, potentially electroactive organisms belonging to the bacterial families *Geobacteraceae, Desulfuromonadaceae* and archaeal families *Methanocalculaceae* and *Methanobacteriaceae* [131], all of which have been detected in coal environments [38, 55, 132]. Furthermore, organisms derived from subsurface anaerobic environments such as oil reservoirs and marine sediments have been shown to be electroactive [126], suggesting that these organisms may be present in terrestrial coal seams. This study seeks to build on recent work highlighting the feasibility of bioelectrochemically enhanced coal-to-methane conversion by investigating the performance of MECs loaded with subbituminous coal inoculated with coal-derived microorganisms and subsequent methane yields.

Methods

Site and Sample Collection

Coal, water, and microbial samples were collected from the previously described Birney Test Site, located near Birney, MT in the Powder River Basin (PRB) [38]. Formation water from the Flowers-Goodale (FG) coal bed was pumped and retrieved in October 2017 from the FG-09 well. After two well volumes were pumped and discarded, 6-gal plastic jugs were rinsed twice with formation water before being filled and stored at 4ºC prior to microcosm set up. Coal cores were collected during the July 2013 drilling of the Flowers-Goodale monitoring wells (FGM-13

and FGP-13). The 2-inch diameter cores were cut into approximately 12-inch long sections and placed in PVC tubes filled with formation water pumped from the FG-11 well. Microbial cultures were collected from the FG-11 well in October 2017 using a subsurface environmental sampler (SES) (Montana Emergent Technologies, Butte, MT, USA). Prior to field use, the SES was autoclaved and assembled in a Biosafety Cabinet. The SES was loaded with prepared FG coal and pressurized with 5% CO_2 (balance N_2) and transported to the field site. After cleaning the exterior surfaces with 70% ethanol, the SES was lowered down the FG-11 well, opened, and incubated at depth for 3 months. Upon returning to the field site in October 2017, the SES was closed at depth, - sealing the collected microbial sample from the stagnant well bore water and maintaining *in-situ* pressure - and brought to the surface, where it was immediately stored on ice for transport back to Montana State University. Ninety mL of collected slurry were removed from the FG-11 SES in an anaerobic chamber and aliquoted equally to serum bottles prepared with 5g FG coal and 45 mL of filter sterilized, reduced FG formation water before incubation at $21 \pm 1^{o}C$ in the dark for 12 months.

Reactor Construction and Setup

Single chamber MECs were fabricated with modifications as described in Call et al. (2011) [133]. MECs were constructed using 100 mL clear media bottles sealed with butyl rubber stoppers. Anodes were isomolded graphite plates with a thickness of 0.32 cm (Grade GM-10, Graphite Store, Northbrook, IL, USA), cut to dimensions of 5 cm (L) x 1.5 cm (W), providing a surface area of A_{AN}=19.2 cm^2. All Anodes were polished sequentially with 400 grit and 1500 grit sandpaper, sonicated to remove particulate debris, soaked in 1M HCl overnight, and rinsed three times with Milli-Q water. A hole was drilled using a #67 drill bit near the top center of the graphite anode to allow for electrical connection. Titanium wire (0.08 cm diameter, Grade 2; McMaster-Carr) was cut to 10 cm length and bent into a J-hook on one end. The J-hook was

inserted into the prepared hole in the graphite anode and crimped to create a secure electrical connection. The electrical connections between the wire and the graphite plate were checked and any electrodes with a contact resistance greater >1.0Ω were discarded. Similarly, cathodes of the same length and width were prepared from stainless steel mesh (Type 316, mesh size 100 x 100; McMaster-Carr). Cathodes were polished using 400 and 1500 grit sandpaper, rinsed three times with Milli-Q water, rinsed with 70% ethanol, and rinsed once more with Milli-Q. Based on the surface area of the individual wires, the surface area of the mesh cathode was approximately A_{CAT}=30 cm^2. Electrical connections were created as described above using stainless steel wire (Type 304, 0.08 cm diameter, McMaster-Carr) and checked for adequate contact resistances. The respective cathode and anode wires were pushed through butyl rubber stoppers and the electrode-stopper assemblies were inserted into the media bottles after the reactors were anoxically prepared with coal and FG formation water, as described below.

Reactor Inoculum and Media

All MEC reactors were set up in triplicate using anoxic techniques. The FG coal core (depth 384-385') was opened in an anaerobic glove bag, where it was dried and crushed. Crushed coal was sieved to an effective size range of 0.85-2.00 mm and UV sterilized for 30 min. One-mm diameter Borosilicate glass beads were autoclaved and used in lieu of coal to provide carbon-free substrate for controls. MECs were loaded with 10 g of prepared coal or GB. FG formation water was filtered with a 0.2 µm bottle top filter to remove particulate organic matter and sparged overnight with anoxic 5% CO_2 (balance of N_2). MECs were inoculated with 10 mL of previously collected FG enrichment consortium, and prepared formation water was added to obtain a final liquid culture volume of 100 mL. Uninoculated controls were setup in triplicate by omitting the FG enrichment consortium. A complete table of experimental treatments can be found in Table A.1

Table A.1: Summary of experimental treatments. Treatments without an applied voltage were not connected to the power supply and were used as unpolarized controls. All treatments had the same MEC reactor design including electrode-stopper assemblies.

Treatment	Substrate	Inoculum	E_{AP} (V)
F1	coal	FG Enrichment	1.0
F2	coal	FG Enrichment	0.0
F3	coal	-	1.0
G1	glass beads	FG Enrichment	1.0
G2	glass beads	FG Enrichment	0.0
G3	glass beads	-	1.0

Reactor Operation and Sampling

Immediately following inoculation, MECs were operated in parallel under an applied whole cell voltage of E_{AP}=1.0V using a direct current power supply (Model 2410, Keithly Instruments Inc., Beaverton, OR, USA). For parallel operation, two separate sets of test leads (positive and negative) were soldered together at one end, with one set connected to the positive terminal of the power supply and the second set to the negative power supply. Each positive test lead had a 10Ω resistor connected in series for recording the voltage produced by each reactor to calculate produced current using Ohm's law (I=V/R). To polarize the cells, the positive test leads were connected to the reactor anodes and the negative test leads were connected to the cathodes. Inoculated MECs with coal or GB were left unpolarized to be used as no applied voltage controls.

MEC headspace gases (CH_4, CO_2, and H_2) were analyzed approximately every 2 weeks. Headspace CH_4 and CO_2 was analyzed using an SRI Instruments (Torrance, CA, USA) Model 8601 GC equipped with a thermal conductivity detector (TCD) interfaced with PeakSimple Chromatography software. Ultra-high purity helium carrier gas and a Supelco HayeSep-D packed

stainless-steel column (6 feet x 1/8" O.D) were used for separation. One mL of headspace gas was sampled from each MEC and manually injected with a carrier gas pressure of 8 psi and the oven and TCD temperatures of 40ºC and 150ºC, respectively. Headspace H_2 was analyzed using an SRI Instruments (Torrance, CA, USA) Model 8601C Multi-Gas Column GC equipped with dual flame ionization (FID) and thermal conductivity (TCD) detectors interfaced with PeakSimple Chromatography software. Ultra-high purity nitrogen and three columns setup in multi-gas configuration, an 18' HayeSep-D precolumn, a 6' HayeSep D, and a 6' molecular sieve 5A column were used for separation. One mL of headspace gas was sampled from each MEC and manually injected with a carrier gas pressure of 13 psi, an oven temperature of 50ºC, a TCD temperature of 100ºC and an FID temperature of 300ºC. Both headspace gas samples were taken simultaneously and 2.0 mL of anoxic 5% CO_2 (balance N_2) was injected to replace the sample volume. The current produced from each reactor was analyzed by measuring the voltage across the 10Ω resistor wired in series on each positive lead using a handheld multimeter (MM600, Klein Tools, Lincolnshire, IL) prior to sampling headspace gases.

Confocal Microscopy Imaging and Electrode Biofilm Quantification

On day 149, all MECs were destructively sampled for confocal laser scanning microscopy (CLSM) imaging. Reactor electrode-stopper assemblies were removed, and electrodes were cut from their respective wires. Both the anodes and cathodes were cut into three pieces along the transverse plane. Two pieces were set aside for DNA extraction and PFA fixation. The remaining electrode pieces were dried and embedded in 1% (w/v) low-melt agarose (Bio-rad Laboratories, Hercules, CA, USA) and allowed to solidify for 20 min. Once solidified, the electrodes were dehydrated in an ethanol series (50%, 80%, 95%) for 1 min each and dried in an oven at 46ºC for 20 min. Embedded electrodes were stored at 4ºC until further processing. Embedded electrodes were placed in sterile petri dishes and stained with SYBR Green

(Invitrogen; Life Technologies, Carlsbad, CA, USA, 40X final concentration) in the dark for 20 min. After staining, embedded electrodes were rinsed with 0.2 μm filter sterilized DI water three times to remove excess stain. Embedded electrodes were imaged with a Leica TCS SP5 II upright confocal microscope (Wetzlar, Germany) using a 25X water immersion objective, 0.95 NA, WD 2.5mm. Fluorophore excitation lasers and emission bandwidths were as follows: SYBR Green (ex 497/em 520) 488 nm excitation, 500-550 nm emission collection; autofluorescence, 561 nm excitation, 580-700 nm emission collection; and reflection imaging, 488 nm excitation. A minimum of three randomly selected images were collected to enumerate cell biomass. Z-stacks were collected in 0.36-1.60 μm steps, depending on the image. Electrode biomass 3D structure was reconstructed from the CLSM images using IMARIS software (version 7.7.2). Biofilm volume (SYBR Green) and electrode surface area (reflection) for each channel imaged was determined using the volume and surface area calculation function in the IMARIS software. Volume and surface area calculation parameters were optimized to sample and image specific properties, maintaining consistency between replicates. SYBR Green images were smoothed at a surface area detail level of 1.18 μm^2, thresholding was based on the background subtraction method, and all voxels greater than 10 were collected. Calculated biomass volume was normalized to the surface area of the electrode surface (R_{VA}) in the corresponding field of view analyzed.

Results

Current Generation

In MECs, current is produced when strictly anaerobic, exoelectrogenic bacteria oxidize biodegradable organic matter and transfer electrons directly to the anode surface while releasing protons (H^+). Due to thermodynamic limitations, current generation must be forced by applying a

small voltage between the electrodes. The electrons produced by the oxidation of organic matter in addition to the electrons supplied by the power source is enough to overcome the thermodynamic energy barrier and reduce the produced protons at the cathode, producing hydrogen gas (H_2). By measuring current produced at the anode, the activity of exoelectrogenic bacteria can be assessed. In the inoculated, polarized coal treatment (F1), current increased immediately, with the fastest rate of current production occurring between day 19 and 34, suggesting that the activity of anode-associated microorganisms reached a maximum on day 34 (Figure A.1). On this day, 0.13±0.03 mA of current was generated from the anode. Current in this treatment decreased until day 98, suggesting that fermentative and exoelectrogenic bacteria had depleted the biodegradable fraction of the coal and therefore were unable to transfer electrons directly to the anode. Current was calculated using Ohm's law by measuring the voltage produced from each cell across a 10Ω resistor wired in series with the corresponding positive test lead.

Current in the uninoculated, polarized coal treatment (F3) remained around 0.02 mA until day 34 and then current rapidly increased until day 61, reaching a maximum 0.16±0.07 mA. While this treatment was uninoculated, microorganisms likely were introduced with the coal substrate despite UV pretreatment. The generation of current suggests these organisms were able to use the anode as a terminal electron acceptor once substrates were available for anode-associated exoelectrogens. The peak in current generation occurred 30 days after the inoculated, polarized, coal treatment, providing evidence that the rate of coal degradation was significantly depressed without the presence of the FG enrichment culture. After day 61, current decreased until day 128, where it stabilized at 0.04±0.01 mA. The presence of low, stable current at the end of the study suggests electrons were still being transferred to the anode and that coal oxidation was still occurring at the time of destructive sampling. The maximum current density (current normalized to anode surface area) achieved over the course of the 148-day study in the F1 and F3 treatments was 0.07±0.03 A/m^2 and 0.08±0.03 A/m^2, respectively. These current densities are

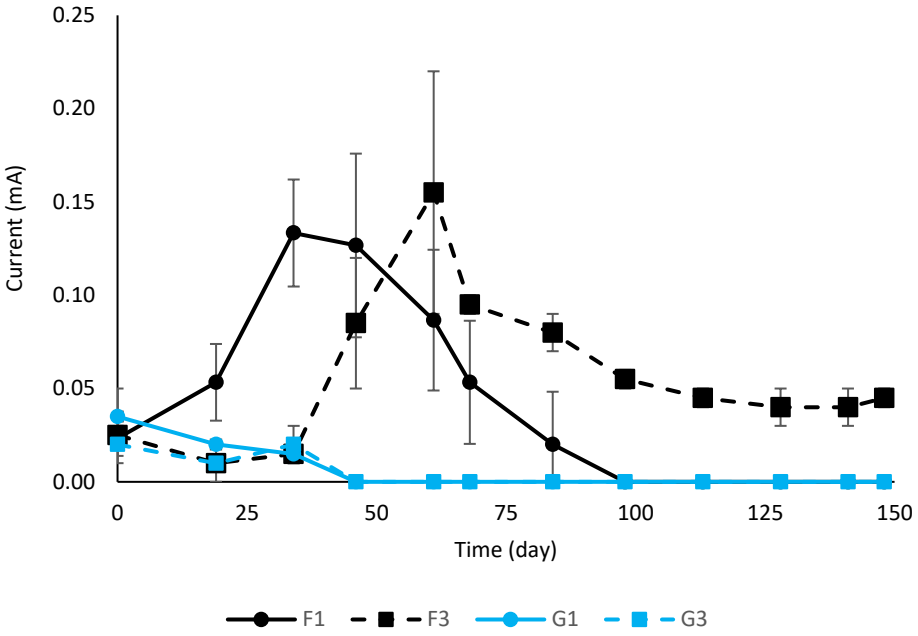

Figure A.1: Current generated from MEC treatments with an applied whole cell voltage of E_{AP}=1.0V. Error bars represent one standard deviation of triplicate measurements.

lower than current densities achieved with similar single chamber MECs polarized with a <1.0V whole cell voltage fed with acetate [134]. Due to the syntrophic nature of coal degradation, lower current density relative to a simple substrate like acetate is expected. Furthermore, the cathodic reduction efficiency was also lower when MECs were fed with coal versus other substrates studied. The cathodic reduction efficiency at the peak of hydrogen production before methane was detected (day 84), r_{cat}, was 11.1% in the F3 treatment. By day 148, the cathodic reduction efficiency decreased drastically to 1.4% due to the consumption of hydrogen, likely by hydrogenotrophic methanogens. Cathodic reduction efficiency in the F1 treatment was challenging to elucidate due to the non-significant effect of voltage on methane production relative to the unpolarized, inoculated treatment (F2). Current production in treatments containing glass beads as a non-carbon substrate had small, measurable current generation from day 0 to day 46. In the inoculated and uninoculated, polarized glass beads treatment (G1, G3 respectively),

initial current production could have been the result of the oxidation of soluble organic matter transferred to the reactor with the inoculum or dissolved organic carbon in the formation water. The suppression of current suggests that any carbon substrates available for exoelectrogen utilization were depleted by day 46. Current was not measured in the unpolarized coal and glass beads treatments because they were not treated with an applied voltage.

Headspace Gas Production

Over the course of the 148-day study, methane production was observed in all MECs with coal substrate, while significant methane production in MECs with non-carbon substrate (glass beads) was not observed (Figure A.2). Methane was detected in inoculated MECs with an E_{AP}=1.0V (F1) and inoculated, unpolarized MECs (F2) on day 19. In these treatments, methane increased until day 98 before leveling out for the remainder of the study. By the end of the 148-day period, cumulative methane production was 47.2±3.6 μmol CH_4/g coal and 45.1±4.9 μmol CH_4/g coal, respectively, suggesting that the effect of applied voltage on methane production was negligible. Furthermore, time series analysis revealed that at no point during the experiment was the methane production between F1 and F2 significantly different (p>0.05). However, the methane production rate in treatment F1 began to increase rapidly on day 34, corresponding with the maximum measured current generation. As expected, methane production increased as the rate of coal degradation reached a maximum. Cumulative methane production leveled out on day 98, the same day that current dropped to 0 mA in this treatment. This result suggests that methane production was correlated with current generation in the polarized treatment, although the cumulative methane recovery was not greater than the unpolarized treatment. Methane production in the F1 treatment appeared to be correlated with the activity of anode-associated exoelectrogenic microorganisms. While coal-to-methane conversion was not enhanced, to the

authors' knowledge, this is the first demonstration of electroactive microorganisms derived from the PRB terrestrial subsurface environment.

Interestingly, detectable methane was produced in the uninoculated, polarized treatment (F3) on day 98 (Figure A.2 A). Once methane production was observed, production increased for the remainder of the study, reaching a maximum of 30.0±6.4 μmol CH_4/g coal on day 148. Significant hydrogen production was only observed in the uninoculated, polarized treatment (F3). Hydrogen was detected in this treatment on day 19 and reached a maximum of 25.8±0.6 μmol H_2/g coal on day 84 (Figure A.2 B). After day 84, the mass of hydrogen in the headspace of the F3 treatment decreased rapidly, coinciding with an increase in headspace methane, suggesting that hydrogen-utilizing methanogens were enriched in the uninoculated, polarized treatment. These methanogens were likely present in the coal substrate prior to reactor loading but were dormant until day 84 due to limited substrate availability. Because a coal-associated enrichment culture was not used to inoculate this treatment, coal-degradation was most likely slow, limiting the availability of soluble organic intermediates such as acetate and C1-compounds to be used for methane production via acetoclastic or methylotrophic methanogenesis. Hydrogen production in the F3 treatment was also correlated with current generation. The maximum accumulation of hydrogen in the headspace of the F3 treatment occurred on day 84, and the fastest rate of detectable hydrogen production occurred between days 46 and 68. The current generation in this treatment reached a maximum on day 61, suggesting that hydrogen production was directly related to current generation, as expected. Furthermore, current generation stabilized on day 128, which corresponded with the leveling off of hydrogen production. Because current was still being generated even though hydrogen did not continue to accumulate, it appears as though hydrogen was being consumed at the end of the study. Continued methane production during this time suggests that hydrogen was being consumed by hydrogen-utilizing methanogenic archaea. Stoichiometrically, the production of 1 mole CH_4 via hydrogenotrophic methanogenesis requires

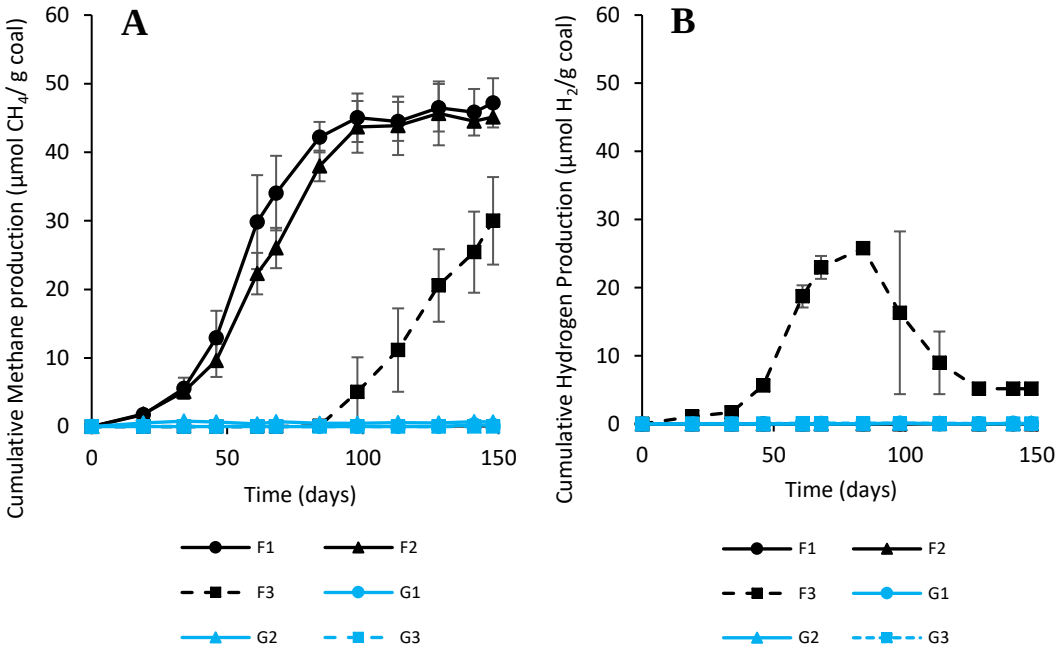

Figure A.2: (A) Cumulative methane and (B) hydrogen production over the course of the 148-day study. Error bars represent one standard deviation of replicate measurements.

4 moles of H_2 and 1 mol CO_2. Based on stoichiometry constraints alone, the reduction of hydrogen in the headspace of the F3 treatment cannot account for all the observed produced methane, suggesting other coal-to-methane pathways, such as acetoclastic methanogenesis, contributed to methane production or that hydrogen consumption via acetogenesis, occurred.

Carbon dioxide was produced in all MECs with coal as the substrate, while headspace carbon dioxide decreased in MECs with glass beads as the carbon-free substrate, suggesting a small amount of CO_2 consumption or dissolution (Figure A.3). In coal treatments, carbon dioxide production began immediately, with the fastest rate of CO_2 production occurring between day 0 and day 19. The CO_2 production rate during this time interval was 0.55±0.05 µmol CO_2/g coal/day, 0.54±0.01 µmol CO_2/g coal/day, and 0.68±0.05 µmol CO_2/g coal/day for F1, F2, and F3, respectively. After day 18, CO_2 production slowed down, but CO_2 concentrations continued to increase gradually for the duration of the study. At the end of the 148-day study, F1, F2, and

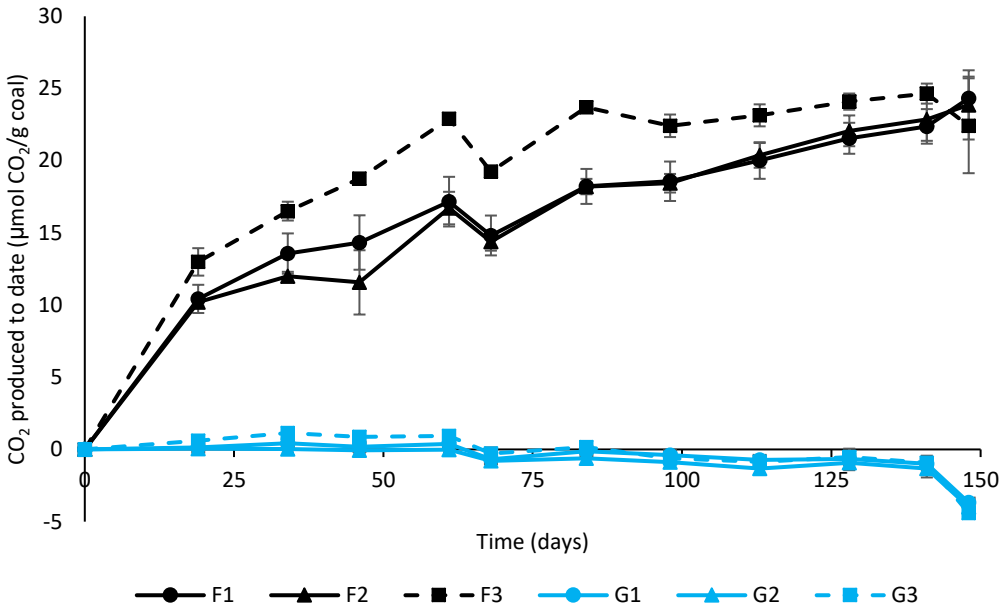

Figure A.3: Cumulative carbon dioxide production over the course of the 148-day study. Negative production represents a consumption of headspace CO_2. Error bars represent one standard deviation of replicate measurements.

F3 produced 24.3±1.5 µmol CO_2/g coal, 23.9±2.4 µmol CO_2/g coal, 22.4±3.3 µmol CO_2/g coal. Analogous to the methane results, the effect of voltage on total CO_2 production or production rate was not statistically significant. In the uninoculated, polarized coal treatment (F3), CO_2 production appeared to stop on day 84, while it continued to increase in the inoculated treatments (F1, F2). The leveling out of CO_2 production on day 84 in F3 also corresponds with the production of methane and the consumption of hydrogen, providing further evidence that one source of methane production was hydrogenotrophic methanogenesis.

Electrode Biofilm Quantification

CLSM revealed attached biomass on MEC electrodes when reactors were loaded with coal (Figure A.4). Biofilm coverage was generally greater on the stainless cathodes than the graphite anodes, but differences were not statistically significant, likely due to high variability

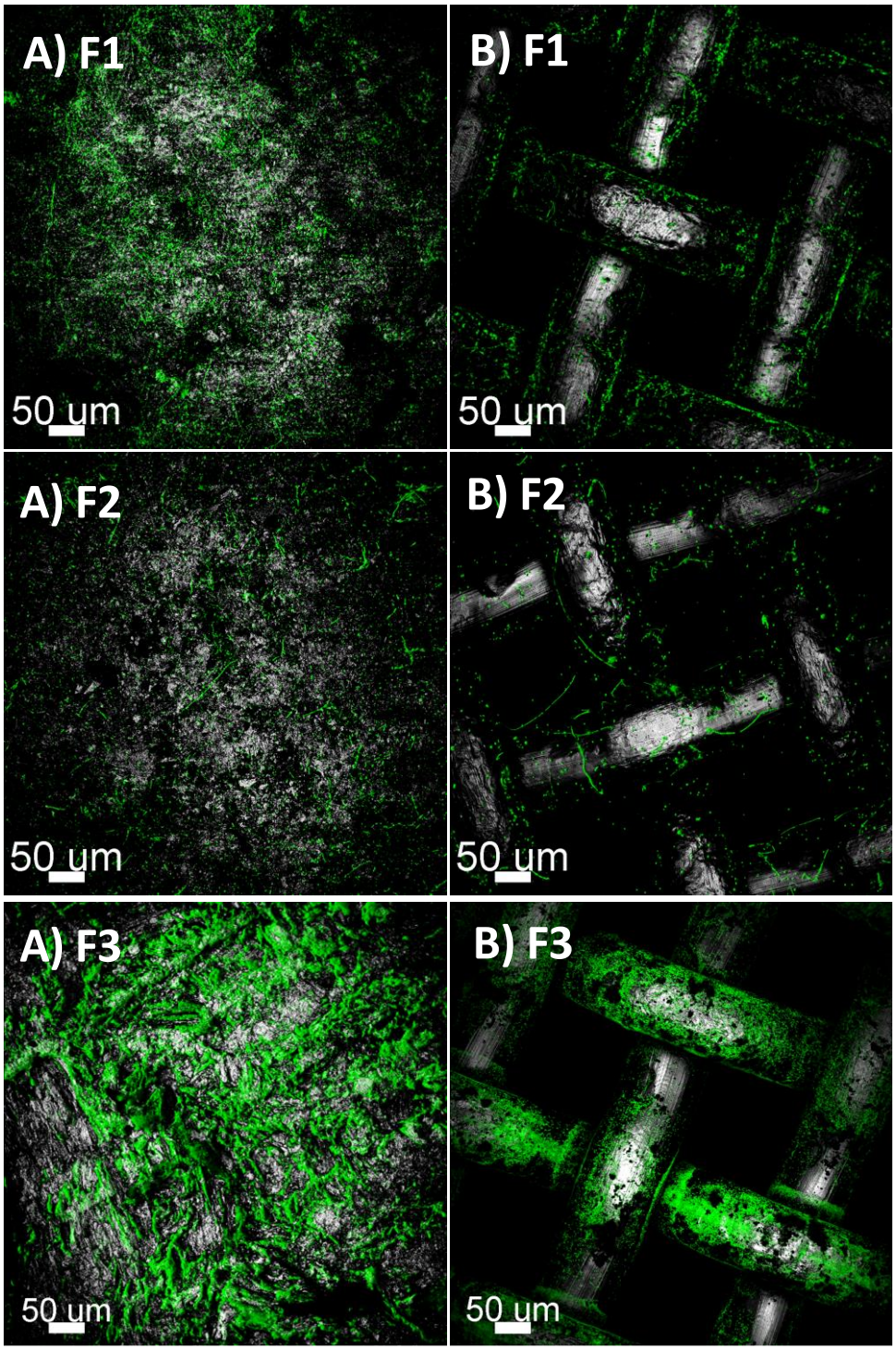

Figure A.4: 3D reconstructions of CLSM z-stack (A) stainless-steel anode and (B) isomolded graphite cathode images. Identified cells are stained with SYBR Green nucleic acid stain.

between replicates. For the inoculated, polarized (F1) treatment, $R_{VA\text{-}AN}$ was 0.7±1.4 $\mu m^3/\mu m^2$ while $R_{VA\text{-}CAT}$ was 3.2±1.6 $\mu m^3/\mu m^2$. Inoculated, unpolarized MECs (F2) also had biomass accumulation on electrode surfaces, but the biofilm volume to electrode surface area ratio was lower. For this treatment, $R_{VA\text{-}AN}$ was 0.3±0.1 $\mu m^3/\mu m^2$ and $R_{VA\text{-}CAT}$ was 1.1±0.7 $\mu m^3/\mu m^2$. The increase in electrode biofilm coverage in reactors with an E_{AP}=1.0V suggests that the polarized electrodes enhanced microbial adhesion and that the microbial community was interacting with the electrode surface. Considering that current generation was significant in the F1 treatment (unmeasured in F2), it is likely that anode biofilms were able to oxidize the available organic matter (coal or coal fermentation products) and utilize the electrode as a terminal electron acceptor. Significant microbial accumulation on the F1 cathode suggests that cathode-associated microorganisms may have utilized hydrogen gas evolved at the surface. Hydrogen was not detected in the headspace of this treatment, but hydrogenotrophic archaea have been reported to utilize hydrogen at nanomolar concentrations [33], indicating that any evolved hydrogen may have been immediately consumed at the cathode surface. While methane production via direct electron transfer from the cathode to the attached microorganisms has been reported [114, 122], no distinct evidence of this process was observed. Interestingly, CLSM imaging revealed significant attached biomass on the electrodes of uninoculated, polarized MECs (F3). Electrode biofilm coverage in this treatment was highly variable, even though hydrogen production was not. The anode and cathode did not have significantly different biofilm volume to electrode surface area ratios, with $R_{VA\text{-}AN}$=2.4±1.4 $\mu m^3/\mu m^2$ and $R_{VA\text{-}CAT}$=2.6±2.3 $\mu m^3/\mu m^2$. Furthermore, the anode and cathode biofilm morphology in the F3 treatment was not consistent with the inoculated F1 and F2 treatments, providing additional evidence that microorganism introduced from the coal were enriched. Both polarized and unpolarized MECs with glass beads as a substrate exhibited negligible anode biofilm accumulation, with $R_{VA\text{-}AN}$=0.01±0.00 $\mu m^3/\mu m^2$, $R_{VA\text{-}AN}$=0.0±0.0

$\mu m^3/\mu m^2$, $R_{VA\text{-}AN}$=0.04±0.02 $\mu m^3/\mu m^2$ for G1, G2, and G3, respectively, validating the claim that anode attachment is dependent on the presence of an organic substrate. Cathodic biofilms were detected in all three glass beads MEC treatments. Limited current production in these treatments suggests that attached biomass was not electroactive.

Cathodic biomass coverage for the inoculated, glass beads treatments, G1 and G2, was $R_{VA\text{-}CAT}$=0.3±0.0 $\mu m^3/\mu m^2$ and $R_{VA\text{-}CAT}$=1.5±0.5 $\mu m^3/\mu m^2$. In the absence of current production due to the lack of substrate utilization at the anode, electrons are not being transferred to the cathode, regardless of electrode polarization. As a result, any difference in attached biomass between these treatments is likely the result of spatial variability inside the reactor due to a lack of mixing. Cathode biomass accumulation in the uninoculated, polarized treatment (G3, $R_{VA\text{-}CAT}$=0.5±0.2 $\mu m^3/\mu m^2$), suggests that reactor contamination was possible, most likely during enrichment preparation or during the electrode embedding process. During electrode embedment, the same batch of agarose was used for some treatments, including G3, resulting in possible cross-contamination. The G3 treatment exhibited unique morphology (image not shown) compared to other coal treatments, with all cells resembling rod-like morphology, while filamentous structures were not observed.

Discussion

MECs are a developing technology targeted at energy and value-added product recovery from waste stream treatment. While MEC research has been focused on scale-up and integration into mature wastewater treatment operations, there is also the potential to use this technology for energy recovery, storage, and carbon sequestration in geologic reservoirs [34, 118]. Coal represents a complex organic substrate that theoretically could be utilized in MECs. Coupled with the recent interest in utilizing coal seams and abandoned mines for carbon sequestration [84, 135-

137], exploring the possibility of enhanced coal-to-methane conversion via electromethanogenesis is intriguing. MECs loaded with coal substrate were inoculated with a PRB coal microbial community to explore the effect of applied voltage on coal-to-methane conversion. In this study, applying a whole cell voltage of 1.0V to inoculated reactors did not result in enhanced methane production compared to the unpolarized treatment. This result is inconsistent with previously reported research using coal as a substrate in MECs. Piao et al. (2018) reported a methane yield from the bioelectrochemical conversion of lignite using an E_{AP}=1.0V of 2249.1 µmol CH_4/g lignite, which was orders of magnitude greater than the methane yield obtained from their unpolarized control (30.7 µmol CH_4/g lignite) and the highest reported laboratory scale coal-to-methane yield to date [37].

While enhanced coal-to-methane conversion was not observed in this study, current generation and anodic biofilms were detected, indicating that coal-associated microorganisms were able to utilize the coal substrate and use the solid electrode as a terminal electron acceptor. In these treatments, current generation was correlated with methane production, with maximum current generation corresponding with the fastest methane production rate. However, current density is not always representative of MEC performance due to the potential to generate current loops without accumulating hydrogen or methane. Most known exoelectrogens can only extract electrons from simple organic substrates such as volatile fatty acids to produce current [33] and therefore require syntrophic interaction with polymer fermenting bacteria in order to utilize complex organic matter, such as coal. This syntrophic requirement complicates MEC performance due to the competition for electrons. For example, coal fermentation products include H_2 and acetate. Acetate can be utilized by exoelectrogens to produce current and homo-acetogens can utilize the produced H_2 to reduce carbon dioxide, producing additional acetate. This acetate can then be utilized once more by exoelectrogens, resulting in produced current without value-added product accumulation. Additionally, some anode respirating bacteria (ARBs)

can utilize hydrogen as an electron donor [130]. Because hydrogen was not detected in the headspace of the inoculated, polarized coal treatment but significant current generation was, it is likely that homoacetogens and ARBs scavenged a portion of produced hydrogen, limiting hydrogenotrophic methanogenesis.

Current generation, hydrogen, and methane were all detected in the uninoculated, polarized MEC coal treatment, suggesting that coal-associated microorganisms were transferred to the reactors during coal loading. While most likely at low relative abundance due to UV pretreatment, these organisms were able to utilize the available coal organic substrate to transfer electrons to the anode, resulting in current generation and hydrogen production. Hydrogen accumulated in these reactors for 84 days, suggesting that the applied voltage overcame the thermodynamic energy barrier to reduce protons at the cathode. Because these reactors were not inoculated, competition from homoacetogens and other hydrogen scavenging organisms was likely limited, resulting in current production that correlated highly with hydrogen accumulation. During this time, methane was not detected in these treatments, suggesting that methanogenic archaea or electrotrophic organisms at the cathode were not active. After day 84, headspace hydrogen decreased, and methane production began. The amount of methane produced could not be explained stoichiometrically by hydrogen consumption alone, suggesting other types of methane production occurred, such as acetoclastic methanogenesis, or that hydrogen consumption was faster than cathodic hydrogen evolution. While exoelectrogens have been described to have higher specific growth rates (μ_{max}) [138] and lower Monod half saturation constants (K_s) than acetoclastic methanogens when growing on acetate [111, 139], acetate scavenging may have occurred due to anode biofilm reaction-diffusion disadvantages. While hydrogen and methane were both produced in this treatment, current density and cathodic conversion efficiency were both well below the range of typically reported values [31], which is likely the result of overpotentials and high ohmic losses, in addition to the recalcitrant nature of coal.

Confocal microscopy revealed accumulated biomass on all coal MEC electrodes, with polarized electrodes having higher biofilm volume to electrode surface area ratios. Biofilm coverage and thickness has been reported to affect MEC performance, with thin, uniform biofilms resulting in high current densities due to decreased mass transfer limitations and decreased ohmic losses from the electrode biofilms [100, 102]. In coal MECs, cathodes generally had higher R_{VA} ratios than the complementary anodes, but due to high variability among replicates these differences were not statistically significant. Biofilm morphologies between the polarized, inoculated (F1) and polarized, uninoculated (F3) treatments were qualitatively very different. The anode and cathode biofilm in the F1 treatment appeared to contain filamentous organisms in addition to smaller, colony forming organisms. In contrast, the F3 treatment had a uniform sheet-like biofilm, with little noticeable heterogeneity. F1 was inoculated with a multi-species, coal-derived microbial consortium, while any microorganisms in the F3 treatment were likely introduced with the coal at low relative abundance and enriched by the applied voltage. Substrate competition in the F3 treatment was likely negligible, resulting in the selection of specific, electroactive organisms, resulting in less heterogeneity. However, R_{VA} in the F3 treatment was highly variable between replicates, suggesting that the organisms introduced with the coal may not have been consistent across treatments. Further investigation of inoculated and uninoculated coal fed MECs is needed. Particularly, reactor materials and design need to be optimized to reduce overpotentials, resistive losses, and variability. Advanced electrochemical techniques such as cyclic voltammetry should be utilized to evaluate system performance and elucidate bioelectrochemical mechanisms. Furthermore, the description and activity of exoelectrogens present in coal associated PRB microbial communities should be evaluated using simple substrates such as acetate to establish additional proof of concept.

Conclusion

Polarizing single chamber MECs loaded with coal using a whole cell voltage of 1.0V promoted the enrichment of exoelectrogens derived from an *in-situ* PRB consortium. Produced current in polarized treatments and the subsequent cathodic reduction of protons to hydrogen gas in the uninoculated treatment provides evidence that exoelectrogens were able to use the graphite anode as a terminal electron acceptor. Low current density and low cathodic reduction efficiency suggests that recalcitrant coal may limit exoelectrogen activity due to syntrophic requirements and coal fermentation/hydrolysis product competition. Furthermore, applied voltage in inoculated treatments did not result in enhanced coal-to-methane conversion or detectable hydrogen evolution compared to inoculated, unpolarized controls, suggesting that the MEC system did not result in improved thermodynamic and kinetic conditions for coal-to-methane conversion. Elevated biofilm volume to electrode surface area ratios in coal treatments with an applied voltage suggests electrode polarization may have enhanced biomass attachment on both graphite anodes and stainless-steel cathodes, but definitive conclusions correlating MEC system performance to biofilm coverage could not be determined due to high variability. Further research evaluating the viability of electroactive coal-seam microorganisms and the effect of applied voltage is needed to determine the feasibility of bioelectrochemical enhanced *in-situ* coal to methane conversion.

APPENDIX B

QUANTIFYING COAL TO METHANE CONVERSION AND GAS ADSORPTION IN ALGAL AMENDED COAL MICROCOSMS

Motivation

Quantifying the effect of algal amendment on coal-to-methane conversion accurately in batch microcosms is challenging due to the presence of three phases: solid coal, liquid media, and headspace gas. This three-phase equilibrium involves pH dependent dissolution of gaseous carbon dioxide and methane into aqueous solution and the adsorption of these species to the solid coal geopolymer. The adsorption process is often neglected when methane is quantified in batch systems, likely resulting in an underestimation of coal-to-methane conversion. However, the majority of gas-in-place in CBM reservoirs is found in the adsorbed phase, resulting in a disconnect between laboratory research and field relevance. The objective of this study was to determine the effect of algal amendment on coal-to-methane conversion in batch microcosms loaded with different amounts of coal and to quantify subsequent gas adsorption.

Methods

Microcosm Setup

All microcosms were set up in triplicate using anoxic techniques in 26 mL Balch tubes sealed with butyl rubber stoppers and aluminum crimp seals. The FG coal core (depth 384-385') was opened in an anaerobic glove bag, where it was dried and crushed. Crushed coal was sieved to an effective size of 0.85-2.00 mm. One mm diameter Borosilicate glass beads were autoclaved and used in lieu of coal to provide carbon-free substrate for controls.

Microcosms were set up with 1g, 2g, or 5g of coal. FG formation water was filtered with a 0.2 µm bottle top filter, sparged overnight with anoxic 5% CO_2 (balance of N_2) and reduced with 1 mM sulfide ($Na_2S^{\bullet}9H_2O$). For each coal amount condition, amended microcosms were set up with a final amendment concentration of 0.1 g/L ^{13}C-algae. Additional unamended microcosms for each coal amount condition were set up as controls. Each microcosm was

inoculated with 1 mL of previously collected FG enrichment consortium, as described in Chapter Two, and prepared formation water was added to obtain a final liquid culture volume of 10 mL. Microcosms with 1g, 2g, and 5g of coal had headspace volumes of 16.0, 15.2, and 12.8 mL, respectively. All microcosms were incubated at 21±1ºC in the dark for 405 days. Headspace gas was sampled and analyzed every 2-6 weeks.

Headspace Gas Analysis

Headspace gases (CH_4 and CO_2) were analyzed using an SRI Instruments (Torrance, CA, USA) Model 8601 GC equipped with a thermal conductivity detector (TCD) interfaced with PeakSimple Chromatography software. Ultra-high purity helium carrier gas and a Supelco HayeSep-D packed stainless-steel column (6 feet x 1/8" O.D) were used for separation. One mL of headspace gas was sampled from each microcosm and manually injected with a carrier gas pressure of 8 psi and the oven and TCD temperatures of 40ºC and 150ºC, respectively. To measure isotope ratios of $^{13}CH_4$:$^{12}CH_4$ and $^{13}CO_2$:$^{12}CO_2$, 500 µL of headspace gas was manually injected into an Agilent 6890 GC 5973 electron impact ionization mass selective detector (Agilent Technologies, Palo Alto, Ca, USA) equipped with a GS-Carbonplot column (60m x 0.320 mm I.D. x 1.50 µm film thickness) and interfaced with Agilent Enhanced ChemStation software. The following operation parameters were used: 500 uL split ratio 30:1 injection, constant flow at 1 ml/min, injector temperature of 185ºC, interface temperature of 60ºC, and scan range m/z 2-100. Ultra-high purity helium was the carrier gas. Both headspace gas samples were taken simultaneously and 1.5 mL of anoxic 5% CO_2 (balance N_2) was injected to replace the sample volume. Isotope ratios were analyzed using the GC-MS deconvolution method previous described [50].

Quantifying Adsorbed Gas

At the end of the 405-day study, all microcosms were destructively sampled to quantify the amount of methane and carbon dioxide adsorbed to the coal. The liquid media from each Balch tube was transferred to fresh Balch tubes prepared with N_2 at atmospheric pressure. The liquid media was allowed to equilibrate with the N2 headspace for 24 hr before gas samples were obtained as described above. The headspace of the Balch tube with the residual coal was exchanged with N2 to decrease the pressure and create a concentration gradient for gas desorption. Gases were allowed to desorb for 24 hr before headspace gas samples were taken. Lastly, the Balch tubes were connected to a Teledyne ISCO Syringe pump (insert manufacturer info) for vacuum desorption at an initial pressure of -7 psi for 10 min. After 10 min, gas samples were obtained from the pump cylinder volume after returning the system to atmospheric pressure.

Statistical Analysis

Differences in final methane production, methane production rates, carbon dioxide production, carbon dioxide production rates, $^{12}CH_4$ production, and maximum $^{12}CH_4$ production rates for each coal amount and amendment condition were compared using a Generalized Linear Model (GLM) with Tukey interaction. A p-value less than 0.05 determined significance.

Results

Total Methane Production

^{13}C-algae amended (+) and unamended microcosms (-) with different amounts of coal all produced methane over the course of the 405-day study (Figure B.1). Methane was detected in all coal treatments on day 15. Methane in the headspace (measured) and liquid phase (calculated) of the 5g(+), 2g(+), and 1g(+) increased until days 84, 118, and 84, respectively. At the end of the 405-day period, these treatments produced 21.1±0.8 μmol CH_4/g coal, 244.7±10.2 μmol CH_4, and

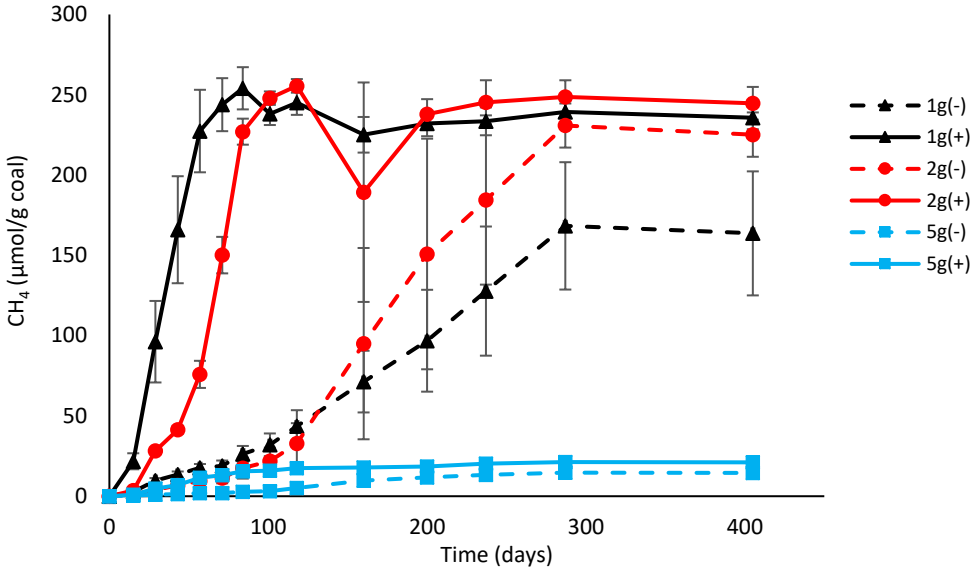

Figure B.1: Detectable methane produced per gram of coal for ^{13}C-algae amended and unamended treatments with 1g, 2g, or 5g of coal versus time over the course of the 405-day study. Amended treatments have an amendment concentration of 0.1 g/L. Error bars represent one standard deviation of triplicate measurements.

235.6±7.1 µmol CH_4/g coal, respectively. Methane in the headspace and liquid phase of all unamended microcosms, 5g(-), 2g(-), and 1g(-), increased until day 287 of the experiment. At the end of the study, these treatments produced 14.5±1.3 µmol CH_4/g coal, 225.2±13.8 µmol CH_4/g coal, and 163.7±38.6 µmol CH_4/g coal, for the 5g(-), 2g(-), and 1g(-) coal treatments respectively. The differences in final methane production between the amended and unamended treatments are statistically significant for 1g (p<0.05), while the addition of amendment did not result in significantly different final methane production for 2g and 5g of coal (p>0.99). In the case of the 2g(+) and 1g(+) treatments, an increase in coal amount did not result in an increase in detectable methane when normalized to the mass of coal when amended with ^{13}C-algal amendment (p>0.99). In the absence of algal amendment, an increase in coal mass from 1g to 2g may have resulted in an increase in detectable methane, although the difference was not significant at the 95% confidence level (p=0.06). Both 5g(+) and 5g(-) treatments resulted in less

detectable methane per gram of coal at the end of the study. A complete table of Tukey pairwise comparisons can be found in the Chapter Specific Supplementary Information, Table SB.1. It is hypothesized that this is the result of an increase in gas adsorption due to an increase in coal surface area. Additionally, the coal-to-liquid ratio was not controlled in these microcosms, possibly contributing to the results seen in this study. Previous work has reported higher methane production in microcosms with smaller coal-to-liquid ratios, which is inconsistent with the results reported here. To accurately determine the effect of coal mass on methane production, covariates such as coal to liquid ratio and headspace volume should be controlled in future studies.

The presence of ^{13}C-algal amendment increased methane production rates in microcosms with 1g and 2g of coal but did not have a statistical effect on microcosms with 5g of coal (p=0.21). Between day 15 and day 84, the (detectable) methane production rate for 5g(+), 2g(+), and 1g(+) were 0.2±0.0 µmol CH_4/g coal/day, 3.2±0.1 µmol CH_4/g coal/day, and 3.4±0.1 µmol CH_4/g coal/day, respectively, while the methane production rates for 5g(-), 2g(-), and 1g(-) during this time period were 0.03±0.00 µmol CH_4/g coal/day, 0.2±0.1 µmol CH_4/g coal/day, and 0.3±0.1 µmol CH_4/g coal/day, respectively. Once again, this time interval is not representative of the maximum methane production rate for the unamended treatments. Instead, a more accurate representation of the highest rate of methane production for the unamended treatments was between days 71-287. The methane production rate during this time period for 5g(-), 2g(-) and 1g(-) was 0.06±0.00 µmol CH_4/g coal/day, 1.02±0.05 µmol CH_4/g coal/day and 0.7±0.2 µmol CH_4/g coal/day, respectively. Comparing methane production rates during the fastest period of methane production for each treatment, it was found that amended treatments had higher methane production rates (p<0.05). These results support the hypothesis that algal amendment increases methane production rates and decreases the lag time before methane production commences. Comparing the effects of coal amount on methane production rate for algal amendment treatments, there was not a significant difference (p=0.77) between days 15-84 for the 2g(+) and

1g(+) treatments when normalized to coal mass. Both 2g(+) and 1g(+) had significantly higher methane production rates per gram of coal than 5g(+) (p<0.05) when comparing gas and aqueous phase methane. However, it is hypothesized that this is a result of undetectable methane due to gas adsorption in the 5g(+) treatment. These results suggest that in the presence of ^{13}C-algal amendment, increasing the mass of coal does not result in increased normalized methane production rates (Chapter Specific Supplementary Information, Table SB.2). Between days 71 and 287, unamended treatments 2g(-) and 1g(-) did not have significantly different methane production rates (p=0.09), suggesting that coal mass does not have an effect on methane production rate when considerable amounts of methane are detectable.

Carbon Dioxide Production and Consumption

After accounting for CO_2 added during sampling, it became evident that CO_2 was produced in both amended and unamended microcosms with 1g of coal and 2g of coal (Figure B.2). CO_2 consumption was observed in the headspace of both amended and unamended 5g treatments. Microcosms amended with 5g amendment consumed 9.4±0.0 µmol CO_2/g coal from the headspace while, the 2g(+) and 1g(+) treatments increased the CO_2 amount in the headspace by 31.2±1.1 µmol CO_2/g coal, and 30.3±3.9 µmol CO_2/g coal, respectively. Unamended microcosms with 5 g of coal consumed 7.3±0.2 µmol CO_2/g coal from the headspace while treatments with 2g and 1g of coal increased the amount of CO_2 in the headspace by 25.6±1.3 µmol CO_2/g coal, and 20.1±4.5 µmol CO_2/g coal, respectively. The effect of algal amendment on normalized CO_2 production over the duration of the experiment was not statistically significant (p=0.62) (Chapter Specific Supplementary Information, Table SB.3). Coal mass had a statistically significant effect on normalized CO_2 production (p<0.05), due to the consumption of CO_2 in the 5g treatments. The consumption of CO_2 in the headspace of the 5g treatments is likely the result

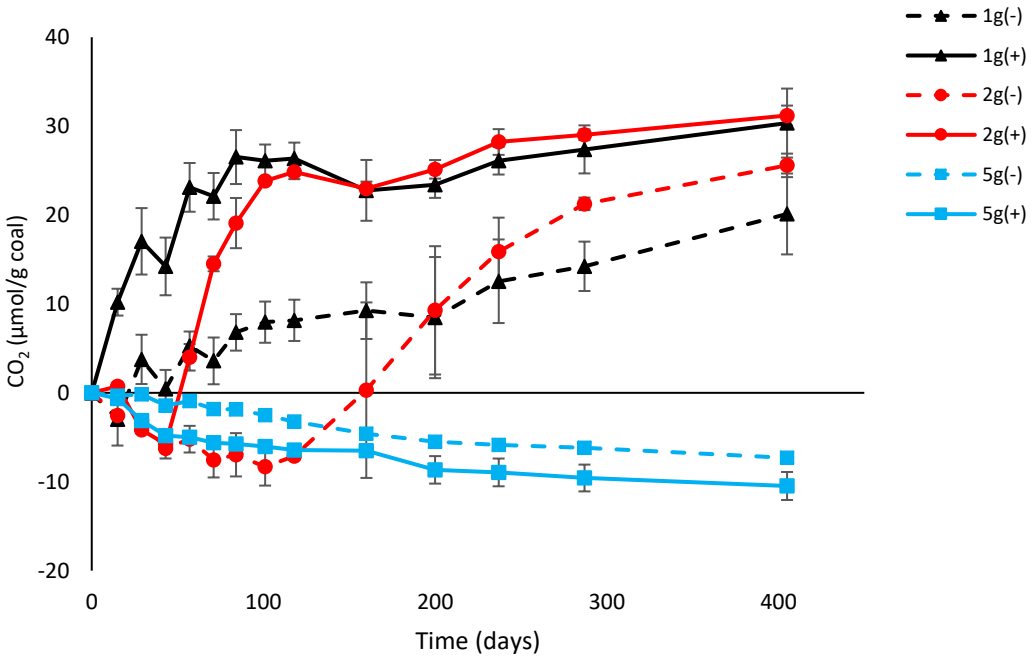

Figure B.2: Carbon dioxide produced per gram of coal for ^{13}C-algae amended and unamended treatments with 1g, 2g or 5g of coal versus time over the course of the 405-day study after accounting for CO_2 added during sample replacement. Negative values represent a net consumption of detectable CO_2. Amended treatments have an amendment concentration of 0.1 g/L. Error bars represent one standard deviation of triplicate measurements.

of gas adsorption and not microbial CO_2 conversion, which is supported by the limited detectable methane in these treatments as well.

The addition of algal amendment had a statistically significant effect on the CO_2 production rate in the headspace of microcosms with different masses of coal. For the 1g(+) treatment, CO_2 was produced at a rate of 0.3±0.0 µmol CO_2/g coal/day, while 1g(-) changed at a rate of 0.1±0.0 µmol CO_2/g coal/day between days 0-84. CO_2 was consumed in both 2g(+) and 2g(-) until day 43 and day 101, respectively, which is likely due to net CO_2 adsorption. CO_2 was produced in the 2g(+) treatment between days 43-118 at a rate of 0.4±0.0 µmol CO_2/g coal/day, while 2g(-) produced CO_2 at a rate of 0.1±0.0 µmol CO_2/g coal/day. For the 2g(-) treatment, days 43-118 are not representative of the fastest CO_2 production rate; instead, CO_2 in the 2g(-) treatment was produced the fastest between days 101-287 at a rate of 0.2±0.0 µmol CO_2/g

coal/day. CO_2 in the headspace of the 5g treatments decreased for the duration of the experiment, with the fastest decrease occurring between days 15-43 for the 5g(+) treatment and days 118-200 for the 5g(-) treatment. The CO_2 consumption rate for these treatments during these time periods was -0.2±0.0 µmol CO_2/g coal/day and -0.03±0.00 µmol CO_2/g coal/day, respectively. All differences in CO_2 production rate between algae amended treatments and unamended treatments were statistically significant when comparing the fastest intervals, regardless of coal mass. Coal mass also had a statistically significant effect on CO_2 production rate (p<0.05) (Chapter Specific Supplementary Information, Table SB.4). However, due to gas adsorption and speciation of CO_2 in these systems, the effect is unclear. CO_2 was consumed in the 2g(+) and 2g(-) initially but CO_2 production still leveled out on the same day as the 1g(+) and 1g(-) treatments (day 118 and day 287), suggesting that the microbial production rate of CO_2 may not truly be different between these samples.

Source of Carbon for Methane Production

Using the carbon balance method (Eq. 2, Chapter Two), the source of carbon for methane production in the microcosms with different amounts of coal was evaluated (Figure B.3). For the 1g(+) treatment, C_{out}/C_{in} was greater than one by day 29 and remained above one for the duration of the experiment. For this treatment, C_{out}/C_{in} reached a maximum of 6.3±0.4 on day 84 and then decreased to 2.0±0.2 by day 405, indicating that by the end of the experiment, 1g(+) produced twice as much additional methane as could be explained by direct amendment conversion alone. For the 2g(+) treatment, C_{out}/C_{in} was greater than one by day 57 and remained above one until day 237. The maximum C_{out}/C_{in} ratio for the 2g(+) treatment was 6.3±0.1, observed on day 101, and the final C_{out}/C_{in} was 0.5±0.3. The final C_{out}/C_{in} ratio less than one for this treatment is another example of how added amendment has a significant effect on methane production rate, but not necessarily on final yield, especially considering uncertainty associated with gas adsorption and

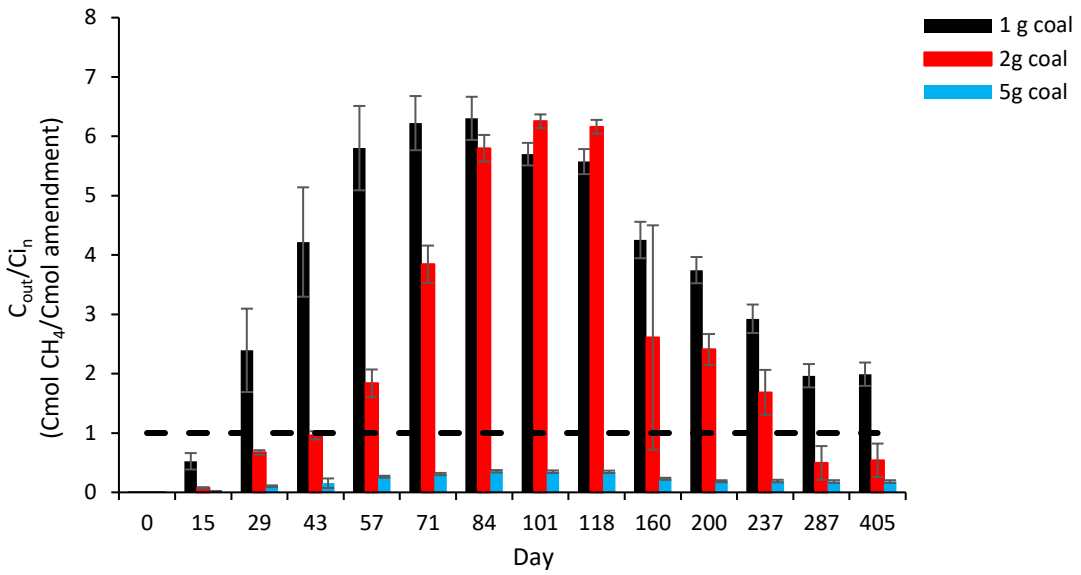

Figure B.3: Amount of carbon detected as methane per gram of coal relative to the amount of carbon added as amendment for ^{13}C-algae amended coal treatments with 1g, 2g and 5g of coal. C_{out}/C_{in} ratios greater than one represents more surplus carbon detected as methane than carbon added as amendment.

the production of other metabolites. C_{out}/C_{in} ratios for the 5g(+) treatment was never observed above one for the duration of the experiment. While this result may be interpreted that additional methane produced in the 5g(+) treatment relative to 5g(-) may be the result of direct amendment conversion as opposed to enhanced coal-to-methane conversion, it is more likely a consequence of gas adsorption due to the increase in surface area associated with an increase in coal mass.

Fate of ^{13}C algal amendment

Microcosms with different amounts of coal produced elevated levels of $^{13}CH_4$ when amended with ^{13}C-algae compared to the complementary unamended treatments by the end of the 405-day period (Supplementary Information, Figure SB.1). Of the total methane produced for the 5g(+), 2g(+), and 1g(+) treatments, 2.3±0.1%, 3.3±0.1%, and 5.5±0.5% was $^{13}CH_4$, respectively. As expected, the percent of methane that was $^{13}CH_4$ decreased as coal amount increased ($p<0.05$) due to the increase in coal-to-amendment ratio. The presence of elevated $^{13}CH_4$ methane in the

5g(+) treatments suggests that even with excess coal, some algal amendment is still converted to methane. By day 405, the percent of total methane that was $^{13}CH_4$ for the 5g(-), 2g(-), and 1g(-) treatments was 1.6±0.1%, 1.6±0.1%, and 1.4±0.1%, respectively, which is comparable to the natural relative abundance of ^{13}C considering the sensitivity of the analysis method.

Microcosms with different amounts of coal amended with ^{13}C-algae produced variable $^{13}CO_2/^{12}CO_2$ ratios (Supplementary Information, Figure SB.1). After the first sampling (day 15), the 5g(+) treatment exhibited 1.1±0.0% $^{13}CO_2$, which is consistent with the natural relative abundance of ^{13}C. Paralleling the decrease in total mass of CO_2 in the headspace, $^{13}CO_2$ dropped to 0.6±0.0% by the end of the 405-day period. The 2g(+) and 1g(+) treatments had elevated $^{13}CO_2/^{12}CO_2$ ratios, with both reaching a maximum of 2.9±0.1 and 4.0±0.2%$^{13}CO_2$ on day 200, respectively. The percent of total CO_2 that was $^{13}CO_2$ decreased to 1.6±0.5% in the 1g(+) treatment and 2.7±0.0% in the 2g(+) treatment by the end of the 405-day period. The presence of ^{13}C-algal amendment had a statistically significant effect on final $^{13}CO_2/^{12}CO_2$ ratios ($p<0.05$), but not for all masses of coal. Amended treatments with 2g and 1g of coal had elevated $^{13}CO_2/^{12}CO_2$ ratios compared to the corresponding unamended treatments, but the $^{13}CO_2/^{12}CO_2$ ratio was not statistically different between 5g(+) and 5g(-). $^{13}CO_2/^{12}CO_2$ ratios for the unamended treatments were consistent with natural relative abundance within the sensitivity limits of the analysis method. The 5g(-) treatment may have decreased slightly from 1.0±0.1% $^{13}CO_2$ on day 15 to 0.6±0.0% $^{13}CO_2$ by day 405. Headspace CO_2 for the 2g(-) and 1g(-) on day 15 was 0.9±0.0% $^{13}CO_2$ and 0.9±0.0% $^{13}CO_2$, respectively, and had a final $^{13}CO_2$ content of 1.0±0.0% and 0.9±0.0% $^{13}CO_2$, respectively.

After accounting for ^{13}C produced in unamended treatments, either as $^{13}CH_4$ and $^{13}CO_2$, significant differences in detectable amendment conversion between 2g(+) and 1g(+) treatments were not observed (Table B.1).

Table B.1: Summary of produced $^{13}CH_4$, $^{13}CO_2$, and amendment conversion after 405 days for 0.1 g/L ^{13}C-algae amended coal treatments with 1g, 2g, and 5g of coal.

Treatment	Total $^{13}CH_4$ µmol	Total $^{13}CO_{2\,(g)}$ µmol	% ^{13}C amendment as $^{13}CH_4$	% ^{13}C amendment as $^{13}CO_2$	% ^{13}C amendment as gas
1g(+)	10.8±0.7	0.5±0.2	25.5±2.1	2.4±0.6	27.3±2.4
2g(+)	14.0 ±1.0	2.4±0.1	21.2±2.9	5.4±0.1	26.5±3.0
5g(+)	2.1±0.1	0.1±0.0	3.0 ±0.3	-0.2±0.0	2.8±0.3

Amendment-to methane conversion was 21.2±2.9% and 25.5±2.1% for 2g(+) and 1g(+), respectively, while amendment-to-$CO_{2(g)}$ conversion was 5.4±0.1% and 2.4±0.6%, resulting in total detectable amendment conversions of 26.5±3.0% and 27.3±2.4%, respectively. This result suggests that increasing the ratio of coal to amendment does not impact the microbial community's ability to convert the algal amendment to gaseous products and that similar amounts of amendment were converted to biomass, organic intermediates or adsorbed products. Amendment conversion in the 5g(+) treatment was difficult to ascertain accurately due to significantly lower amounts of methane and carbon dioxide detected.

Coal-to-Methane Conversion: $^{12}CH_4$

$^{12}CH_4$ production correlated with total CH_4 production in microcosms with different masses of coal throughout the duration of the 405-day study, providing evidence that coal degradation is driving methane production in these systems, regardless of coal amount or amendment condition (Chapter Specific Supplementary Information, Figure SB.2). Amended microcosms with an increased coal-to-amendment ratio did not produce more $^{12}CH_4$ per gram of coal than corresponding unamended treatments. Specifically, 5g(+) produced 20.7±0.8 µmol $^{12}CH_4$/g coal and 5g(-) produced 14.3±1.3 µmol $^{12}CH_4$/g coal (p=0.99), and 2g(+) produced 237.7±9.7 µmol $^{12}CH_4$/g coal, while 2g(-) produced 221.8±13.7 µmol $^{12}CH_4$/g coal (p=0.98).

Amended microcosms with 1g of coal produced statistically more $^{12}CH_4$ than the unamended 1g treatment, with 1g(+) producing 224.8±6.5 μmol $^{12}CH_4$/g coal and 1g(-) producing 161.6±38.2 μmol $^{12}CH_4$/g coal (p<0.05). These results suggest that when the coal-to-amendment ratio increases, the addition of algal amendment does not result in increased cumulative coal degradation per gram of coal relative to corresponding unamended treatments. Comparing the 2g(+) and 1g(+) treatments, increasing the coal-to-amendment ratio did not result in significantly different normalized $^{12}CH_4$ yields (p=0.97), suggesting that in the presence of algal amendment, the fraction of coal that is converted to methane remains similar (Chapter Specific Supplementary Information, Table SB.5).

However, the $^{12}CH_4$ production rate increased with the addition of algal amendment in microcosms with 2g and 1g of coal (Figure B.4). $^{12}CH_4$ production increased until days 84-118 in these treatments, with both treatments producing comparable $^{12}CH_4$ by day 84. The 2g(+) treatment presumably had twice as much surface area for methane adsorption than the 1g(+) treatment, most likely explaining the apparent increase in lag phase for $^{12}CH_4$ production in the 2g(+) treatment. Between day 15 and day 84, $^{12}CH_4$ production mirrored the total production of CH_4, suggesting that coal degradation drives methane production kinetics in algae-amended coal microcosms, regardless of coal mass. During this time interval, amended treatments 5g(+), 2g(+), and 1g(+) had $^{12}CH_4$ production rates of 0.2±0.0 μmol $^{12}CH_4$/g coal/day, 3.2±0.1 μmol $^{12}CH_4$/g coal/day and 3.2±0.1 μmol $^{12}CH_4$/g coal/day, respectively. During this same time interval, unamended treatments had $^{12}CH_4$ production rates of 0.0±0.0.0 μmol $^{12}CH_4$/g coal/day, 0.2±0.1 μmol $^{12}CH_4$/g coal/day and 0.3±0.1 μmol $^{12}CH_4$/g coal/day, respectively. However, a more accurate representation of the highest rate of $^{12}CH_4$ for the unamended treatments was between days 71-287. The $^{12}CH_4$ methane production rates during this time period for 5g(-), 2g(-), and 1g(-) treatments were 0.1±0.00 μmol CH_4/g coal/day, 1.0±0.0 μmol CH_4/g coal/day and 0.7±0.2 μmol CH_4/g coal/day, respectively. Comparing the periods of fastest $^{12}CH_4$ production rate,

amended coal treatments with 2g and 1g of coal had greater $^{12}CH_4$ production rates than analogous unamended treatments (p<0.05). The 5g(+) and 5g(-) did not have statistically different production rates (p=0.68*)* when comparing the fastest period of ^{12}CH4 production for each treatment. When normalized to coal mass, 2g(+) and 1g(+) did not have different $^{12}CH_4$ production rates (p=0.70), while 2g(-) had statistically greater methane production rate than the 1g(-) treatment, suggesting that in the presence of algal amendment, coal degradation rates are not affected by an increase in coal mass between 1 and 2g, but in the absence of algal amendment, detectable coal degradation rates may increase with an increase in coal mass (Chapter Specific Supplementary Information, Table SB.6).

Recovery of Adsorbed Methane and Carbon Dioxide

At the end of the 405-day study, CH_4 and CO_2 were recovered from both the aqueous and adsorbed phase in amended and unamended treatments (Figure B.5). The mass of CH_4 recovered in the aqueous phase of the unamended microcosms, 5g(-), 2g(-), and 1g(-), was 2.4±2.0 μmol CH_4/g coal, 14.0±2.9 μmol CH_4/g coal, and 16.3±5.4 μmol CH_4/g coal, respectively, while the mass recovered in analogous amended treatments was 1.2±1.1 μmol CH_4/g coal, 7.1±2.0 μmol CH_4/g coal, and 7.6±4.6 μmol CH_4/g coal. CH_4 recovery from the aqueous phase was generally higher in unamended treatments than amended treatments. Interestingly, the mass of CH_4 recovered in the 1g and 2g treatments were comparable, while the 5g treatments had significantly less CH_4 dissolved in the aqueous phase. During the atmospheric pressure desorption step (0 psig), the mass of CH_4 recovered from the coal in the 5g(-), 2g(-), and 1g(-) treatments was 0.0±0.0 μmol CH_4/g coal, 1.9±0.1 μmol CH_4/g coal, and 4.7±3.6 μmol CH_4/g coal, respectively. For analagous amended treatments, CH_4 recovery from the atmospheric desorption step was 0.0±0.0 μmol CH_4/g coal, 2.6±0.8 μmol CH_4/g coal, and 4.1±5.7 μmol CH_4/g coal, respectively. Lastly, the CH_4 recovery from the -7 psig vacuum desorption step was 0.0±0.0 μmol CH_4/g coal,

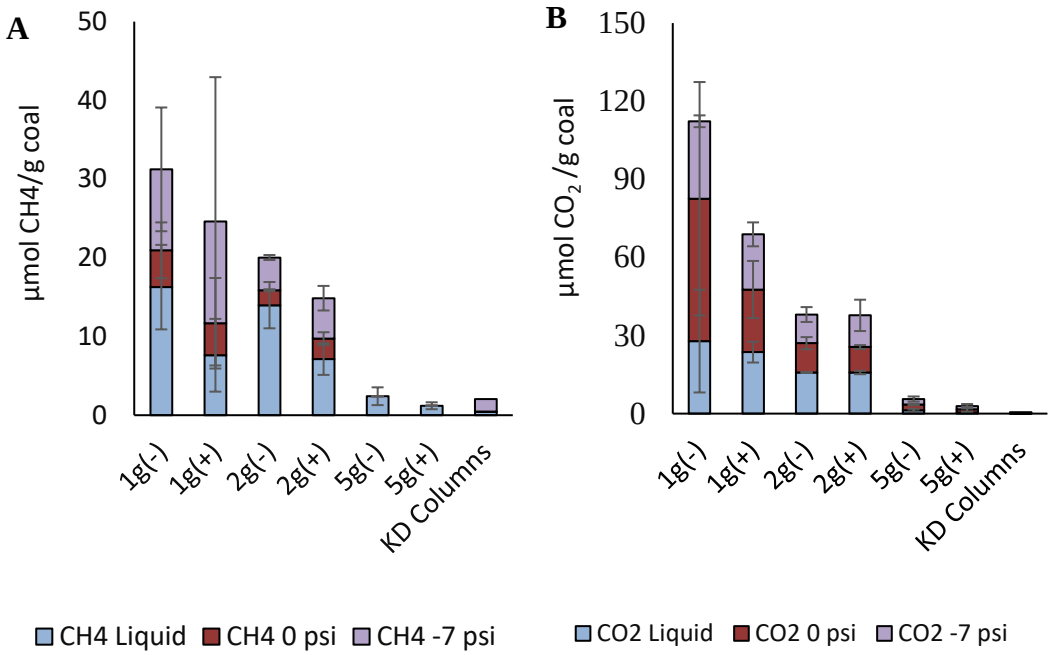

Figure B.4: (A) CH_4 and (B) CO_2 recovered from microcosm liquid and adsorbed to the coal surface after 405 days. Desorption from the coal surface was performed in two steps, an atmospheric pressure desorption step and a -7 psig vacuum step. Error bars represent one standard deviation of triplicate measurements from each step.

4.2±0.3 µmol CH_4/g coal, and 10.3±7.9 µmol CH_4/g coal for 5g(-), 2g(-), and 1g(-), respectively, and 0.0±0.0 µmol CH_4/g coal, 5.1±1.6 µmol CH_4/g coal, and 12.9±18.3 µmol CH_4/g coal for 5g(+), 2g(+), and 1g(+), respectively. Notably, CH_4 was not recovered during the atmospheric pressure desorption step or -7 psig vacuum step, which was not expected. CH_4 recovery was highly variable within a treatment, suggesting that the experimental methods may need reconsideration.

Considering all three desorption steps, the total CH_4 recovery was 2.4±1.1 µmol CH_4/g coal, 20.0±3.4 µmol CH_4/g coal, and 31.2±10.5 µmol CH_4/g coal for the 5g(-), 2g(-), and 1g(-) treatments, respectively, and 1.2±0.4 µmol CH_4/g coal, 14.9±3.1 µmol CH_4/g coal, and 24.6±25.5 µmol CH_4/g coal for 5g(+), 2g(+), and 1g(+), respectively. The CO_2 recovery from the three desorption steps followed a similar trend, with total recovery generally decreasing with increasing

coal mass (Figure B.5B). The total amount of CO_2 recovered from the three desorption steps was 5.6±4.9 μmol CO_2/g coal, 38.1±0.4 μmol CO_2/g coal, and 112.3±40.7 μmol CO_2/g coal for 5g(-), 2g(-), and 1g(-), respectively, and 2.8±0.5 μmol CO_2/g coal, 37.7±4.9 μmol CO_2/g coal, and 68.9±14.4 μmol CO_2/g coal for 5g(+), 2g(+), and 1g(+), respectively. In general, total CO_2 recovery was at least two times greater than CH_4 recovery, which is consistent with the preferential adsorption of CO_2 over CH_4 to coal.

Discussion and Conclusions

Coal is a heavily reduced form of carbon, and due to its recalcitrant nature, *in-situ* coal seam organisms may be substrate limited, preventing an adequate accumulation of biomass necessary for efficient coal-to-methane conversion. To assess the effect of algal amendment on systems with different amounts of coal, both amended and unamended microcosms with 1g, 2g, and 5g of coal were set up. The amended treatment with 1g of coal produced more detectable methane than the analogous unamended treatment, and methane production rates increased in amended microcosms with 2g and 1g of coal relative to unamended treatments, suggesting that algal amendment increases methane production rate even at increased coal-to-amendment ratios. $^{12}CH_4$ production rates paralleled total methane production rates in these treatments, providing evidence that increased methane production in algae amended treatments is driven by an increase in coal degradation. From the headspace measurements, gas adsorption appeared to play a role in the amount of detectable methane in the 2g and 5g treatments. After testing this hypothesis, it was found that the mass CH_4 and CO_2 recovered during the desorption procedure generally decreased with increasing coal mass, suggesting that gas adsorption does not adequately explain the limited headspace CH_4 production in the 5g treatments. The mass of CO_2 recovered was generally greater than the mass of CH_4 recovered, regardless of coal amount, which is consistent with previously

reported adsorption studies showing preferential CO_2 to CH_4 adsorption. Gas recovery from the desorption steps was highly variable within a given treatment. Because headspace gas measurements did not exhibit this same variability, the desorption methods likely need improvement.

Due to the lack of CH_4 and CO_2 recovery in the 5g treatments, an explanation for the limited CH_4 production in the 5g treatment is still being sought. One possible explanation is that coal hydrolysis and fermentation products accumulated in the batch systems and subsequently inhibited methanogenesis. To the author's knowledge, there has been no reported evidence of this occurring, but based on the results of this study it remains a plausible explanation. Accurately quantifying methane in all three phases of these microcosms is important because *in-situ* CBM is predominately found adsorbed to the coal geopolymer [140]. The microbial conversion of coal-to-methane may increase the adsorption capacity of coal by exposing previously unavailable micropores [85]. Amending *in-situ* microbial communities with algal amendment may compound this effect due to the increase in coal degradation, as shown in Chapter 2 of this thesis. An increase in gas-in-place (GIP) due to an increase in methane production and adsorption capacity could increase the economic viability of CBM extraction. Furthermore, coal seams have been investigated for carbon sequestration because CO_2 injection has the potential to enhance methane recovery by displacing methane by competitive adsorption [81]. With this in mind, further exploration of the effects of algal amendment on long term methane production, gas adsorption, and *in-situ* microbial communities will be necessary to determine the effectiveness of using these techniques together.

Conclusions

It was determined that doubling the coal-amendment ratio does not have an impact on detectable methane production rates, suggesting that the benefits of algal amendment addition are

not suppressed when the microbial community has twice as much coal substrate available for metabolism. However, increasing the amount of coal 5-fold resulted in limited detectable CH_4 and a consumption of headspace CO_2. This result could not be explained by gas adsorption alone, as gas desorption tests on the 5g treatment did not recover sufficient quantities of CH_4 and CO_2. As a result, the effect of coal hydrolysis and fermentation intermediate accumulation in batch systems on methanogenesis inhibition should be investigated.

Chapter Specific Supplementary Information

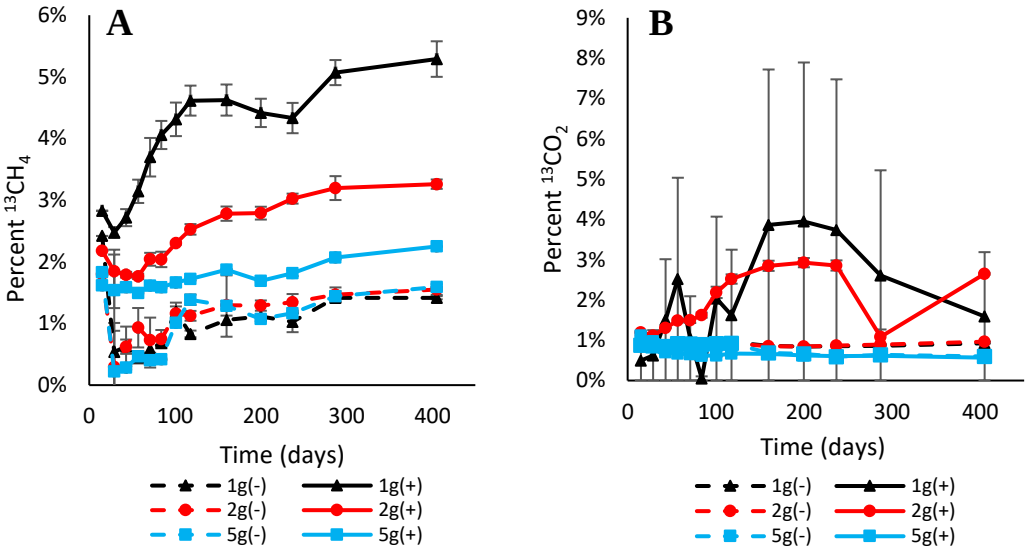

Figure SB.1: (A) Percent of total methane produced that is $^{13}CH_4$ and (B) percent of headspace carbon dioxide that is $^{13}CO_2$ or ^{13}C-algae amended and unamended treatments with 1g, 2g, or 5g of coal over the course of the 405-day study.

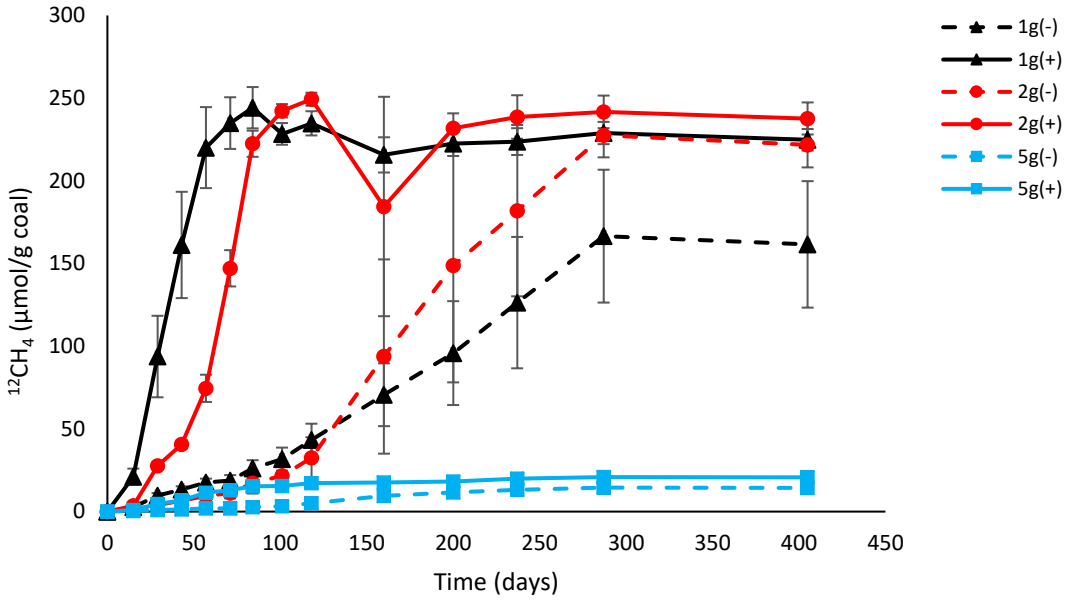

Figure SB.2: Detectable $^{12}CH_4$ per gram of coal produced for ^{13}C-algae amended and unamended treatments with 1g, 2g, or 5g of coal versus time over the course of the 405-day study. Amended treatments have an amendment concentration of 0.1 g/L. Error bars represent one standard deviation of triplicate measurements and adsorbed methane was not evaluated.

Table SB.1: Tukey Pairwise Comparisons from the Generalized Linear Model comparing cumulative CH_4 production (µmol CH_4/g coal) considering different amounts of coal and amendment condition. Means that do not share a letter are significantly different.

Treatment	N	Mean	Grouping		
2g(+)	3	244.696	A		
1g(+)	6	235.633	A		
2g(-)	2	225.191	A	B	
1g(-)	6	163.683		B	
5g(+)	3	21.074			C
5g(-)	3	14.510			C

Table SB.2: Tukey Pairwise Comparisons from the generalized linear model comparing maximum CH_4 production rate (μmol CH_4/g coal/day) considering different amounts of coal and amendment condition. Means that do not share a letter are significantly different.

Treatment	N	Mean	Grouping		
1g(+)	6	3.36627	A		
2g(+)	3	3.23766	A		
2g(-)	2	1.01669		B	
1g(-)	6	0.69167		B	
5g(+)	3	0.20912			C
5g(-)	3	0.05877			C

Table SB.3: Tukey pairwise comparisons from the Generalized Linear Model comparing cumulative CO_2 production (μmol CO_2/g coal) considering different amounts of coal and amendment condition. Means that do not share a letter are significantly different.

Treatment	N	Mean	Grouping	
2g(+)	3	31.1950	A	
1g(+)	6	25.9598	A	
2g(-)	2	25.5855	A	
1g(-)	6	24.5036	A	
5g(-)	3	-7.3110		B
5g(+)	3	-10.4752		B

Table SB.4: Tukey Pairwise Comparisons from the Generalized Linear Model comparing cumulative CO_2 production rate (μmol CO_2/g coal/day) considering different amounts of coal and amendment condition. Means that do not share a letter are significantly different.

Treatment	N	Mean	Grouping				
2g(+)	3	0.408081	A				
1g(+)	6	0.315721		B			
2g(-)	2	0.158981			C		
1g(-)	6	0.080977				D	
5g(-)	3	-0.028085					E
5g(+)	3	-0.204824					F

Table SB.5: Tukey pairwise comparisons from the Generalized Linear Model comparing cumulative $^{12}CH_4$ production (μmol $^{12}CH_4$/g coal) considering different amounts of coal and amendment condition. Means that do not share a letter are significantly different.

Treatment	N	Mean	Grouping		
2g(+)	3	237.698	A		
1g(+)	6	224.803	A		
2g(-)	2	221.821	A	B	
1g(-)	6	161.530		B	
5g(+)	3	20.660			C
5g(-)	3	14.304			C

Table SB.6: Tukey pairwise comparisons from the Generalized Linear Model comparing maximum $^{12}CH_4$ production rate (μmol $^{12}CH_4$/g coal/day) considering different amounts of coal and amendment condition. Means that do not share a letter are significantly different.

Treatment	N	Mean	Grouping			
1g(+)	6	3.29728	A			
2(+)	3	3.17212	A			
2g(-)	2	1.00179		B		
1g(-)	6	0.68144			C	
5(+)	3	0.20582				D
5g(-)	3	0.05791				D

REFERENCES CITED

1. Bell, S.E. and R. York, *Community Economic Identity: The Coal Industry and Ideology Construction in West Virginia.* Rural Sociology, 2010. **75**(1): p. 111-143.
2. Haggerty, J., et al., *Long-term effects of income specialization in oil and gas extraction: The U.S. West, 1980–2011.* Energy Economics, 2014. **45**: p. 186-195.
3. Tester, J.W., Drake, Elisabeth M., Driscoll, Michael J., Golay, Micahel W., Peters, Williams A., *Sustainable Energy: Choosing Among Options*. Second ed. 2012, Cambridge: The MIT Press.
4. Arastoopour, H., *The critical contribution of chemical engineering to a pathway to sustainability.* Chemical Engineering Science, 2019. **203**: p. 247-258.
5. Blondeau, J. and J. Mertens, *Impact of intermittent renewable energy production on specific CO2 and NOx emissions from large scale gas-fired combined cycles.* Journal of Cleaner Production, 2019. **221**: p. 261-270.
6. Gonzalez-Salazar, M.A., T. Kirsten, and L. Prchlik, *Review of the operational flexibility and emissions of gas- and coal-fired power plants in a future with growing renewables.* Renewable and Sustainable Energy Reviews, 2018. **82**: p. 1497-1513.
7. (EIA), U.S.E.I.A., *Annual Energy Outlook 2019*, U.S.D.o. Energy, Editor. 2019. p. 69-86.
8. De Bruin, R.H., Lyman, R.M., Jones, Richard W., Cook, Lance W. , *Coalbed Methane in Wyoming*, W.S.G. Survey, Editor. 2000: Laramie ,Wyoming.
9. Green, M.S., K.C. Flanegan, and P.C. Gilcrease, *Characterization of a methanogenic consortium enriched from a coalbed methane well in the Powder River Basin, U.S.A.* International Journal of Coal Geology, 2008. **76**(1): p. 34-45.
10. Rice, C.A., Ellis, M.S., Bullock J.H Jr., *Water co-produced with coalbed methane in the Powder River Basin, Wyoming: Preliminary compositional data: U.S. Geological Survey Open-File Report 00-372, 20 p.* 2000.
11. Administration, U.S.E.I., *Natural Gas*, U.S.D.o. Energy, Editor. 2019: Washington, D.C.
12. Bills Walsh, K., *Split Estate and Wyoming's Orphaned Well Crisis: The Case of Coalbed Methane Reclamation in the Powder River Basin, Wyoming.* Case Studies in the Environment, 2017.
13. Meredith, E., J. Wheaton, and S. Kuzara, *Coalbed-methane Basics: Ten Years of Lessons from the Powder River Basin, Montana*. 2012: MBMG.
14. Brandt, A.R., *Oil Depletion and the Energy Efficiency of Oil Production: The Case of California.* Sustainability, 2011. **3**(10).
15. Gavenas, E., K.E. Rosendahl, and T. Skjerpen, *CO2-emissions from Norwegian oil and gas extraction.* Energy, 2015. **90**: p. 1956-1966.
16. Crow, D.J.G., et al., *Assessing the impact of future greenhouse gas emissions from natural gas production.* Science of The Total Environment, 2019. **668**: p. 1242-1258.
17. McIntosh, J., et al., *Biogeochemistry of the Forest City Basin coalbed methane play.* International Journal of Coal Geology, 2008. **76**(1): p. 111-118.

18. Barnhart, E.P., et al., *Hydrogeochemistry and coal-associated bacterial populations from a methanogenic coal bed.* International Journal of Coal Geology, 2016. **162**: p. 14-26.
19. Davis, K.J. and R. Gerlach, *Transition of biogenic coal-to-methane conversion from the laboratory to the field: A review of important parameters and studies.* International Journal of Coal Geology, 2018. **185**: p. 33-43.
20. Strąpoć, D., et al., *Biogeochemistry of Microbial Coal-Bed Methane.* Annual Review of Earth and Planetary Sciences, 2011. **39**(1): p. 617-656.
21. Martini, A.M., et al., *Genetic and temporal relations between formation waters and biogenic methane: Upper Devonian Antrim Shale, Michigan Basin, USA.* Geochimica et Cosmochimica Acta, 1998. **62**(10): p. 1699-1720.
22. Newell, K.D., et al., *Geological and geochemical factors influencing the emerging coalbed gas play in the Cherokee and Forest City Basins in Eastern Kansas.* Open-File Report, 2004. **17**.
23. Barnhart, E.P., et al., *Enhanced coal-dependent methanogenesis coupled with algal biofuels: Potential water recycle and carbon capture.* International Journal of Coal Geology, 2017. **171**: p. 69-75.
24. Davis, K.J., et al., *Type and amount of organic amendments affect enhanced biogenic methane production from coal and microbial community structure.* Fuel, 2018. **211**: p. 600-608.
25. Hodgskiss, L.H., et al., *Cultivation of a native alga for biomass and biofuel accumulation in coal bed methane production water.* Algal Research, 2016. **19**: p. 63-68.
26. Davis, K.J., et al., *Biogenic Coal-to-Methane Conversion Efficiency Decreases after Repeated Organic Amendment.* Energy & Fuels, 2018. **32**(3): p. 2916-2925.
27. Fallgren, P.H., et al., *Comparison of coal rank for enhanced biogenic natural gas production.* International Journal of Coal Geology, 2013. **115**: p. 92-96.
28. Robbins, S.J., et al., *The effect of coal rank on biogenic methane potential and microbial composition.* International Journal of Coal Geology, 2016. **154**: p. 205-212.
29. Harris, S.H., R.L. Smith, and C.E. Barker, *Microbial and chemical factors influencing methane production in laboratory incubations of low-rank subsurface coals.* International Journal of Coal Geology, 2008. **76**(1): p. 46-51.
30. Wawrik, B., et al., *Field and laboratory studies on the bioconversion of coal to methane in the San Juan Basin.* FEMS Microbiology Ecology, 2012. **81**(1): p. 26-42.
31. Logan, B.E., et al., *Microbial Electrolysis Cells for High Yield Hydrogen Gas Production from Organic Matter.* Environmental Science & Technology, 2008. **42**(23): p. 8630-8640.
32. Logan, B.E., et al., *Microbial Fuel Cells: Methodology and Technology.* Environmental Science & Technology, 2006. **40**(17): p. 5181-5192.
33. Lu, L. and Z.J. Ren, *Microbial electrolysis cells for waste biorefinery: A state of the art review.* Bioresource Technology, 2016. **215**: p. 254-264.

34. Kawaguchi, H., et al., *Methane production by Methanothermobacter thermautotrophicus to recover energy from carbon dioxide sequestered in geological reservoirs.* Journal of Bioscience and Bioengineering, 2010. **110**(1): p. 106-108.
35. Kuramochi, Y., et al., *Electromethanogenic CO2 Conversion by Subsurface-reservoir Microorganisms.* Energy Procedia, 2013. **37**: p. 7014-7020.
36. Lobato, J., et al., *Lagooning microbial fuel cells: A first approach by coupling electricity-producing microorganisms and algae.* Applied Energy, 2013. **110**(Supplement C): p. 220-226.
37. Piao, D.-M., Y.-C. Song, and D.-H. Kim, *Bioelectrochemical Enhancement of Biogenic Methane Conversion of Coal.* Energies, 2018. **11**(10).
38. Barnhart, E.P., et al., *Investigation of coal-associated bacterial and archaeal populations from a diffusive microbial sampler (DMS).* International Journal of Coal Geology, 2013. **115**: p. 64-70.
39. Flores, R.M., et al., *Methanogenic pathways of coal-bed gas in the Powder River Basin, United States: The geologic factor.* International Journal of Coal Geology, 2008. **76**(1): p. 52-75.
40. Park, S.Y. and Y. Liang, *Biogenic methane production from coal: A review on recent research and development on microbially enhanced coalbed methane (MECBM).* Fuel, 2016. **166**: p. 258-267.
41. Colosimo, F., et al., *Biogenic methane in shale gas and coal bed methane: A review of current knowledge and gaps.* International Journal of Coal Geology, 2016. **165**: p. 106-120.
42. Jaramillo, P., W.M. Griffin, and H.S. Matthews, *Comparative Life-Cycle Air Emissions of Coal, Domestic Natural Gas, LNG, and SNG for Electricity Generation.* Environmental Science & Technology, 2007. **41**(17): p. 6290-6296.
43. Jenner, S. and A.J. Lamadrid, *Shale gas vs. coal: Policy implications from environmental impact comparisons of shale gas, conventional gas, and coal on air, water, and land in the United States.* Energy Policy, 2013. **53**: p. 442-453.
44. Jones, E.J.P., et al., *Stimulation of Methane Generation from Nonproductive Coal by Addition of Nutrients or a Microbial Consortium.* Applied and Environmental Microbiology, 2010. **76**(21): p. 7013.
45. Ulrich, G. and S. Bower, *Active methanogenesis and acetate utilization in Powder River Basin coals, United States.* International Journal of Coal Geology, 2008. **76**(1): p. 25-33.
46. Ritter, D., et al., *Enhanced microbial coalbed methane generation: A review of research, commercial activity, and remaining challenges.* International Journal of Coal Geology, 2015. **146**: p. 28-41.
47. Bi, Z., et al., *A formation water-based nutrient recipe for potentially increasing methane release from coal in situ.* Fuel, 2017. **209**: p. 498-508.
48. Nichols, H.W. and H.C. Bold, *Trichosarcina polymorpha Gen. et Sp. Nov.* Journal of Phycology, 1965. **1**(1): p. 34-38.

49. Gardner, R.D., et al., *Use of sodium bicarbonate to stimulate triacylglycerol accumulation in the chlorophyte Scenedesmus sp. and the diatom Phaeodactylum tricornutum.* Journal of Applied Phycology, 2012. **24**(5): p. 1311-1320.
50. Davis, K., *Organic Amendments for Enhancing Microbial Coalbed Methane Production*. 2017, Montana State University: Bozeman, MT. p. pg 202-209.
51. Rounick, J.S. and M.J. Winterbourn, *Stable Carbon Isotopes and Carbon Flow in Ecosystems.* BioScience, 1986. **36**(3): p. 171-177.
52. Orem, W.H., et al., *Organic intermediates in the anaerobic biodegradation of coal to methane under laboratory conditions.* Organic Geochemistry, 2010. **41**(9): p. 997-1000.
53. Hoehler, T.M. and B.B. Jørgensen, *Microbial life under extreme energy limitation.* Nature Reviews Microbiology, 2013. **11**: p. 83.
54. Stouthamer, A.H., *A theoretical study on the amount of ATP required for synthesis of microbial cell material.* Antonie van Leeuwenhoek, 1973. **39**(1): p. 545-565.
55. Schweitzer, H., et al., *Changes in microbial communities and associated water and gas geochemistry across a sulfate gradient in coal beds: Powder River Basin, USA.* Geochimica et Cosmochimica Acta, 2019. **245**: p. 495-513.
56. Flores, R.M., *Chapter 4 - Coalification, Gasification, and Gas Storage*, in *Coal and Coalbed Gas*, R.M. Flores, Editor. 2014, Elsevier: Boston. p. 167-233.
57. O'Keefe, J.M.K., et al., *On the fundamental difference between coal rank and coal type.* International Journal of Coal Geology, 2013. **118**: p. 58-87.
58. Suárez-Ruiz, I. and C.R. Ward, *Chapter 2 - Basic Factors Controlling Coal Quality and Technological Behavior of Coal*, in *Applied Coal Petrology*, I. Suárez-Ruiz and J.C. Crelling, Editors. 2008, Elsevier: Burlington. p. 19-59.
59. Ward, C.R. and I. Suárez-Ruiz, *Chapter 1 - Introduction to Applied Coal Petrology*, in *Applied Coal Petrology*, I. Suárez-Ruiz and J.C. Crelling, Editors. 2008, Elsevier: Burlington. p. 1-18.
60. Scott, A.C. and I.J. Glasspool, *Observations and experiments on the origin and formation of inertinite group macerals.* International Journal of Coal Geology, 2007. **70**(1): p. 53-66.
61. Hower, J.C., et al., *Notes on the origin of inertinite macerals in coals: Observations on the importance of fungi in the origin of macrinite.* International Journal of Coal Geology, 2009. **80**(2): p. 135-143.
62. Sýkorová, I., et al., *Classification of huminite—ICCP System 1994.* International Journal of Coal Geology, 2005. **62**(1): p. 85-106.
63. Teichmüller, M., *The genesis of coal from the viewpoint of coal petrology.* International Journal of Coal Geology, 1989. **12**(1): p. 1-87.
64. Fakoussa, R.M. and M. Hofrichter, *Biotechnology and microbiology of coal degradation.* Applied Microbiology and Biotechnology, 1999. **52**(1): p. 25-40.
65. Drobniak, A. and M. Mastalerz, *Chemical evolution of Miocene wood: Example from the Belchatow brown coal deposit, central Poland.* International Journal of Coal Geology, 2006. **66**(3): p. 157-178.

66. Vorres, K.S., *The Argonne Premium Coal Sample Program.* Energy & Fuels, 1990. **4**(5): p. 420-426.
67. Takahashi, S., et al., *Development of a prokaryotic universal primer for simultaneous analysis of bacteria and archaea using next-generation sequencing.* PloS one, 2014. **9**(8): p. e105592.
68. Baker, G.C., J.J. Smith, and D.A. Cowan, *Review and re-analysis of domain-specific 16S primers.* Journal of Microbiological Methods, 2003. **55**(3): p. 541-555.
69. Kozich, J.J., et al., *Development of a dual-index sequencing strategy and curation pipeline for analyzing amplicon sequence data on the MiSeq Illumina sequencing platform.* Appl. Environ. Microbiol., 2013. **79**(17): p. 5112-5120.
70. Caporaso, J.G., et al., *QIIME allows analysis of high-throughput community sequencing data.* Nature methods, 2010. **7**(5): p. 335.
71. Quast, C., et al., *The SILVA ribosomal RNA gene database project: improved data processing and web-based tools.* Nucleic acids research, 2012. **41**(D1): p. D590-D596.
72. Wang, Q., et al., *Naive Bayesian classifier for rapid assignment of rRNA sequences into the new bacterial taxonomy.* Appl. Environ. Microbiol., 2007. **73**(16): p. 5261-5267.
73. Haas, B.J., et al., *Chimeric 16S rRNA sequence formation and detection in Sanger and 454-pyrosequenced PCR amplicons.* Genome research, 2011. **21**(3): p. 494-504.
74. Gray, N.D., et al., *The quantitative significance of Syntrophaceae and syntrophic partnerships in methanogenic degradation of crude oil alkanes.* Environmental microbiology, 2011. **13**(11): p. 2957-2975.
75. Ünal, B., et al., *Trace Elements Affect Methanogenic Activity and Diversity in Enrichments from Subsurface Coal Bed Produced Water.* Frontiers in Microbiology, 2012. **3**(175).
76. Meslé, M., G. Dromart, and P. Oger, *Microbial methanogenesis in subsurface oil and coal.* Research in Microbiology, 2013. **164**(9): p. 959-972.
77. De Vrieze, J., et al., *Methanosarcina: The rediscovered methanogen for heavy duty biomethanation.* Bioresource Technology, 2012. **112**: p. 1-9.
78. Gründger, F., et al., *Microbial methane formation in deep aquifers of a coal-bearing sedimentary basin, Germany.* Frontiers in Microbiology, 2015. **6**(200).
79. Munson, M.A., D.B. Nedwell, and T.M. Embley, *Phylogenetic diversity of Archaea in sediment samples from a coastal salt marsh.* Applied and Environmental Microbiology, 1997. **63**(12): p. 4729.
80. Meng, M., et al., *Adsorption characteristics of supercritical CO2/CH4 on different types of coal and a machine learning approach.* Chemical Engineering Journal, 2019. **368**: p. 847-864.
81. Busch, A. and Y. Gensterblum, *CBM and CO2-ECBM related sorption processes in coal: A review.* International Journal of Coal Geology, 2011. **87**(2): p. 49-71.

82. Busch, A., Y. Gensterblum, and B.M. Krooss, *Methane and CO2 sorption and desorption measurements on dry Argonne premium coals: pure components and mixtures.* International Journal of Coal Geology, 2003. **55**(2): p. 205-224.
83. Crosdale, P.J., B.B. Beamish, and M. Valix, *Coalbed methane sorption related to coal composition.* International Journal of Coal Geology, 1998. **35**(1): p. 147-158.
84. Prinz, D., et al. *Investigations on the micro-and mesoporous structure of coals of varying rank: a combined small angle neutron scattering (SANS) and gas adsorption experiments study*. in *Proceedings of the 2001 international coalbed methane symposium*. 2001.
85. Zhang, R., et al., *Changes in pore structure of coal caused by coal-to-gas bioconversion.* Scientific Reports, 2017. **7**(1): p. 3840.
86. Singh, D.N. and A.K. Tripathi, *Coal induced production of a rhamnolipid biosurfactant by Pseudomonas stutzeri, isolated from the formation water of Jharia coalbed.* Bioresource Technology, 2013. **128**: p. 215-221.
87. Fry, J.C., et al., *Prokaryotic Populations and Activities in an Interbedded Coal Deposit, Including a Previously Deeply Buried Section (1.6–2.3 km) Above ~150 Ma Basement Rock.* Geomicrobiology Journal, 2009. **26**(3): p. 163-178.
88. Shimizu, S., et al., *Molecular characterization of microbial communities in deep coal seam groundwater of northern Japan.* Geobiology, 2007. **5**(4): p. 423-433.
89. Beckmann, S., et al., *Acetogens and Acetoclastic Methanosarcinales Govern Methane Formation in Abandoned Coal Mines.* Applied and Environmental Microbiology, 2011. **77**(11): p. 3749.
90. Shin, S.G., et al., *Use of order-specific primers to investigate the methanogenic diversity in acetate enrichment system.* Journal of Industrial Microbiology & Biotechnology, 2008. **35**(11): p. 1345-1352.
91. Mittal, M. and K.J. Rockne, *Indole production by Pseudomonas stutzeri strain NAP-3 during anaerobic naphthalene biodegradation in the presence of dimethyl formamide.* Journal of Environmental Science and Health, Part A, 2008. **43**(9): p. 1027-1034.
92. Deziel, E., et al., *Biosurfactant production by a soil pseudomonas strain growing on polycyclic aromatic hydrocarbons.* Applied and Environmental Microbiology, 1996. **62**(6): p. 1908.
93. Zhang, Z., et al., *Degradation of n-alkanes and polycyclic aromatic hydrocarbons in petroleum by a newly isolated Pseudomonas aeruginosa DQ8.* Bioresource Technology, 2011. **102**(5): p. 4111-4116.
94. Juhasz, A.L., M.L. Britz, and G.A. Stanley, *Degradation of high molecular weight polycyclic aromatic hydrocarbons by Pseudomonas cepacia.* Biotechnology Letters, 1996. **18**(5): p. 577-582.
95. Zheng, C., et al., *Characterization and emulsifying property of a novel bioemulsifier by Aeribacillus pallidus YM-1.* Journal of Applied Microbiology, 2012. **113**(1): p. 44-51.
96. Kügler, J.H., et al., *Surfactants tailored by the class Actinobacteria.* Frontiers in Microbiology, 2015. **6**(212).

97. Bognolo, G., *Biosurfactants as emulsifying agents for hydrocarbons.* Colloids and Surfaces A: Physicochemical and Engineering Aspects, 1999. **152**(1): p. 41-52.
98. Lovley, D.R. and K.P. Nevin, *A shift in the current: New applications and concepts for microbe-electrode electron exchange.* Current Opinion in Biotechnology, 2011. **22**(3): p. 441-448.
99. Jiang, Y. and R. Jianxiong Zeng, *Expanding the product spectrum of value added chemicals in microbial electrosynthesis through integrated process design—A review.* Bioresource Technology, 2018. **269**: p. 503-512.
100. Torres, C.I., A. Kato Marcus, and B.E. Rittmann, *Kinetics of consumption of fermentation products by anode-respiring bacteria.* Applied Microbiology and Biotechnology, 2007. **77**(3): p. 689-697.
101. Torres, C.I., et al., *Selecting Anode-Respiring Bacteria Based on Anode Potential: Phylogenetic, Electrochemical, and Microscopic Characterization.* Environmental Science & Technology, 2009. **43**(24): p. 9519-9524.
102. Torres, C.I., A. Kato Marcus, and B.E. Rittmann, *Proton transport inside the biofilm limits electrical current generation by anode-respiring bacteria.* Biotechnology and Bioengineering, 2008. **100**(5): p. 872-881.
103. Torres, C.I., et al., *A kinetic perspective on extracellular electron transfer by anode-respiring bacteria.* FEMS Microbiology Reviews, 2010. **34**(1): p. 3-17.
104. Kumar, R., L. Singh, and A.W. Zularisam, *Exoelectrogens: Recent advances in molecular drivers involved in extracellular electron transfer and strategies used to improve it for microbial fuel cell applications.* Renewable and Sustainable Energy Reviews, 2016. **56**: p. 1322-1336.
105. TerAvest, M.A. and C.M. Ajo-Franklin, *Transforming exoelectrogens for biotechnology using synthetic biology.* Biotechnology and Bioengineering, 2016. **113**(4): p. 687-697.
106. Abdalla, A.M., et al., *Hydrogen production, storage, transportation and key challenges with applications: A review.* Energy Conversion and Management, 2018. **165**: p. 602-627.
107. Chae, K.-J., et al., *Selective inhibition of methanogens for the improvement of biohydrogen production in microbial electrolysis cells.* International Journal of Hydrogen Energy, 2010. **35**(24): p. 13379-13386.
108. Catal, T., K.L. Lesnik, and H. Liu, *Suppression of methanogenesis for hydrogen production in single-chamber microbial electrolysis cells using various antibiotics.* Bioresource Technology, 2015. **187**: p. 77-83.
109. Chae, K.-J., et al., *Methanogenesis control by employing various environmental stress conditions in two-chambered microbial fuel cells.* Bioresource Technology, 2010. **101**(14): p. 5350-5357.
110. Kadier, A., et al., *Surpassing the current limitations of high purity H2 production in microbial electrolysis cell (MECs): Strategies for inhibiting growth of methanogens.* Bioelectrochemistry, 2018. **119**: p. 211-219.
111. Lawrence, A.W. and P.L. McCarty, *Kinetics of Methane Fermentation in Anaerobic Treatment.* Journal (Water Pollution Control Federation), 1969. **41**(2): p. R1-R17.

112. Villano, M., et al., *Carbon and nitrogen removal and enhanced methane production in a microbial electrolysis cell.* Bioresource Technology, 2013. **130**: p. 366-371.
113. Liu, W., et al., *Microbial electrolysis contribution to anaerobic digestion of waste activated sludge, leading to accelerated methane production.* Renewable Energy, 2016. **91**: p. 334-339.
114. Cheng, S., et al., *Direct Biological Conversion of Electrical Current into Methane by Electromethanogenesis.* Environmental Science & Technology, 2009. **43**(10): p. 3953-3958.
115. In 't Zandt, M.H., et al., *Nutrient and acetate amendment leads to acetoclastic methane production and microbial community change in a non-producing Australian coal well.* Microbial biotechnology, 2017. **11**(4): p. 626-638.
116. Gallagher, L.K., et al., *The effect of coal oxidation on methane production and microbial community structure in Powder River Basin coal.* International Journal of Coal Geology, 2013. **115**: p. 71-78.
117. Huang, Z., M.A. Urynowicz, and P.J.S. Colberg, *Stimulation of biogenic methane generation in coal samples following chemical treatment with potassium permanganate.* Fuel, 2013. **111**: p. 813-819.
118. Sato, K., H. Kawaguchi, and H. Kobayashi, *Bio-electrochemical conversion of carbon dioxide to methane in geological storage reservoirs.* Energy Conversion and Management, 2013. **66**: p. 343-350.
119. Zhen, G., et al., *Understanding methane bioelectrosynthesis from carbon dioxide in a two-chamber microbial electrolysis cells (MECs) containing a carbon biocathode.* Bioresource Technology, 2015. **186**: p. 141-148.
120. Cruz Viggi, C., et al., *Magnetite particles triggering a faster and more robust syntrophic pathway of methanogenic propionate degradation.* Environmental science & technology, 2014. **48**(13): p. 7536-7543.
121. Zhen, G., et al., *Promoted electromethanosynthesis in a two-chamber microbial electrolysis cells (MECs) containing a hybrid biocathode covered with graphite felt (GF).* Chemical Engineering Journal, 2016. **284**: p. 1146-1155.
122. Villano, M., et al., *Bioelectrochemical reduction of CO2 to CH4 via direct and indirect extracellular electron transfer by a hydrogenophilic methanogenic culture.* Bioresource Technology, 2010. **101**(9): p. 3085-3090.
123. Feng, Q., et al., *Polarized electrode enhances biological direct interspecies electron transfer for methane production in upflow anaerobic bioelectrochemical reactor.* Chemosphere, 2018. **204**: p. 186-192.
124. Feng, Q., et al., *Bioelectrochemical enhancement of direct interspecies electron transfer in upflow anaerobic reactor with effluent recirculation for acidic distillery wastewater.* Bioresource Technology, 2017. **241**: p. 171-180.
125. Zhao, Z., et al., *Evaluation on direct interspecies electron transfer in anaerobic sludge digestion of microbial electrolysis cell.* Bioresource Technology, 2016. **200**: p. 235-244.
126. Lovley, D.R., *Happy together: microbial communities that hook up to swap electrons.* The Isme Journal, 2016. **11**: p. 327.

127. Rotaru, A.-E., et al., *A new model for electron flow during anaerobic digestion: direct interspecies electron transfer to Methanosaeta for the reduction of carbon dioxide to methane.* Energy & Environmental Science, 2014. **7**(1): p. 408-415.
128. Pisciotta, J.M., et al., *Enrichment of Microbial Electrolysis Cell Biocathodes from Sediment Microbial Fuel Cell Bioanodes.* Applied and Environmental Microbiology, 2012. **78**(15): p. 5212.
129. Jeremiasse, A.W., H.V.M. Hamelers, and C.J.N. Buisman, *Microbial electrolysis cell with a microbial biocathode.* Bioelectrochemistry, 2010. **78**(1): p. 39-43.
130. Parameswaran, P., et al., *Syntrophic interactions among anode respiring bacteria (ARB) and Non-ARB in a biofilm anode: electron balances.* Biotechnology and Bioengineering, 2009. **103**(3): p. 513-523.
131. Ishii, S.i., et al., *Bioelectrochemical Stimulation of Electromethanogenesis at a Seawater-Based Subsurface Aquifer in a Natural Gas Field.* Frontiers in Energy Research, 2019. **6**(144).
132. Yang, X., et al., *Potential of biogenic methane for pilot-scale fermentation ex situ with lump anthracite and the changes of methanogenic consortia.* Journal of Industrial Microbiology & Biotechnology, 2018. **45**(4): p. 229-237.
133. Call, D.F. and B.E. Logan, *A method for high throughput bioelectrochemical research based on small scale microbial electrolysis cells.* Biosensors and Bioelectronics, 2011. **26**(11): p. 4526-4531.
134. Call, D. and B.E. Logan, *Hydrogen Production in a Single Chamber Microbial Electrolysis Cell Lacking a Membrane.* Environmental Science & Technology, 2008. **42**(9): p. 3401-3406.
135. Karacan, C.Ö. and G.D. Mitchell, *Behavior and effect of different coal microlithotypes during gas transport for carbon dioxide sequestration into coal seams.* International Journal of Coal Geology, 2003. **53**(4): p. 201-217.
136. Zhao, J., et al., *A comparative evaluation of coal specific surface area by CO2 and N2 adsorption and its influence on CH4 adsorption capacity at different pore sizes.* Fuel, 2016. **183**: p. 420-431.
137. Mohanty, M.M. and B.K. Pal, *Sorption behavior of coal for implication in coal bed methane an overview.* International Journal of Mining Science and Technology, 2017. **27**(2): p. 307-314.
138. Lee, H.-S., C.I. Torres, and B.E. Rittmann, *Effects of Substrate Diffusion and Anode Potential on Kinetic Parameters for Anode-Respiring Bacteria.* Environmental Science & Technology, 2009. **43**(19): p. 7571-7577.
139. Finney, C.D. and R.S. Evans, *Anaerobic Digestion: The Rate-Limiting Process and the Nature of Inhibition.* Science, 1975. **190**(4219): p. 1088.
140. Pillalamarry, M., S. Harpalani, and S. Liu, *Gas diffusion behavior of coal and its impact on production from coalbed methane reservoirs.* International Journal of Coal Geology, 2011. **86**(4): p. 342-348.